PRODUCTION AND EQUILIBRATION OF QUARK-GLUON PLASMA IN ULTRA RELATIVISTIC HEAVY-ION COLLISIONS
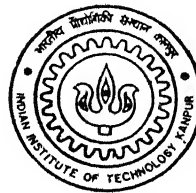
by

GOURANGA CHANDRA NAYAK

DEPARTMENT OF PHYSICS
INDIAN INSTITUTE OF TECHNOLOGY KANPUR
JULY, 1998

PRODUCTION AND EQUILIBRATION OF QUARK-GLUON PLASMA IN ULTRA RELATIVISTIC HEAVY-ION COLLISIONS

A Thesis Submitted
in Partial Fulfillment of the Requirements
for the Degree of
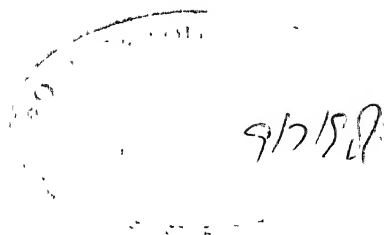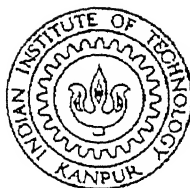Doctor of Philosophy

by
GOURANGA CHANDRA NAYAK

to the
DEPARTMENT OF PHYSICS
INDIAN INSTITUTE OF TECHNOLOGY, KANPUR
July, 1998

Dedicated to my parents to whom I love very much

CERTIFICATE

It is certified that the work contained in this thesis entitled *Production and equilibration of quark-gluon plasma in ultra relativistic heavy-ion collisions* by *Gouranga Chandra Nayak* has been carried out under my supervision and that this work has not been submitted elsewhere for a degree.

V. Ravishankar
Department of Physics
Indian Institute of Technology
Kanpur

9 July, 1998

Acknowledgements

I would like to express my deepest gratitude to my supervisor Professor V. Ravishankar, for introducing me to this field. During last five years, his useful guidance and suggestions helped me in completing my work. Apart from helping me in my academic endevour he has been very friendly with me providing solutions to many of my personal problems. In my personal opinion he was very friendly and helpful to me during my stay in I I T Kanpur

It is a great pleasure for me to acknowledge Professor Rajeev S. Bhalerao (TIFR), who made available the original numerical program, which was modified according my needs.

I would like to thank Professor Deshdeep Sahdev and Professor Satyendra Kumar for their useful suggestions during my Ph.D. period.

I would take this oppertunity to thank Professor Rajiv V. Gavai (TIFR), who has discussed a lot with me (by E-mail) to learn the J/ψ problem from very begning. Without him and Professor Pankaj Jain it would have been very difficult for me to persue studies on this topic. I thank Professor Pankaj Jain for this discussions. I also acknowledge Professor S. D. Joglekar, Professor M. K. Verma for useful discussions.

I would like to thank Sudhansu (IISC), Pranab Bhai, Uzzal, Vikas, Dandapat sir, Bandu, Tapu, Goutam, Ashutosh, Anirban, Dixit for making my stay at IIT a memorable one

I am thankful to my parents, Akshaya, Apa, Lili, Kuni, Reena, Chhuajhia for their sacrifice and constant encouragement, without which it would not been possible to complete this work.

Finally, I am thankful to leenu for bringing a lot of inspiration and encouragement in my life

Nayak

SYNOPSIS

Name of Student **Gouranga Chandra Nayak**   Roll No **9210966**

Degree for which submitted: **Ph.D.**   Department: **Physics**

Thesis Title: **Production and equilibration of quark-gluon plasma in ultra relativistic heavy-ion collisions**

Name of thesis supervisor: **Dr. V. Ravishankar**

Month and year of submission: **July, 1998**

The study of production of quark-gluon plasma (QGP) in the laboratory is fascinating for a variety of reasons. It is interesting beacuse, this phase did exist for first few microseconds in the early universe and perhaps also exists in the stellar matter at high density. Further, a study of QGP provides a test of QCD in a new scale (high energy density) in its non-perturbative regime. It is also expected to improve our understanding of other fundamental concepts such as the nature of confinement and and chiral symmetry.

From quantum chromodynamics as input dynamics for strong interaction between quarks and gluons, we can directly predict this state of matter by large scale computer simulations. The results of computer simulations provided a quantitative confirmation of the idea that hadronic

matter at sufficiently high density will undergo a transition to a state of matter of deconfined quarks and gluons, *i.e.* quark-gluon plasma. On the experimental side, there has been much effort in the direction of detecting this phase of matter. In the last decade two experiments at SPS of CERN and AGS of BNL were done which succeded in achieving a high energy density, although the creation of QGP itself is not confirmed. Future experiments at relativistic heavy-ion collidres (RHIC) of BNL and large hadron colliders (LHC) of CERN will hopefully able to produce energy density high enough for the production (and equilibration) of QGP

The most difficult task in these experiments is the detection of quark-gluon plasma. This is because, the plasma exists for a very short time in a very small volume and a direct detection is not possible. The signatures suggested are necessarily indirect and the prominent ones are. (1) J/ψ suppression, (2) electromagnetic probes such as dilepton and direct photon production. and (3) strangeness enhancement. The measurement of these signatures involve both theoretical and experimental constraints. The main experimental difficulty lies in singling out the contributions arising from the non-qgp sources. The major theoretical difficulty in the calculation of these signatures arise from the poorly understood space time evolution of the quark-gluon plasma in these ultra relativistic heavy-ion collisions.

The space time evolution of the quark-gluon plasma evolution at these experiments has been generally described by hydrodynamics assuming that the equilibration is almost instantaneously reached. In reality, the various stages by which the complete evolution of quark-gluon plasma are to be described are, i) pre-equilibrium, ii) equilibrium. where one actually studies the thermalised quark-gluon plasma. iii) cooling and iv) hadronisation. It is crucial and very much necessary to study the pre-equilibrium stage in the ultra relativistic heavy-ion collisions, for it has direct impact on the plasma evolution and also on the measured signatures in the experiments.

In this thesis we study the pre-equilibrium evolution of quark-gluon plasma in URHIC by employing color flux-tube model.

In chapter 1 we introduce the topic and provide the necessary background. It contains an overview of the theoretical and experimental status of the field. A brief description of the proposed signatures is presented in this chapter.

chapter 2 contains an extensive description of the pre-equilibrium evolution of quark-gluon plasma within color flux-tube model. In this model the two nuclei that undergo a central collision at RHIC and LHC are highly Lorentz contracted as thin plates. These two Lorentz contracted nuclei pass through each other and, in the process, acquire a non-zero color charge ($\langle Q \rangle = 0$, $\langle Q^2 \rangle \neq 0$), by exchanging soft gluons. This leads to creation of a chromoelectric field between two receeding nuclei, which polarise the QCD vacuum and produces quarks and gluons via Schwinger mechanism (with suitable adaptions and modifications). The quarks and gluons so produced collide with each other and get accelerated by the background chromoelectric field. In this chapter we set up the transport equations in an extended phase space (which include color in addition to coordinate and momenta) to study the production and equilibration of quark-gluon plasma in ultra relativistic heavy-ion collisions.

In chapter 3 we solve the non-Abelian transport equations for $q\bar{q}$ plasma in SU(2) gauge group. In this exercise which is essentially a warm up for the more realistic study which we perform in the next chapter, it is shown that the non-Abelian features are crucial and the so called Abelian dominance which was studied so far is not justified. We obtain the distribution function of quarks and gluons which carry explicit color charges those are abscent in any other study. The physical quantities such as local energy density, number density and temperature of the plasma are determined for this $q\bar{q}$ plasma.

In chapter 4 we again solve non-Abelian transport equations to include gluons in addition to $q\bar{q}$ in SU(3) group which is the realistic gauge group for strong interaction. We made a detailed comparison with the SU(2) results as well as with other p-QCD based approaches such as parton cascade model.

A calculation of the dilepton rate is presented in **chapter 5** using the distribution of quarks and antiquarks within color flux-tube model. It is shown that the pre-equilibrium production of dilepton pair is dominant for very small transverse mementum of the dilepton pair, whereas the Drell-Yan contribution is dominant over large transverse momentum of the dilepton pair

In **chapter 6**, we propose a new source term for quarks and gluons as is appropriate for URHIC. We treat the time dependence of the background field dynamically, and also project the amplitudes to a coherent basis in the extended phase space, so as to obtain a legitmate classical source term. We show that the 'source' is also necessarily a sink both of which exhibit special characters in the phase space. We make a detailed comparison with the source term which are obtained using rather ad-hoc prescriptions.

In **chapter 7** we have studied J/v suppressions in a thermally equilibrating quark-gluon plasma at RHIC using short-distance QCD. The evolution of the system is taken from parton cascade model. The suppression is found to be 100 percent at RHIC energy. A discussion on the validity of the models, which describe the evolution of the quark-gluon plasma, is presented from this study.

chapter 8 contains a very brief literature survey of the other models available for the study of the pre-equilibrium evolution of quark-gluon plasma. It also contains a very brief description of the lattice approaches towards this field.

This thesis is based on the following publications/papers

1. Pre-equilibrium evolution of a non-abelian plasma– **Gouranga C Nayak** and V Ravishankar, *Phys. Rev D* 55 (1997) 6877.

2. Pre-equilibrium evolution of quark-gluon plasma– **Gouranga C Nayak** and V Ravishankar, *Phys. Rev. C* 58 (1998) 356

3. J/Ψ supressions in a thermally equilibrating quark-gluon plasma at RHIC – **Gouranga C Nayak**, *Journal of high energy physics* **02** (1998) 005

4. Dilepton emissions from an equilibrating non-abelian plasma – **Gouranga C Nayak**, *Report no* hep-ph/9801321

5. Quark-antiquark and gluon production from a space-time dependent chromoelectric field – **Gouranga C Nayak** and V Ravishankar, *to be communicated*

Contents

List of Tables

List of Figures

Chapter 1

Introduction

In recent times particle physicists and nuclear physicists have evinced a lot of interest in studying a new phase of matter, namely, quark-gluon plasma(QGP). It is theoretically established that this state of matter consists of unbound quarks and gluons at a temperature about 200 MeV. Such a phase did exist in the early stage of the evolution of our universe, $\sim 10^{-4}$ second after Big Bang. As the universe expanded and cooled down, it went through a phase transition to the hadronic matter that we see today. To study this phase and to re-create the early universe in the laboratory is a challenging task for both the theorists and the experimentalists.

Quantum chromodynamics (QCD), which successfully describes the strong interaction between quarks and gluons, has predicted the possibility of such a phase. Within QCD, quarks carry three types of color charges which interact among themselves via gluons, which are the non-abelian gauge bosons. Unlike the Abelian theory where photons do not carry any electric charge, gluons in the non-Abelian theory (described by the gauge group SU(3)) carry a charge which

is a vector in eight-dimensional space. Within this theory, quarks belong to the fundamental representation of SU(3) group and gluons to its adjoint representation This theory explains many phenomena observed at the present day experiments.

However the full range of QCD is not solved till today. This is because, the perturbative calculation is not applicable over the large distance scale due to the nature of the strong interaction between quarks and gluons. This regime needs to be studied within the frame work of non-perturbative QCD So far, computer simulations on the lattice[1] provide the only reliable method available for the non-perturbative study. More importantly lattice QCD predicts a phase transition between the hadronic state to a quark-gluon phase. It also predicts that at a critical temperature T_c the dimensionless energy density measure, ϵ/T^4, increases abruptly from a value near that of an ideal pion gas ($\simeq 1$) to a value that of an ideal quark-gluon gas. This increase in the energy density, $\Delta\epsilon$, represents some thing like "latent heat of deconfinement". This suggests that for a stable and large system of vanishing net baryon density, there occurs a deconfined phase of the quarks and gluons, called quark-gluon plasma. This deconfinement phase transition is expected to occur at a temperature of the order $T_c = 150 MeV$ corresponding to an energy density of $\epsilon_c = $ 1-3 GeV/fm^3. Energy densities of this magnitude which did exist in the early universe is expected to be obtained in small volumes ($\sim 100 fm^3$) and for a short time ($\sim 5 - 10 fm$) in high energy heavy-ion collisions. Abundant multiple scattering among the incident nucleons in the heavy-ion collisions and the many secondaries produced during these processes are expected to give rise such an energy density.

As no direct observation exists in these experiments for the initial energy density released, it has to be determined from the distribution of the final state hadrons. The formula obtained

from the Bjorken model[2] which is generally used to estimated the energy density is

$$\epsilon = \frac{dE_T/dy}{\pi R^2 \tau_0} \tag{1.1}$$

where $\tau_0 = 1fm$ being the formation time and $R = 1.15A^{1/3}$. The quantity dE_T/dy in the above equation is proportional to the final multiple distribution dN/dy which increases as the number of binary nucleon-nucleon interaction increases. In order to obtain such an energy density through large multiple collisions, it is required that the two nuclei in the collision should be large and accelerated to high energy.

During the last decade such experiments involving heavy-ion collisions have been done at the AGS[3] of BNL and the SPS[4] of CERN with $E_{lab} = 14$ and 200 A GeV. Both are fixed target experiments and hence produce a low centre of mass energy (E_{cm}). Although the results of these experiments suggest an extremely rich physics which can not be explained by a straight forward extrapolation of nucleon-nucleon collisions, it is still not clear whether (an equilibrated) quark-gluon plasma is created in these experiments, in particular at SPS (Pb-Pb collisions at at $E_{cm} = 17$ GeV). The future heavy-ion collider experiments at RHIC (Au-Au collision) of BNL and LHC (Pb-Pb collision) of CERN with $E_{cm} = 200$ A GeVand 5.5 A TeV respectively will provide the best opportunity to study such a phase. These values of high energy imply that at the moment of maximum nuclear overlap the energy densities are of the order of $\epsilon_i \sim 250$ (7500) GeV/fm^3 at RHIC (LHC), which is much higher than the critical energy density for deconfinement caluculated from lattice QCD.

The most important task on hand is a detection of QGP, assuming that it is produced. As the plasma exists for a short time ($\sim 5 - 10fm$) over a small volume ($\sim 100fm^3$), it is not directly accesible in these experiments. Indirect signatures are proposed to detect this phase and the prominents among them are : (1) J/ψ suppression[5], (2) electromagnetic probes such

as dilepton and direct photon production[6, 7], and (3) strangeness enhancement[8].

• J/ψ **suppression**

According to the proposal of Matsui and Satz, the J/ψ production is suppressed in the presence of a deconfined QGP medium due to Debye screening. At high temperature the Debye screening length which is calculated from lattice QCD is smaller than the J/ψ bound state radius. This forbids the binding of $c\bar{c}$ to J/ψ. Although suppression of J/ψ is seen in heavy-ion collisions, still it is not clear that it is due to screening only. This is because, J/ψ is also supressed in p-A collisions and A-B collisions at SPS, where there is no QGP phase. This can be seen from Fig-1.1 where the survival probability of J/ψ is plotted against various nuclei in different experiments.

The suppression of J/ψ in the above cases is due to the presence of a nuclear medium. The inelastic collision between $c\bar{c}$ and nucleon explains the data in p-A collisions and A-B collisions at SPS. Although a recent measurement of J/ψ by NA50 experiment (see Fig-1.1) is not explained by the presence of a nuclear medium, it is still not clear whether this supression can be understood in terms of the presence of a deconfined medium. Recently Kharzeev and Satz have employed the results of Bhanot and Peskin (1979) to study the interaction of heavy quarkonium with gluons. This work provides a dynamical basis to study the J/ψ suppression by using short-distance QCD. Within this formalism J/ψ dissociates to $D\bar{D}$ due to the interaction with hard gluons which are present in the deconfined medium. This mechanism is expected to give rise a huge suppression of J/ψ at RHIC and LHC[9, 10]. Besides this, various authors have devloped different proposals for explaining the NA50 data without assuming any deconfined medium[11–14].
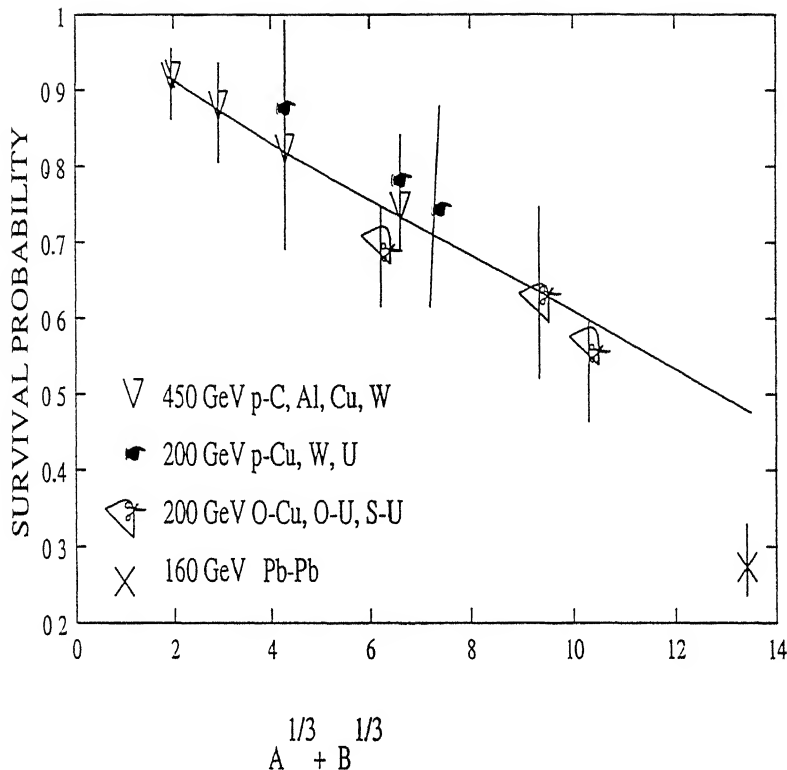
Figure 1.1: The J/ψ survival probability after absorption through nuclear matter. Here A and B are the mass number of the colliding objects. The full line is the sutvival probability for the proton-nucleus (nucleus-nucleus) systems, calculated with a cross section $\sigma = 6.2$ mb. The marks are the experimental datas, as mentioned in the figure.

In short, although a supression of J/ψ is seen in these existing experiments, no clear conclusive evidence for the existence of quark-gluon plasma can be assured. A detailed description of the recent theoritical and experimental developements on J/ψ production and its suppression is presented in chapter 7.

• **Electromagnetic probes**

Dileptons and single photons have long been proposed as useful probes of the plasma[7]. Once produced, they hardly interact with the strong matter and thus carry the details of the circumstances of their production. The major processes for dilepton and photon production in URHIC are, (i) hard parton scattering, (ii) electromegnetic decay of hadrons and (iii) production from

partons present in QGP (thermal production). The hard parton scatterings produce high p_t lepton pairs and photons which are calculated from pQCD. The leading order processes are quark-antiquark anihillation and quark-gluon compton scattering. This is simillar to hadronic collisions. On the other hand, electromagnetic decay of produced hadrons is the main source of dilepton and photon production which obscure the signal of interest (thermal production), which are produced from QGP. More importantly, the thermal emission of dilepton and direct photon is not well understood either theoretically (due to lack of proper description of the space time evolution of QGP) or experimentally. These thermal lepton pairs and thermal photons are expected to be important signatures of QGP because, their measurement is probably the only possibility to have a direct access to the transient dense and high temperature phase of a heavy-ion collision. Using thermal parton distributions, the emission rate of thermal dilepton and photon is calculated in a simillar way as the high p_t direct photon and dilepton calculation using the structure functions of nucleons inside nucleus. It is expected that in high energy heavy-ion collisions such as at RHIC and LHC, the thermal production will be more than the other processes.

At present, a lot of effort are being made both theoretically and experimentally to understand the thermal production of dileptons and photons from the quark-gluon plasma. This is one of the hot topic in the search of QGP. A detailed description of this topic is presented in chapter 5.

• Strangeness enhancement

Strangeness enhancement was proposed as a possible signature of the QGP state, almost 17 years ago[15]. Recall that QGP is formed when the matter density is 10 times greater than that of the nuclear matter. The energy corresopnding to the temperatute which is greater than

that of the critical temperature is larger than the mass of the $s\bar{s}$ pair ($\simeq$ 300 MeV). Therefore, the $s\bar{s}$ will occur at almost the same rate as $u\bar{u}$ or $d\bar{d}$ in the QGP at high temperature. In the hadron gas the strange particles are produced through associated production during the collision of two typically non-strange hadrons. The threshold energy to produce this strange particle is determined by the mass of the strange hadron pair. The reaction with the lowest threshold is $p + n - > \Lambda^0 + K^+ + n$ which requires 671 MeV. On the otherhand. as we have discussed, in a QGP the threshold for the strangeness production is only around 300 MeV. Therefore, the strangeness production in the QGP is favoured from the production in the hadron gas. The strangeness enhancement has been investigated by many experimental groups[16] and recently it has been one of the important topics in relativistic heavy-ion collisions.

The signals discussed above had been initially studied by assuming an equilibrated QGP. However, the measurement of these signals in the actual experiment. involve the contributions from all the stages of evolution of the system. In order to make a convincing case for observation of QGP, the observation of several signals must be supported with a reasonable description of the interactions of the final state particles. The formation and study of quark-gluon plasma in future experiments, will crucially depend upon a detailed microscopic understanding of the plasma. Questions relating to its formation. evolution and hadronisation deserve a much better study.

Of particular importance to us is the production and the evolution of quark-guon plasma after two nuclei collide with each other. It is expected that in the center-of-mass frame, two highly Lorentz contracted nuclei pass through each other and deposit their kinetic energy gradually behind them[17]. A qualitatively accepted space-time evolution of these reactions is schematically illustrated in Fig-1.2. The various stages by which the complete evolution of quark-gluon
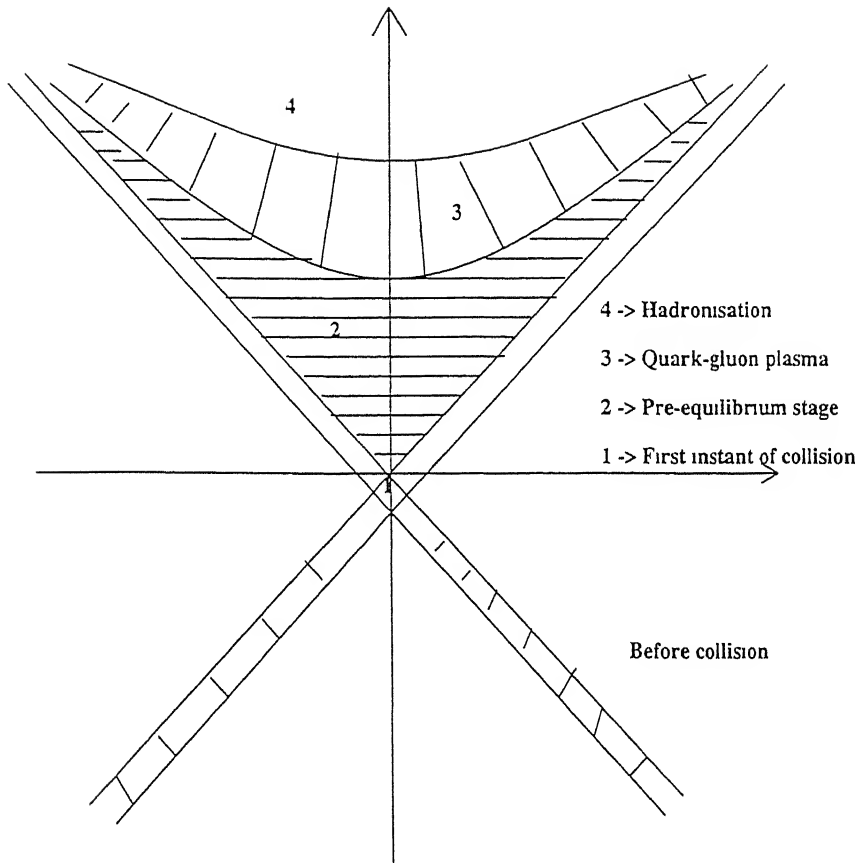
Figure 1.2: A typically accepted space time evolution picture of the nucleus-nucleus collisions in ultra relativistic heavy-ion collisions

plasma is described in URHIC are, ı) pre-equilibrıum, ıı) equilibrium. where one actually studies the thermalised quark-gluon plasma, iıı) cooling and iv) hadronisation. In the very early stage of this collisıon, the partons are being produced and they collide with each other ın the pre-equilibrıum stage to form the equilibrated quark-gluon plasma ın the stage (ii). It ıs expected that most of the entropy and transverse energy are produced in this satge. The dynamics of partons durıng the first few fermi determines the ınitial (and boundary) conditions for the hydrodynamic expansion of the plasma phase. The validity of the calculations involving hydrodynamic expansion. assuming very fast local thermodynamic equilıbrium after the partons are produced, is to be checked and a proper study of pre-equilibrium dynamics is needed. In particular, we want to know how the partons evolve, under what conditions they thermalise,

the time scale of equilibration and the typical energy density soon after the thermalisation Without these inputs there are always uncertainties in choosing the equilibration time and the initial temperature which crucially determines the predictions of all the signatures. To study these questions systematically in a realistic model, a detailed study of the pre-equilibrium stage during the very early stage of the high energy nuclear collisions is necessary.

As mentioned, the production of an equilibrated quark-gluon plasma in stage (ii) crucially depends on the pre-equilibrium evolution. and hence all the signatures in the experiments. Indeed it has been pointed out[9, 10] that J/ψ suppression which is generally attributed to the equilibrium stage can also arise from the pre-equilibrium stage, an observation which is true for strangeness enhancement as well. The contribution of the pre-equilibrium stage to the dilepton production and the direct photon production would be even more pronounced, and a careful study of the above signals ought to shed light on this stage of the plasma.

In this thesis we discuss the production and the equilibration of quark-gluon plasma(QGP) in URHIC by employing the Flux-tube Model[18, 19] which is a generalization of the familiar Lund string model[20] widely used for e^+e^- and $p-p$ collisions. A chapter wise summary is given in the synopsis (see page v).

Chapter 2

Pre-equilibrium evolution of quark-gluon plasma

2.1   Introduction

The space-time evolution of quark-gluon plasma created in ultra relativistic heavy-ion collisions is governed by hydrodynamics, once it reaches equilibrium The relativistic hydrodynamic equations are:

$$\partial_\mu T^{\mu\nu}(r) = 0 \tag{2.1}$$

and

$$\partial_\mu n^\mu(r) = 0, \tag{2.2}$$

where $T^{\mu\nu}(r)$ is the local energy-momentum tensor and $n^\mu(r)$ is related to the local number density $n(r)$ by $n(r) = n^\mu(r)u_\mu(r)$ with $u_\mu(r)$ being the flow velocity. In the absence of any dissipation the energy-momentum tensor is written in terms of energy density $\epsilon(r)$ and the pressure $p(r)$ as

$$T^{\mu\nu}(r) = -g^{\mu\nu}p(r) + (\epsilon(r) + p(r))u^\mu(r)u^\nu(r), \tag{2.3}$$

where $\epsilon(r) = T_{\mu\nu}u^\mu(r)u^\nu(r)$. If one further neglects the transverse expansion in the early stage and considers only the longitudinal expansion, we then arrive at the equation[2]:

$$\frac{d\epsilon}{d\tau} + \frac{\epsilon + p}{\tau} = 0, \tag{2.4}$$

first proposed by Bjorken to describe space-time evolution of QGP In the above equation, $\tau = \sqrt{(t^2 - z^2)}$ is the proper time.

As these hydrodynamical equations are applicable only in equilibrium, which is attained at certain time after the two nuclei have collided with each other it is desirable to determine the equilibration time by some microscopic approach. After all, the initial conditions that govern the hydrodynamical evolution (Eqn 2.4) can only be obtained from a careful study of the pre-equilibrium regeime in heavy-ion collisions For an ideal quark-gluon plasma of massless partons, the equation of state is given by[17]

$$p = a(T)T^4 \tag{2.5}$$

and

$$\epsilon \simeq 3a(T)T^4 \tag{2.6}$$

$$s = \frac{\epsilon + p}{T} \simeq 4a(T)T^3 \tag{2.7}$$

and

$$n = b(T)T^3. \tag{2.8}$$

Here s is the entropy density, T is the temperature, n is the number density of the plasma and the quantities are given by

$$a(T) = \frac{\pi^2}{90}(16 + \frac{21}{2}n_f) \qquad (2.9)$$

$$b(T) = \frac{\zeta(3)}{\pi^2}(16 + 9n_f) \qquad (2.10)$$

with n_f being the number of flavours. It follows from the above equation of state together with Bjorken's scaling picture that the temperature of the plasma scales like $T(\tau) \propto \tau^{-1/3}$, energy density like $\epsilon(\tau) \propto \tau^{-4/3}$ and number density like $n(\tau) \propto \tau^{-1}$.

The major difficult task is the detailed study of the poorly understood pre-equilibrium stage of the collisions. Crudely speaking, this pre-equilibrium stage is the duration between the moment when the two nuclei just pass through each other to the actual establishment of an equilibrated quark-gluon plasma. While most of the earlier work refers to the equilibrium stage studied by employing the hydrodynamic evolution, it is necessary to study the pre-equilibrium stage for the above mentioned reasons. Indeed, without a proper study of the pre-equilibrium stage there are always uncertainties in the predictions of all the signatures in the ultra relativistic heavy-ion collisions (at RHIC and LHC). Any pre-equilibrium study also presupposes a production mechanism for QGP, and here, we study the pre-equilibrium evolution of quark-gluon plasma in ultra relativistic heavy-ion collisions (URHIC), within color flux-tube model. The color flux-tube model is a generalization of the familiar Lund string model widely used for e^+e^- and $p-p$ collisions[20]. A brief description of the model is given below.

2.2 Color Flux-tube model

In this model the two nuclei that undergo a central collision at RHIC and LHC are highly lorentz contracted as thin plates[21, 22] (The two nuclei in collision at RHIC and LHC travel almost at a speed that of light). These two lorentz contracted nuclei pass through each other and, in the process, acquire a non-zero color charge ($\langle Q \rangle = 0$, $\langle Q^2 \rangle \neq 0$), by exchanging soft gluons. So one may figuratively call such nuclei after collision as color capacitor plates between which a strong chromoelectric field is created. The nuclei which act as color capacitor plates produce a chromo-electric field between them[21, 22] The strength of the field which naturally depends on the strength of the color charge residing on the plates cannot be fixed from first principles. We can only fix that phenomenologically, say by identifying the field energy with the energy in the central region as estimated by Bjorken[2] This strong electric field creates $q\bar{q}$ and gluon pairs via the Schwinger mechanism which enforces the instability of the vacuum in the presence of an external field. The partons so produced. collide with each other and also get accelerated by the background field. The mutual collisions drive the system towards equilibrium with suitable modulation from the background acceleration Within this model a set of transport equations are solved to study production and equilibration of quark-gluon plasma in URHIC. A brief description of works done on this model is given below.

In the approach of Baym[18], the partons are assumed to be created soon after the two nuclei have collided with each other, and are further assumed to equilibrate almost instantaneously thereafter (with a very small collision time). This quark-gluon gas then proceeds to expand hydrodynamically. Subsequent work of Kajantie and Matsui[19], incorporated a dynamic particle production by introducing a source term via the Schwinger mechanism[23] in the Boltzmann equation, and they also studied the equilibration in the relaxation time approximation. On the

other hand, Bialas *et al*[24] generalized the Baym analysis by introducing the effect of the background field on the otherwise hydrodynamic flow. A self consistent study of the system was carried out by Banerjee *et al*[25] who combined the effect of both the background field and the collisions on the quark-antiquark system. Finally, by employing the same analysis as of Banerjee *et al*, Asakawa and Matsui[28] have studied the rate of dilepton production by $q\bar{q}$ annihilation. as a function of (proper) time. All the above analyses ignore the gluon component.

However some of the crucial features which have not been considered in these earlier studies remains to be justified. First of all in the analyses of Kajantie *et al*[19] and Banerjee *et al*[25], the source term acquires a time dependence by virtue of the time dependence that the electric field suffers because of the particle production. The production of particles is then strictly governed by a time dependent field, in which case a perturbative mechanism will take over from the non-perturbative Schwinger mechanism. Note that the latter holds only for a uniform constant field. All the previous studies employing the flux tube model employ the non-perturbative expression. 2) The source term is derived for QED processes and needs to be redone for QCD processes at hand. It is apparent that the QCD effect will show up most manifestly in the gluon production; there is no corresponding counterpart in QED. In other words it is necessary to obtain a source term for gluons. 3) It is well known from earlier studies of Yang-Mills equations that there are inequivalent gauge field configurations which yield the same field tensor[26], and hence the same energy momentum tensor. This feature which is again absent in the Maxwell case has to be taken into account in this study. Recall that the lattice studies at any given energy density implicitly sum over the contributions coming from all such inequivalent configurations[27]. 4) Finally, the inherent non-linearity and the local gauge invariance which characterize the Yang-Mills equations lead to an added complexity; the equations do not possess a unique solution, even after gauge fixing. and even if one considers only static configurations. Consequently, one

needs to scan, with some suitable weightage, all the solutions for the given initial conditions, and sum over all such configurations It is not clear if any procedure is known that allows an implementation of this requirement

We have attempted here to fill this gap partially within color flux-tube model by solving transport equations in an extended phase space

2.3   Transport equation in an extended phase space

In the study of production and equilibration of quark-gluon plasma in ultra relativistic heavy-ion collisions one needs to know the distribution of quarks and gluons, $f(x, p)$, in the usual phase space. The determination of all physical quantities in the experiments crucially depend on this distribution functions of quarks and gluons. At equilibrium the above distribution functions are the standard Fermi-Dirac distribution function for the quarks and anti-quarks and Bose-Einstein distribution function for gluons. In the non-equilibrium stage the time devlopement of the phase-space distributions $f_a(x, p)$ for the partons of species a $= q_f, \bar{q}_f$, g (f being the quark flavors) is described by the relativistic transport equation (Boltzmann equation):

$$\left[p_\mu \partial^\mu + F_{\mu\nu} p^\nu \partial_p^\mu \right] f_a(x, p) = C_a(x, p) + S_a(x, p) \qquad (2.11)$$

with some known initial condition of $f_a(x, p)$ at $t = t_0$, when the two nuclei begin to overlap at RHIC and·LHC. The first term in the left hand side of the above equation corresponds to the usual convective flow and the second term is the Lorentz force term. S and C on the right hand side correspond to the source term for parton production and collision term among the partons (described in chapter 3).

The above equation is written in the usual six dimensional phase space and does not carry any information on the time evolution of the color charge, which is a dynamical quantity for non-Abelian plasma. Thus, as such, these transport equations which are valid for an abelian plasma are not applicable to quark-gluon plasma. It is our purpose to emphasize and study a crucial feature of the quark-gluon phase. *viz*, the inherently non- Abelian nature of the plasma. (Note that all the earlier macroscopic approaches[18, 19, 24, 25, 28] are in the so called Abelian approximation). Put simply, the non-Abelian features are completely ignored in the space time evolution, and the Boltzmann equation describes the dynamics which is essentially that of a Maxwell fluid, be it in the source term or in the background field term. The approach of Geiger and Kapusta[17] does incorporate the non-Abelian features in their basic Feynman diagrams, but is neverthless incomplete in that the distribution function in its final form does not carry any color degee of freedom.

We will now set up the relevant equations with the color degree of freedom, following several works of Heinz[29]. In non-abelian theory the color charge is a continuously varying function of time. The precession of the color charge(Q^a) obeys Wong's equation[30]:

$$\frac{dQ^a}{d\tau} = f^{abc} u_\mu Q^b A^{c\mu} \tag{2.12}$$

which supplements the Lorentz force equation

$$\frac{dp^\mu}{d\tau} = Q^a F^{a\mu\nu} u_\nu. \tag{2.13}$$

Here $A^{a\mu}$ is the gauge potential, and f^{abc} is the structure constant of the gauge group. In order

to include the color charge in the phase-space, we consider an extended one particle phase space of dimension $d = 6 + (N^2 - 1)$ in SU(N) The extended phase space is taken to be the direct sum $R^6 \oplus G$, where G is the(compact) space corresopnding to the given gauge group In short, in addition to the usual 6 dimensional phase space of coordinates and momenta we now have another eight coordinates corresponding to the eight color charges in SU(3). In this extended phase space a typical transport equation reads as[31]:

$$\left[p_\mu \partial^\mu + Q^a F_{\mu\nu}^a p^\nu \partial_p^\mu + f^{abc} Q^a A_\mu^b p^\mu \partial_Q^c \right] f(x, p, Q) = C(x, p, Q) + S(x, p, Q) \qquad (2.14)$$

Here $f(x, p, Q)$ is the single particle distribution function in the extended phase space The above equation is gauge and Lorentz invariant[31]. The first term in the left hand side of equation (2.14) corresponds to the usual convective flow, the second term is the non-Abelian version of the Lorentz force term and the last term corresponds to the precession of the charge as described by Wong's equation. Note that, in general we have to write separate equations for quarks, antiquarks and gluons since they belong to different representations of the gauge group. For anti-quarks the distribution function $\bar{f}(x, p, Q)$ obeys a simillar equation, with Q^a replaced by $-Q^a$ (i.e. the second term in the above equation changes sign). These equations are closed with the Yang-Mills equation, given by

$$(D_\mu F^{\mu\nu})^a(x) = j^\nu(x) = g \int p^\nu Q^a [f_q(x, p, Q) - \bar{f}_q(x, p, Q) + f_g(x. p, Q)] dP dQ \qquad (2.15)$$

The integration measures in the above equation are

$$dP = 2\theta(p_0)\delta(p^2 - m^2)\frac{d^4 p}{(2\pi)^3} = \frac{d^3 p}{(2\pi)^3 p_0} \qquad (2.16)$$

$$dQ = \delta(Q^a Q^a - q^2)\delta(d_{abc} Q^a Q^b Q^c - \bar{q}^3)d^8 Q. \qquad (2.17)$$

Using these distribution functions we obtain the local number density and local energy density of the quark-gluon plasma by the equations

$$n(\tau) = \int dP dQ (p^\mu u_\mu)(f_q(x,p,Q) + \bar{f}_q(x,p,Q) + f_g(x,p,Q)) \qquad (2.18)$$

$$\epsilon(\tau) = \int dP dQ (p^\mu u_\mu)^2(f_q(x,p,Q) + \bar{f}_q(x,p,Q) + f_g(x,p,Q)) \qquad (2.19)$$

In the next chapter we shall consider the simplest of the non-Abelian group *viz* $SU(2)$ to highlight the dynamical role of the color degree of freedom. The realistic guage group $SU(3)$ applicable for QGP will be studied in detail in chapter 4 Both the chapters contain rather ad hoc adaptation of the Schwinger formola for $q\bar{q}$ and gg production that will be reconsidered in chapter six. A full study of the transport equation with the new source term is beyond the scope of this thesis That will be reported elsewhere.

Chapter 3

Solution of transport equations and evolution of $q\bar{q}$ plasma

3.1 Transport equations for q$\bar{q}$ plasma

In this chapter we discuss the production and the evolution of quark-antiquark plasma in URHIC by employing the Flux-tube Model[18, 19], in particular to obtain a time devlopment of the quark and antiquark distribution function. As mentioned earlier, in this model the two nuclei that undergo a central collision at ultra high energies are lorentz contracted as thin plates[21, 22]. These two lorentz contracted nuclei pass through each other and, in the process, acquire a non-zero color charge ($\langle Q \rangle = 0$, $\langle Q^2 \rangle \neq 0$), by exchanging soft gluons. So one may figuratively call such nuclei after collision as color capacitor plates between which a strong chromoelectric field

is created. This field creates $q\bar{q}$ and gluon pairs *via* the Schwinger mechanism which enforces the instability of the vacuum in the presence of an external electric field The partons so produced will collide with each other and also get accelerated by the parent background field. The mutual collisions drive the system towards equilibrium with suitable modulation from the background acceleration. In all the earlier studies (e g [19, 25]) a set of transport equations are solved within this model in the abelian approximation, *i.e.* the model was valid for an electromegnetic plasma. We now attempt to study the evolution of a non-Abelian plasma by solving transport equations which are written in an extended phase space of coordinate, momenta and color.

As mentioned eariler, for simplicity and also to get a feeling for how crucial is the non-abelian effect in the study of quark-gluon plasma can be, we shall study the gauge group SU(2). and consider only a $q\bar{q}$ plasma. We will solve the transport equations in SU(3) in the next chapter with gluons taken into consideration. For SU(2) charges that we are interested in. the non-Abelian extension of Eqn.(2.14) reads

$$\left[p_\mu \partial^\mu + Q^a F^a_{\mu\nu} p^\nu \partial^\mu_p + \epsilon^{abc} Q^a A^b_\mu p^\mu \partial^c_Q\right] f(x, p, Q) = C(x, p, Q) + S(x. p, Q). \qquad (3.1)$$

Note that we do not have to write a separate equation for anti-quarks since they belong to the same color representation as quarks. The quarks considered in this chapter does not possess any other quantum number such as the electric charge. In reality the situation is of course different. Indeed, the antipodal points on the sphere (corresponding to the color part of the phase-space with a fixed charge) represent the particle and anti-particle. Wong's equation (Eqn 2.12) may be recast in the more convenient form

$$\frac{d\vec{Q}}{d\tau} = u_\mu \vec{Q} \times \vec{A}^\mu \tag{3.2}$$

where the arrows now denote the direction in the color space. In the same notation, the transport equation obtains the form

$$\left[p^\mu \partial_\mu + \vec{Q} \cdot \vec{F}_{\mu\nu} p^\mu \partial_p^\nu + p^\mu \vec{Q} \times \vec{A}_\mu \cdot \frac{\partial}{\partial \vec{Q}} \right] f(x, p, \vec{Q}) = C(x, p, \vec{Q}) + S(x, p, \vec{Q}). \tag{3.3}$$

For the model at hand, let us take the 'plates' to be moving along the z-direction. Also we restrict to only that field configuration for which there exists a gauge choice such that the gauge potentials commute with each other every where. Keeping this in mind, we make the gauge choice where only the components $A^{\mu a} = (A^{03}, A^{33})$ are non-vanishing and the other components are zero. With this choice, the resulting electric field points in the '3' direction in the color space. We next require a boost invariant description[2] of the distribution functions as well as the other physical quantities which may be determined thereof, even as the system is evolving. We now proceed to impose the Lorentz gauge condition, which has to be done such that the chromoelectric field depends on the boost-invariant(along the axis of collision) quantity $\tau = (t^2 - z^2)^{1/2}$ Observing that the system is effectively (1+1) dimensional, in the t-z plane, we write

$$\vec{A}^\mu = \epsilon^{\mu\nu} \partial_\nu \vec{G}(\tau) \tag{3.4}$$

where the indices μ, ν take values 0, 3 and $\vec{G}$ is a Lorentz scalar function depending only on τ. The above choice automatically implements the Lorentz gauge condition $\partial_\mu \vec{A}^\mu = 0$. Clearly, the

chromoelectric field $\vec{E}$ is dependent only on τ, and is given by

$$\vec{E}(\tau) = \left[\frac{d^2}{d\tau^2} + (2/\tau)\frac{d}{d\tau} \right] \vec{G}(\tau) \tag{3.5}$$

(It will be seen below that all the derivation in this chapter is obtained in terms of E(τ), not G(τ). However this relation (Eqn. 3.5) is important (see chapter 6) when we use new source term (from τ dependent electric field) for particle production.)

The Wong equation (Eqn 3.2) guarantees the conservation of the magnitude of the vector charge $\vec{Q}$, which may now be held fixed. Being the analogue of the Larmor equation for a charged particle in an external magnetic field, it also conserves the component of the charge that is parallel to the background chromoelectric field. It is, therefore, convenient to resolve the SU(2) charge in the polar coordinates. Writing

$$Q_1 = Q sin\theta cos\phi; \quad Q_2 = Q sin\theta sin\phi; \quad Q_3 = Q cos\theta, \tag{3.6}$$

it is straight forward to verify that

$$\left(\vec{Q} \times \frac{\partial}{\partial \vec{Q}} \right)_3 = \frac{\partial}{\partial \phi} \tag{3.7}$$

The last equation will lead to considerable simpification in solving the transport equation.

Let us now consider the collision term. The color plate model can be looked upon as an effective version of a more complete microscopic theory describing the interactions of quarks and gluons. Hence, we employ the simple relaxation time hypothesis, with a phenomenological parameter

τ_c, the relaxation time, to be obtained from microscopic computations. It then follows that

$$C = \frac{-p^\mu u_\mu (f - f_{eq})}{\tau_c} \qquad (3.8)$$

where f_{eq} is the eqilibrium distribution function, with local (space time dependent) values of the thermodynamic quantities. While it has been customary to take f_{eq} to be one of an ideal gas, with some support from the parton cascade model (pcm) analysis of Geiger and Kapusta[17], recent lattice studies suggest that the quark-gluon phase is possibly a non-perturbative phase, being ideal only at $T \simeq 5T_c$. Since we are not dealing with a true system here, we shall conveniently take f_{eq} to be that of an ideal Fermi gas with a local temperature, evolving as a function of the proper time τ. Apart from space time dependence this distribution function carries color in its definition[32]. We thus have

$$f_{eq} = \frac{2}{\exp((p^\mu - A^\mu)u_\mu/T(\tau)) + 1}, \qquad (3.9)$$

where u^μ is the flow velocity,

$$u^\mu = (cosh\eta, 0, 0, sinh\eta). \qquad (3.10)$$

which is written in terms of the (space-time) rapidity $tanh\eta = z/t$.

It can be verified that with the above choice of the potential

$$A^\mu u_\mu = 0, \qquad (3.11)$$

and the above equation boils down to the familiar form

$$f_{eq} = \frac{2}{\exp(p^{\mu})u_{\mu}/T(\tau)) + 1}. \tag{3.12}$$

Now we demand the boost invariance following Bjorken's picture according to which the longitudinal boosts are the symmetry operations on the single particle distribution. The boost invariant parameters on which f can depend are, apart from the charge coordinates,

$$\tau = (t^2 - z^2)^{1/2}, \; \xi = (\eta - y), \; p_t = (p_0^2 - p_l^2)^{1/2} \tag{3.13}$$

where $y = \tanh^{-1}(p_l/p_0)$ is the momentum rapidity. It is convenient to write separate equations for quarks and anti-quarks, *a la* the Abelian case. If we therefore identify the quark states with the points on the upper hemisphere of the color sphere, and the antiquarks with the lower hemisphere, by a trivial relabeling, we may write two equations,

$$\left[\frac{\partial}{\partial\tau} - \left(\frac{\tanh\xi}{\tau} + \frac{g\cos\theta E(\tau)}{p_t\cosh\xi}\right)\frac{\partial}{\partial\xi} + g\frac{d}{d\tau}G(\tau)\tanh\xi\frac{\partial}{\partial\phi}\right] f(\tau,\xi,p_t,\theta,\dot\phi)$$
$$+\frac{f}{\tau_c} = \frac{f_{eq}}{\tau_c} + \frac{\Sigma(\tau,p_t,\xi,\theta)}{p_t\cosh\xi} \tag{3.14}$$

$$\left[\frac{\partial}{\partial\tau} - \left(\frac{\tanh\xi}{\tau} - \frac{g\cos\theta E(\tau)}{p_t\cosh\xi}\right)\frac{\partial}{\partial\xi} + g\frac{d}{d\tau}G(\tau)\tanh\xi\frac{\partial}{\partial\phi}\right] \bar{f}(\tau,\xi,p_t,\theta,\dot\phi)$$
$$+\frac{\bar{f}}{\tau_c} = \frac{f_{eq}}{\tau_c} + \frac{\Sigma(\tau,p_t,\xi,\theta)}{p_t\cosh\xi} \tag{3.15}$$

with the first of them for the quarks and the next for the anti-quarks. The angle variable θ varies from 0 to $\pi/2$ in both the equations.

Finally, Σ is the (non perturbative) Schwinger's expression for pair production and is given by

$$\Sigma(\tau,\xi,p_t.\theta) = -\frac{gE\cos\theta}{8\pi^3}\ln\left[1-\exp\left(-\frac{2\pi p_t^2}{gE\cos\theta}\right)\right](\frac{\alpha}{\pi})^{1/2}\exp(-\alpha\xi^2) \qquad (3.16)$$

where we have inserted the Gaussian dependence on ξ by hand. Note that the non-Abelian nature features dominantly *via* the $\cos\theta$ term This occurence plays an important role in the evolution of the system.

After having set up the relevant equations (not all yet since energy-momentum conservation is to be imposed), we observe that the above differential equation possesses the formal solution

$$f(\tau,\xi,p_t\theta,\phi) = \int_0^\tau d\tau'\exp(\frac{\tau'-\tau}{\tau_c})\left[\frac{\Sigma(\tau',\xi',p_t.\theta)}{p_t\cosh\xi'} + \frac{f_{eq}(\tau',\xi',p_t)}{\tau_c}\right] \qquad (3.17)$$

where $\xi(\tau')$ is given by

$$\xi' = \sinh^{-1}\left[\frac{\tau}{\tau'}\sinh\xi + \frac{g\cos\theta}{p_t\tau'}\int_{\tau'}^\tau d\tau''E(\tau'')\right] \qquad (3.18)$$

It is thus clear that f does not depend on $\dot\phi$, so the $\frac{\partial}{\partial\phi}$ term contributes nothing to the transport equation. However the θ dependence is still involved through out the formalism which shows the non-Abelian effects. The corresponding distribution $\bar{f}$ for antiquark can be written by just changing g to $-g$ in f as can be checked out easily

The transport equation has to be supplemented with the conservation constraint

$$\partial_\mu T^{\mu\nu}_{mat} + \partial_\mu T^{\mu\nu}_{YM} = 0, \tag{3 19}$$

since it is the field energy that is being pumped in order to produce the $q\bar{q}$ pairs More explicitly,

$$\partial_\mu T^{\mu\nu}_{mat} = -J^a_\mu F^{\mu\nu}_a \equiv -\partial_\mu T^{\mu\nu}_{YM} \tag{3.20}$$

with

$$T^{\mu\nu}_{mat} = \int p^\mu p^\nu (f + \bar{f}) d\Gamma d\Omega_Q \tag{3.21}$$

where the measures $d\Omega_Q = \sin\theta d\theta d\phi$, $d\Gamma = \frac{\gamma d^3 p}{(2\pi)^3 p_0} = \frac{\gamma p_t dp_t d\xi}{(2\pi)^2}$ and $J^\mu_a = \int p^\mu Q_a (f - \bar{f}) d\Gamma d\Omega_Q$. Here we have taken the value of the degeneracy factor $\gamma = 2$ corresponding to two flavours. Since energy and momentum are conserved in each collision, the moment of the sum of the collision term vanishes.

$$\int p^\nu (C) d\Gamma d\Omega_Q = 0 \tag{3.22}$$

Now taking the first moments of the Boltzmann equation and integrating over the color degrees of freedom for f and $\bar{f}$ and making use of the conservation of energy and momentum, we obtain

$$\partial_\mu T^{\mu\nu}_f + gE(\tau) \int d\Gamma d\Omega_Q p^\nu \frac{\partial (f - \bar{f})}{\partial \xi} + 2 \int d\Gamma d\Omega_Q S = 0 \tag{3.23}$$

where

$$T_f^{\mu\nu} = \mathrm{diag}(E^2/2, E^2/2, E^2/2, -E^2/2) \tag{3 24}$$

is the energy momentum tensor for the field We may solve for the electric field by employing the same procedure as in[25], and by employing the symmetry $\bar{f}(\tau, \xi. p_T, \theta) = f(\tau, -\xi, p_T, \theta)$. We thus obtain the equation governing the decay of the source field to be

$$\frac{dE(\tau)}{d\tau} - \frac{2g\gamma}{2\pi} \int_0^\infty dp_t p_t^2 \int_0^\infty d\xi \sinh\xi \int_0^{\pi/2} d\theta \sin\theta[f - \bar{f}] + \frac{4\pi}{7}\bar{a}|E(\tau)|^{3/2} = 0 \tag{3.25}$$

where $\bar{a} = a\zeta(5/2)\exp(0.25/\alpha)$, $a = c(g/2)^{5/2}\frac{\gamma}{(2\pi)^3}$ and $c = \frac{1}{(4\pi^3)}$. Finally, $\zeta(5/2) = 1.342$ is the Reimann zeta function.

Equations (3.25) and (3 17) are as yet underdetermined since the local temperature $T(\tau)$ is free. In order to fix the form of $T(\tau)$, we appeal to the relaxation time approach that we are employing, and assume that the the particle energy density differs negligibly from the equilibrium energy density. We may then relate, by an ansatz, the proper energy density which is defined by

$$\epsilon(\tau) = \int d\Gamma d\Omega_Q (p^\mu u_\mu)^2 (f + \bar{f}) \tag{3.26}$$

to the temperature by its equilibrium value, whence,

$$T(\tau) = \left(\frac{15}{(7\gamma\pi^3)}\epsilon(\tau)\right)^{1/4}. \tag{3 27}$$

It may be mentioned that the weaker condition of energy-momentum conservation that we have employed here , in fact. satisfies the Yang-Mills equations $D_\mu \vec{F}^{\mu,\nu} = \bar{j}^\nu$ as well.

Finally, we pause briefly to discuss the effects of hard thermal loops that have been emphasized recently[33]. They have been derived from the classical transport equation as well by Kelly et al[34, 35] The latter derivation, which is important for us here, is based on an analysis of the Vlasov equation which properly describes the expansion of an already equilibrated gas, in a back-ground field but with with no source or sink. It is, therefore, necessary to determine whether the more complete transport equation such as the one that we have here will have any effect on the results of Ref.[34, 35] Conversely, it is also necessary to determine how the hard thermal loops will affect the purely classical results that will be obtained here. Let us recall that the derivation of Kelly et al[34, 35] consists of a systematic expansion of the distribution function as well as the background field term in powers of the coupling constant. The zeroth order term is merely the Fermi-Dirac term for the quarks. Since we are solving here the approach to the equlibrium, there is necessarily a dependence of the distribution functions and other physical quantities on g. It remains to disentangle the contribution coming from the hard thermal loops Indeed, observe that the two extra terms that we have at hand here are of higher order in g. First of all, the source term is non-analytic and does not even admit an expansion in powers of g The other collision term is easily seen to be of order g^4 or higher. We thus conclude that the conclusions of Ref.[34, 35] remain unaffected, and we may take over those results in toto, supplementing our classical results

3.2   Computational Procedure

We have adopted here a double-self consistent method to determine $(f, \epsilon, ...)$,following the work of Banerjee et al[25] in the Abelian case. The procedure follows the scheme $\{T(\tau)_{trial}, E(\tau)_{trial}\} \rightarrow$

$\{f, \bar{f} \; E(\tau)\} \;\rightarrow\; \{f, \bar{f}\} \;\rightarrow\; T(\tau) \;\rightarrow\; ...$ by repeated use of equations (3.17), (3.25), (3.17), (3.27). The iteration terminates as soon as a convergence is established in the solutions for $E(\tau), T(\tau)$ All the desired quantities are thereby consistently determined. The same procedure will be employed subsequently.

3.3   Results and discussions

Before we proceed to present and discuss the results, a few comments about the choice of the value of the parameters in the computation We put $g = 4$ throughout our calculations. Since lattice computation results predict a phase transition from the baryonic phase to the quark-gluon phase at densities $\sim 5 - 10 \, GeV/fm^3$, it has also been customary to take an initial energy density in the same range in the Flux tube model. However, greater care needs to be taken before the initial energy densities in URHIC are chosen. Indeed, a fairly reliable estimate of the time required for the partons to be produced in central collisions after the two nuclei have suffered the maximum overlap is $\sim 0.05 - 0.1 \, fm$; a simple dimensional analysis leads to a value of the initial energy density to be $(1/2)E_0^2 \approx 500 - 1000 \, GeV/fm^3$, the precise value depending on the the magnitude of g in $\sqrt{gE} = \frac{1}{\tau_0}$ Since in the color plate model, we set the zero of time not at maximum overlap, but at the instant when the plates have completely crossed each other, we shall take the initial energy density $\epsilon = 300 GeV/fm^3$. We shall also be guided by the results of Geiger and Kapusta[17] in our choice of the values of τ_c, and take $\tau_c = 0.2 fm$, to be a realistic value[17]. The scale for the hydrodynamic limit will be set by the choice for τ_c as well as the formation time τ_0. A typical value for the analysis at hand is 0.001 fm, which we employ here. Finally, we study the other extreme case, the collisionless limit, by the choice $\tau_c = 5 fm$.

It is instructive to compare how the realistic regime behaves in relation to the results that we obtain for the two extreme limits.

We have studied the decay of the chromoelectric field, the evolution of the particle energy and number densities, the evolution of the distribution function and its approach to the equilibrium state We have compared them with the corresponding Abelian results. In addition, we have also evaluated a quintessentially non-Abelian quantity, viz, the expectation value of the angle that the quark charge makes with the direction of the chromoelectric field. In the current model the chromoelectric field not only decays to produce the $q\bar{q}$ pairs, but is itself built up by the receding nuclei which act as color plates. We have, therefore, also studied the particle energy per unit transverse area as a function of ordinary time to highlight this feature.

3.3.1   Discussion of the results

We shall present the results of our analysis in the three regimes corresponding to the hydrodynamic, the realistic, and the collisionless cases. Comparison between the Abelian and the non-Abelian systems will be taken up subsequently.

Consider the hydrodynamic limit first. The physical quantity of utmost importance is the chromoelectric field, whose dynamics is most readily determined in the Flux tube model at hand Indeed, apart from determining the production and the acceleration of the partons in the Flux tube model at hand, it has an additional role which has been emphasized by Svetitsky[36]: the charms which are produced in the pre-equilibrium stage would not only interact with the gas of light quarks and gluons, before either forming a J/ψ or an open charm mesonic state, but will also be influenced by the background field. Thus the study of the evolution of the mean electric

field in the pre-equilibrium stage acquires an added importance. It is a merit of the Flux tube model that we can readily determine the evolution of the background electric field. Note that in contrast, no such information can be extracted in the more microscopic models such as parton cascade model (PCM)[17] and heavy-ion jet interaction generator (HIJING)[37]. In Fig 3 1 the decay of the field is shown Recall that $\tau_c = .001fm$ As can be seen from Fig 3.1, the electric field has hardly decayed at all, with a percentage decay less than 2 %, even at $\tau = 1 5fm$. The corresponding particle energy density, shown in Fig. 3.2 is also negligibly small, with the

Figure 3.1: Decay of the chromoelectric field as a function of proper time (in units of fermi), for $\tau_c = .001fm$ The solid line refers to the non-Abelian case, and the broken line to the Abelian case.

ratio with respect to the initial energy density being $\sim 10^{-5}$. The Abelian situation is an order of magnitude better, but is still hopelessly small. And indeed, the number density is also very small, and as shown in Fig. 3.3 gets saturated at $\sim .05/fm^3$ and the temperature also stabilizes to a value $\sim 40MeV$, which is much less than the temperatures required. Clearly, it is very unlikely that the plasma does not go through a prequilibrium phase.

The behaviour of the system for $\tau_c = 0.2$ and $5fm$ is in sharp contrast to the case discussed
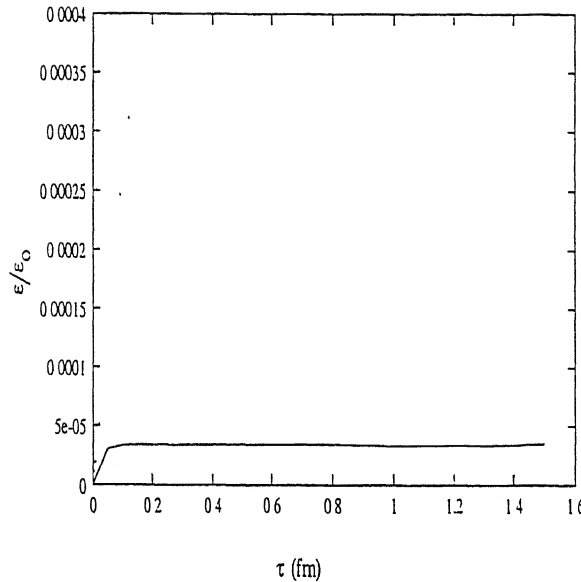
Figure 3.2: The particle energy density scaled w.r.t the initial field energy density as a function of proper time (in units of fermi), for $\tau_c = 001 fm$. The solid line refers to the non-Abelian case, and the broken line to the Abelian case.

above There is a significant decay of the electric field, which is shown in Figs. 3.4 and 3.5 for the two respective values of τ_c. The electric field decays by about 15% of the original value, at $\tau = 1 5 fm$. The corresponding energy densities are also not very different, and yield $\sim 10 - 15\%$ of the initial field energy density (see Figs. 3.6 and 3.7). The corresponding temperatures are $\sim 300 MeV$, which is quite realistic. Note that the parton cascade model[17] predicts a value about 300 MeV at $2.4 fm$. The real difference between the collisionless case and the "realistic" case is in the number density. Indeed as Figs. 3.8 and 3.9 show, the plasma produced for $\tau_c = 0.2 fm$ has a number density $\sim 15 - 20/fm^3$, the corresponding number for $\tau_c = 5 fm$ is three to four times smaller. In other words, the system is more dense in the former case than the latter. Clearly, this distinction should show up in signatures such as dilepton production which are sensitive to both the number as well as the energy density.

It thus follows that the flux tube model, with the incorpration of the color degrees of freedom, definitely rules out instantaneous equilibration as envisaged in the approach of Baym[18];

Figure 3.3: The particle number density as a function of proper time (in units of fermi), for $\tau_c = .001 fm$. The solid line refers to the non-Abelian case, and the broken line to the Abelian case.

further, it also distinguishes the collisionless limit from realistic values of equilibration time.

Finally, it should be emphasized that the flux tube model as employed here not only pumps in the field energy to particle production. but also contributes to the field energy by virtue of the recession of the color charged nuclei from each other. In fact, a crude estimate of the time required to convert all the plate energy to the field energy turns out to be $\sim 5fm$ for $200 GeV/$nucleon In any case, it is therefore misleading to interpret the ratios we have shown in Figs. 3.2,3.6 and 3.7 as the fraction of the total field energy that has gone into the particles. To emphasize this, we have evaluated the dependence of the field and particle energies per unit area by integrating over the contribution along the longitudinal direction. The results are shown in Fig. 3.10, from which it is clear that there is a lot more energy in the field than in the particles. For the same reason, it is also misleading to interpret the field energy density at $\tau = 0$ as the counterpart of the energy densities employed in lattice computations to study the transition from the hadronc to the QGP phase.
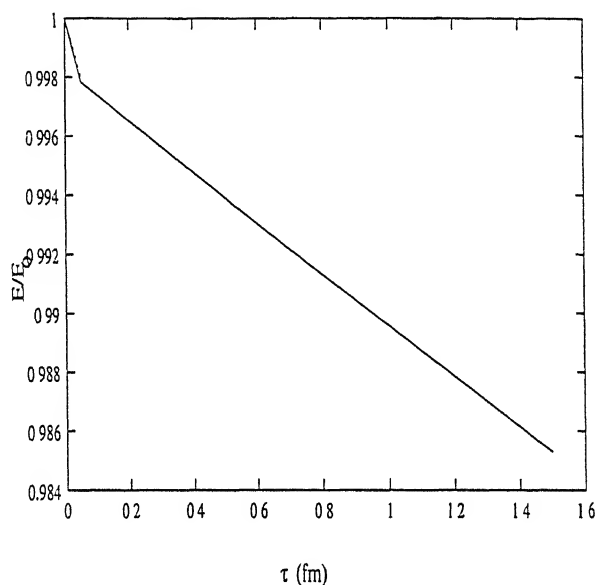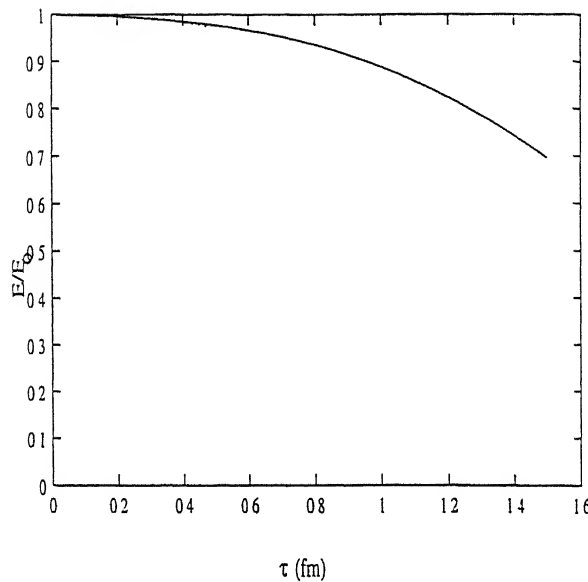
Figure 3.4: Decay of the chromoelectric field as a function of proper time (in units of fermi), for $\tau_c = 2fm$. The solid line refers to the non-Abelian case, and the broken line to the Abelian case.

3.3.2 Comparison with Abelian results

It is clear from Figs. 3.1-3.9 that the Abelian and the non-Abelian results bear little resemblence, belying the expectation that the "Abelian dominance" holds in this case The difference is most dramatically highlighted at $\tau_c = 0\,2fm$. Whereas almost all the initial field has decayed in the Abelian case, only 30% has done so in the non-Abelian case. Accordingly, The particle energy density is larger by a factor of ~ 5 , the number density by a factor of ~ 4, and yields an abnormally large value of $\sim 800MeV$ for the temperature. Earlier Abelian calculations[19, 25, 28] yielded reasonable values for the temperature because of unrealistic values for the initial field energy It is a universal feature that the non-Abelian plasma is rarer and cooler than its Abelian counterpart. In the hydrodynamic limit, the Abelian ananlysis yields a temperature $\sim 200MeV$, in contrast to $\sim 40MeV$ in the non-Abelian case. Thus the incorporation of the color degree of freedom rules out instantaneous hydrodynamic evolution. Of course, a colorless plasma does not have reasonable temperature for any other τ_c.
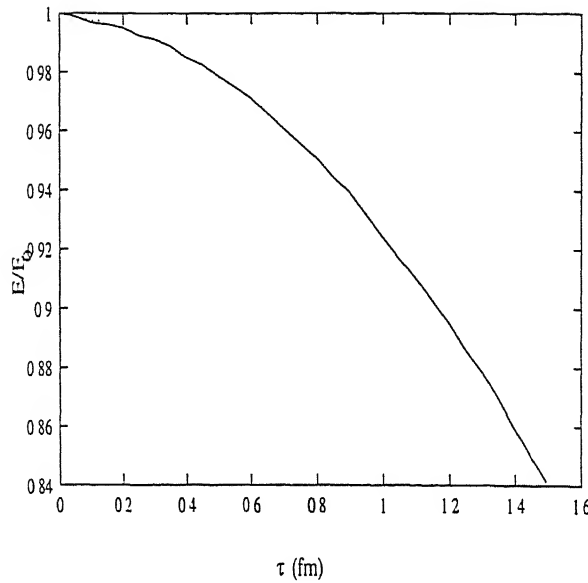
Figure 3.5: Decay of the chromoelectric field as a function of proper time (in units of fermi), for $\tau_c = 5fm$. The solid line refers to the non-Abelian case, and the broken line to the Abelian case.

Yet another interesting aspect that emerges from our studies is in the close interplay between the value of τ_c and the color degree of freedom While the field decays faster in the non-Abelian case in the hydrodynamic limit, the trend reverses at $\tau_c = 0.2fm$ and gets restored in the collisionless limit. In contrast, the particle energy density is smaller for a colored plasma in hydrodynamic limit. Further, it continues to be so at $\tau_c = 0.2fm$ but becomes larger than the Abelian case in the collisionless limit. These non-trivial manifestations of the color charge may be expected to have an important bearing on the other bulk properties of the plasma.

In order to gain some insight into the above features, we have also evaluated the expectation value of $\Theta \equiv < cos^2\theta >$ which yields the rms value that the particle charge makes with the field direction in the color space. Note that the above quantity is gauge invariant, and hence physical. Fig. 3.11 shows $\Theta(\tau)$ for $\tau_c = 0.2fm$. It may be seen that the value saturates around 0.25, corresponding to $\theta \sim \pi/3$. The corresponding value in the non-Abelian case is strictly zero. The effect of the background field is thus reduced, leading to dominance of the collision

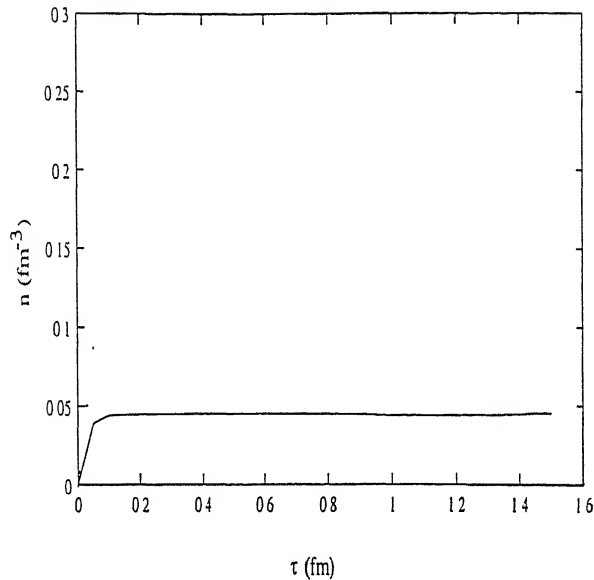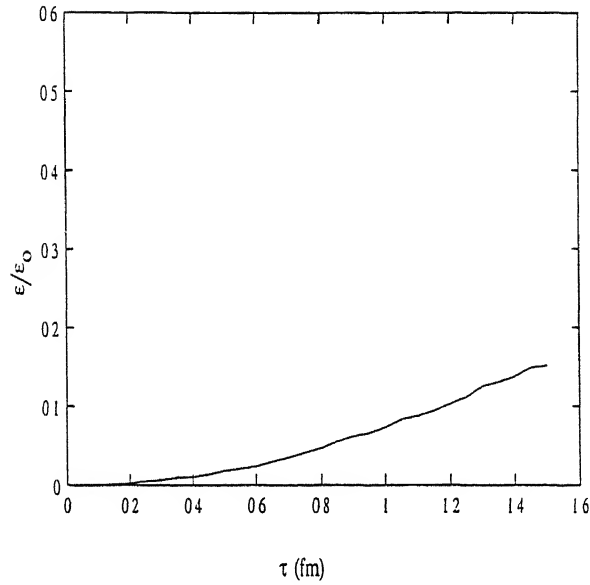Figure 3 6: The particle energy density scaled w.r.t the initial field energy density as a function of proper time (in units of fermi), for $\tau_c = 2fm$. The solid line refers to the non-Abelian case, and the broken line to the Abelian case.
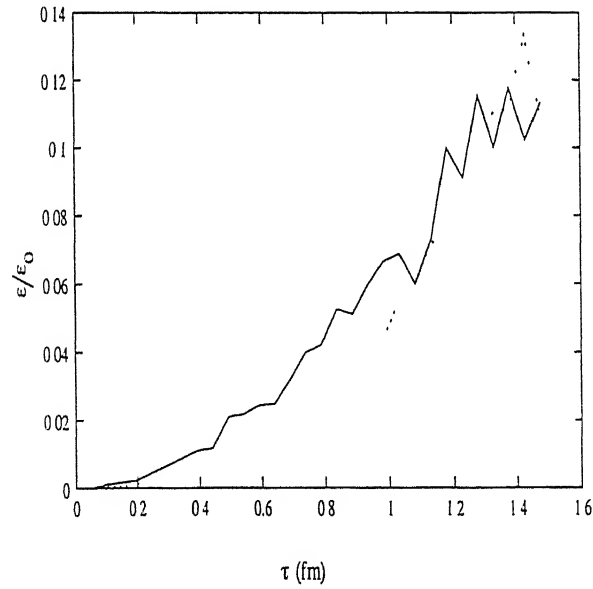
Figure 3.7: The particle energy density scaled w r.t the initial field energy density as a function of proper time (in units of fermi), for $\tau_c = 5fm$. The solid line refers to the non-Abelian case, and the broken line to the Abelian case.
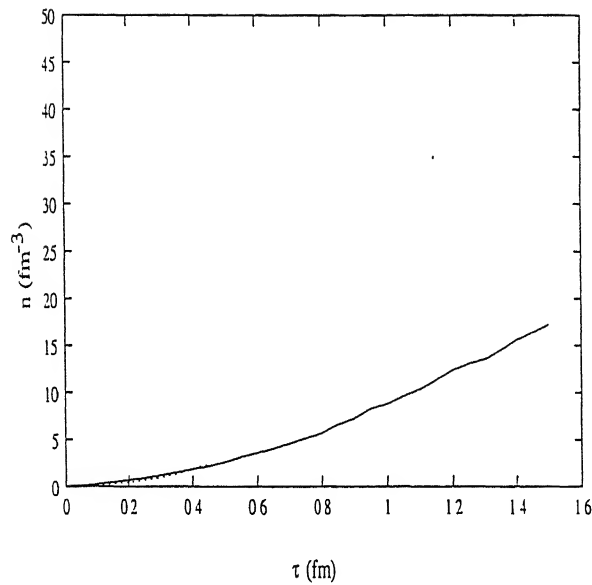
Figure 3.8: The particle number density as a function of proper time (in units of fermi), for $\tau_c = 2fm$. The solid line refers to the non-Abelian case, and the broken line to the Abelian case.
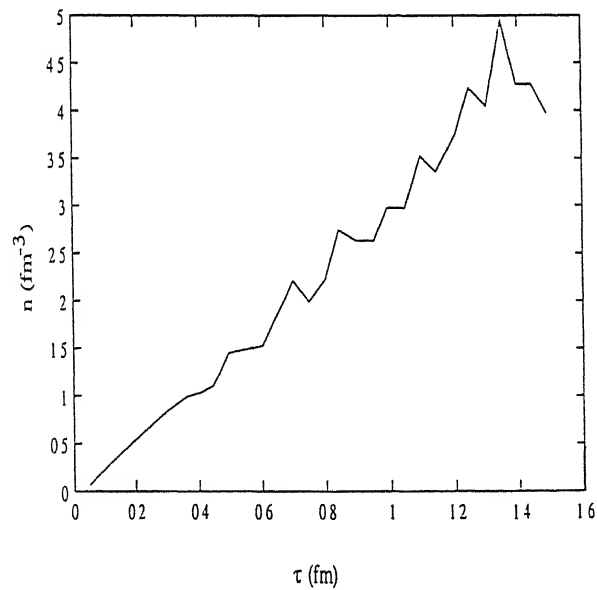
Figure 3.9: The particle number density as a function of proper time (in units of fermi), for $\tau_c = 5fm$. The solid line refers to the non-Abelian case, and the broken line to the Abelian case.
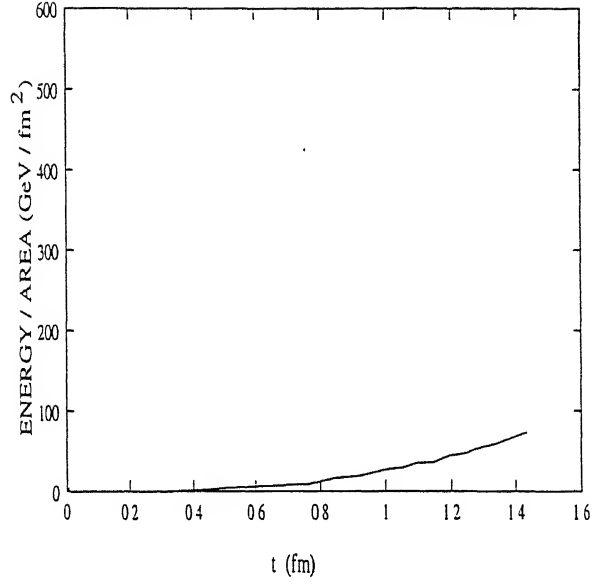
Figure 3.10: The particle energy/unit transverse area (solid line) and the field energy/unit transverse area (dashed line) as a function of time (in fermi). The energy densities are in GeV/fm^2 and $\tau_c = .2fm$.
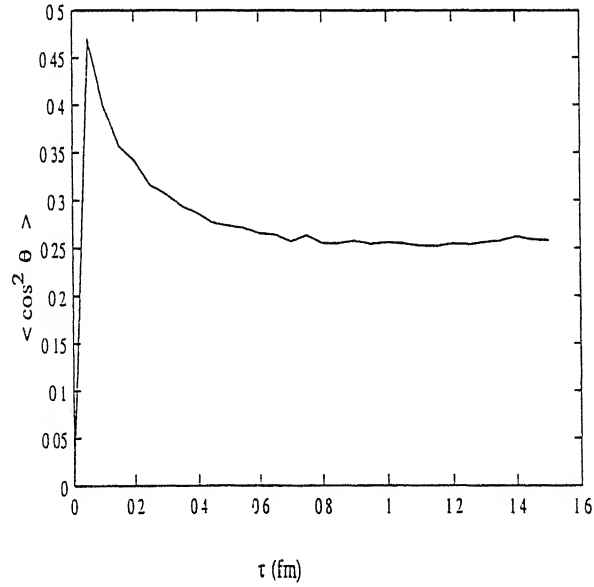
Figure 3.11: $<cos^2\theta>$ as a function of proper time (in fermi) at $\tau_c = .2fm$.

term in the expansion of the particles. Indeed, it shows up most clearly in the approach to the equilibrium, where one now expects that the plasma equilibrates the fastest in the direction normal to that of the field (in the color space). This is corroborated as may be seen in Fig. 3.12
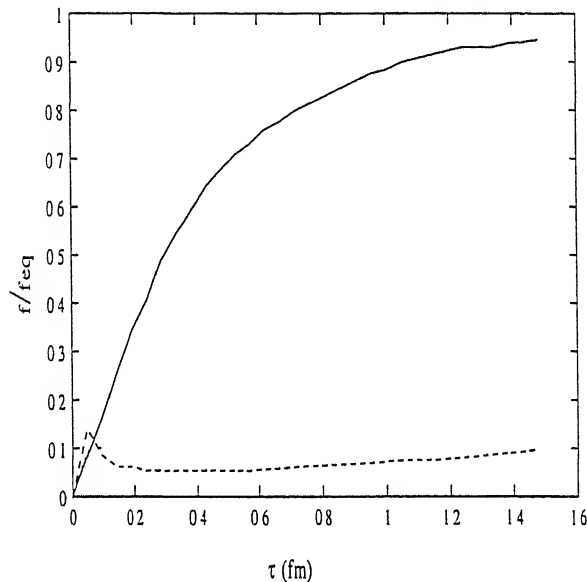
Figure 3.12: f/f_{eq} as a function of proper time at $p_t = 200 MeV$, $\xi = 0$ and $\tau_c = 0.2 fm$ for three different angles corresponding to $cos\theta = 0$ (solid line), $cos\theta = .25$ (dash line just below the solid line), and $cos\theta = 1$ (the other dash line). Note that the equilibration is fastest at $\theta = \pi/2$.

3.4   CONCLUSION

To conclude, we have studied the production and the equilibration of a genuinely non-Abelian plasma with the color degree of freedom incorporated in both the source and the background field term in the transport equation. In the $SU(2)$ gauge theory that we have considered here, the distribution function is defined in the extended phase space. We find that this approach recaptures in an elegant manner many of the findings of the more microscopic parton cascade

model. It has the further advantage that it indeed exhibits the color degree of freedom manifestly, and allows us to compute various gauge invariant quantities Significantly, we also find that the Abelian approximation. employed hitherto in most studies of equilibration of QGP is rather too drastic to be used for any quantitative analysis and comparison with the experiments The study also almost rules out instantaneous equilibration, and also strongly suggests that the collisionless limit may also not be the favoured in URHIC.

To be sure, we have not made any comparison with the experimental findings here, for the simple reason that we are as yet dealing with a simpler gauge group , and ignored the gluonic component altogether. The indications from the present study are unmistakable, though. Indeed. the particle production is enhanced because of increase in the phase space available, and for the same reason the plasma will be cooler than the Abelian counterpart. The energy goes to the color degree of freedom. and does not simply heat the system as it would happen in a colorless plasma. If we consider the realistic $SU(3)$ case, this feature will get further accentuated: For the same initial configuration, we may expect a rarer and a cooler plasma. Of course. there are other features which are intrinsic to $SU(3)$: there is yet another Casimir invariant, and the gluon term will also have to be incorporated. They will be considered in the next chapter.

Chapter 4

Solution of transport equations and evolution of quark-gluon plasma

---

4.1 Transport equations for quark-gluon plasma

In the last chapter we have studied the evolution of a non-abelian $q\bar{q}$ plasma within the color flux-tube model where it was shown that the non-abelian features have a major role in the evolution of the system in a manner that was not captured in any of the earlier studies[18, 19, 25]. It was pointed out that it was unlikely that the system would equilibrate instantaneously. However, for simplicity, we had ignored the gluonic component and considered the simpler gauge group SU(2). In this chapter, we remedy both the drawbacks; we consider the gauge group SU(3) as is appropriate for a real plasma. We also include the gluons, which have been completely

41

ignored so far We pay attention to the detailed evolution, and its prediction for different bulk properties of the plasma in this chapter. Signatures such as dilepton production within this model will be studied in the next chapter.

There are models such as HIJING[37] and PCM[38] which study the pre-equlibrium dynamics via perturbative QCD (pQCD). The production and the evolution of hard and semi-hard partons are studied by a master rate equation in HIJING and by a transport equation in PCM. While they may be reliable in the study of hard partons, these perturbative approaches are admittedly insufficient to study the dynamics of the soft partons[37], in particular, their production. Being perturbative, they do not incorporate any of the non-perturbative aspects such as the formation of the strings and their break up, which is studied even in pp collisions. The addition of soft partons to hard and semi- hard partons changes the bulk properties of plasma, such as temperature and energy density. Xu $et\ al.$[10] have observed that this addition leads to an enhanced suppression of J/ψ, which can be understood to be a consequence of increased number density and a lowered temperature of QGP. In our study, we employ the Schwinger mechanism[23] for particle production, which is quintessentially non-perturbative. Even if one were to employ a perturbative version, as a time dependent electric field would require[39], which we shall propose in chapter six, it may be noted that an initial electric field as a classical saddle point owes its existence to non-perturbative processes, viz, the soft gluon exchanges that take place between the two nuclei. On the whole, one may expect that the pQCD based studies[37, 38] will be useful in the hard regime, and that the flux tube like models will be required to study the soft regime which will become increasingly prominent as the system expands and more and more secondaries are produced[40]. Indeed, it should be possible to develop a unified approach to study the hard and the soft components, say $a\ la$ the approach of Eskola and Gyulassy[41] who have included the minijets in their so called chromoviscous hydrodynamics which is again based

on the flux tube model. This needs a separate study.

For our purpose here. the transport equations we solve in the SU(3) gauge group to describe the evolution of quarks and gluons (see chapter 2 for a detail description) are:

$$\left[p_\mu \partial^\mu + Q^a F^a_{\mu\nu} p^\nu \partial^\mu_p + f^{abc} Q^a A^b_\mu p^\mu \partial^c_Q\right] f(x,p,Q) = C(x,p,Q) + S(x,p,Q). \qquad (4.1)$$

Here $f(x,p,Q)$ is the single particle distribution function in the extended phase space of dimension 14 which include eight color coordinates in SU(3) gauge group in addition to the usual six dimensional phase space of coordinates and momenta. The first term in the left hand side of the above equation corresponds to the usual convective flow, the second term is the non-abelian version of the Lorentz force term and the last term corresponds to the precession of the charge as described by Wong's equation. S and C on the right hand side of the above equation correspond to the source and collision terms respectively.

Note that we have to write separate equations for quarks, antiquarks and gluons since they belong to different representations of $SU(3)$.

The term gluonic source merits some explanation here. The classical background field that we consider here has, in contrast to the Maxwell field, self interaction. We are interested in the stability of the gluonic vacuum (which is the analogue of the photon vacuum in eletrodynamics) against the fluctuations in the classical background field. An adaptation of the Schwinger mechanism in QED shows that the fluctuations can indeed produce the gluons, *i.e.* the off-shell classical field can spontaneously produce the on-shell radiative gluonic field (see Eqn 4.7). There is, therefore, no ambiguity or double counting in this process. The source term yields asymptotic gluonic states, and further interaction between the gluons is treated separately by a collision

term.

It is very difficult to solve the transport equation written above, in general. And we have a set of three coupled equations here As was done in the earlier chapter we make a few assumptions. First of all, we admit only those potentials which can be brought to a form where the only surviving components are $A^{\mu a} = (A^{01}, A^{31})$. This choice restricts $F^{\mu\nu}$ to be "Maxwell" like, also pointing in the "1" direction in the color space. This restriction is not entirely arbitrary as it is known[42] that the non-Maxwellian configurations - where the charges, the gauge potential and the fields do not lie in the same direction in the group space - do not produce particle pairs, in general. Secondly, we require a boost invariant description of the physical quantities[2]. Accordingly, we demand that the distribution functions also be functions of only boost invariant quantities. Finally, we work within the Lorentz gauge which is implemented elegantly by the choice $A^{\mu a} = \epsilon^{\mu\nu}\partial_\nu G^a(\tau)$, μ, $\nu = 0, 3$, with all the other components zero. $\tau = (t^2 - z^2)^{1/2}$ is the boost invariant proper time.

Now we fix the magnitude of the vector charge Q^a, which corresponds to the first Casimir invariant of SU(3). It is simply the value of the coupling constant. There is also another Casimir invariant, viz. $d^{abc}Q^aQ^bQ^c$, which is also conserved as the QGP evolves. There is, however, no way of fixing its value and the experiments presumably impose no restriction on its allowed values. In fact. the same holds for lattice analyses as well. For this reason, we do not take cognizance of this invariant, and we conveniently resolve the SU(3) charges in the polar coordinates: $Q_i = Q \prod_{k=1}^{i-1} sin\theta_k cos\theta_i$ for $i \neq 8$, and $Q_8 = Q \prod_{k=1}^{7} sin\theta_k$.

As is studied by Heiselberg and Wang[43] a collision term can indeed be obtained from pQCD. Apart from making the equation hopelessly non-linear, this approach would be good only for the hard components. which are not of interest to us here. As aptly pointed by Hung and

Shuryak[44] recently, a microscopic description of collisions gets increasingly cumbersome and also unnecessary as more and more secondaries are produced. On the other hand it is admittedly true that there is no way to reliably obtain a collision term in the non-perturbative regime. So we shall employ a relaxation time approach here, where the relaxation time τ_c will have to be fixed phenomenologically, and in all probability, *a posteriori*. In reference[43] it is proposed that τ_c can be local and have a (weak) dependence on τ. We take τ_c to be constant here. and further refinements may be incorporated after we have a better understanding of the transport phenomena both experimentally and theoretically.

Within the relaxation approach, the collision term is written as

$$C = \frac{-p^\mu u_\mu (f - f^{eq})}{\tau_c}. \tag{4.2}$$

Here f^{eq} is the distribution function, in local equilibrium. Note that the locality can extend to the color space as well apart from space-time. Taking it to be an ideal gas, for simplicity, we write,

$$f^{eq}_{q,g} = \frac{2}{\exp((p^\mu - Q^a A^{\mu a})u_\mu / T(\tau)) \pm 1} \tag{4.3}$$

where the +(-) sign is to be taken for fermions (bosons). Note that we allow a common equilibrium temperature for quarks and gluons. Here $u^\mu = (cosh\eta, 0, 0, sinh\eta)$ is the flow velocity and η is the space time rapidity given by $tanh\eta = z/t$. With our choice of potentials, it follows that $A^\mu u_\mu = 0$, so that the equilibrium distribution function can be written as:

$$f^{eq}_{q,g} = \frac{2}{\exp((p^\mu u_\mu)/T(\tau)) \pm 1} \tag{4.4}$$

Note also that the temperature depends only on the proper time, in accordance with the Bjorken picture. Demanding the same of the distribution functions as well, we require that the longitudinal boosts be symmetry operations on the single particle distribution. As mentioned earlier

the boost-invariant parameters are, apart from the color charges,

$$\tau = (t^2 - z^2)^{1/2}, \; \xi = (\eta - y), \; p_t = (p_0^2 - p_l^2)^{1/2} \tag{4.5}$$

where $y = \tanh^{-1}(p_l/p_0)$ is the momentum rapidity.

The above set of invariant variables also serve to express the source terms for $q\bar{q}$ and gluon pairs which will be obtained by the Schwinger mechanism. The expression for $q\bar{q}$ production (obtained from constant electric field) is given by[45, 46]

$$S_q(\tau, \xi, p_t, \theta_1) = -\frac{gE \cos\theta_1}{8\pi^3} \ln\left[1 - \exp\left(-\frac{2\pi p_t^2}{gE \cos\theta_1}\right)\right] (\frac{\alpha}{\pi})^{1/2} \exp(-\alpha\xi^2) \tag{4.6}$$

and for gluon pair production the corresponding term in SU(3) is given by the relatively stronger term[31, 47]

$$S_g(\tau, \xi, p_t, \theta_1) = (3/2)S_q(\tau, \xi, p_t, \theta_1). \tag{4.7}$$

We take $g = 4$ throughout our calculation.

Now consider the third term $f^{abc}A^{\mu a}Q^b \frac{\partial}{\partial Q^c} f(x, p, Q)$, in the transport equation (4.1). Due to the restriction of the gauge potentials to the form $A^{\mu a} = (A^{01}, A^{31})$, there is an additional simplification in the transport equation. In order to see that, note that equation (4.1) has the formal solution

$$f_{q,g}(\tau, \xi, p_t, Q) = \int_0^\tau d\tau' \exp(\frac{\tau' - \tau}{\tau_c}) \left[\frac{S_{q,g}(\tau', \xi', p_t, Q)}{p_t \cosh\xi'} + \frac{f_{q,g}^{eq}(\tau', \xi', p_t, Q)}{\tau_c}\right], \tag{4.8}$$

where $\xi'(\tau')$ is given by

$$\xi' = \sinh^{-1}\left[\frac{\tau}{\tau'}\sinh\xi + \frac{g \cos\theta_1}{p_t \tau'}\int_{\tau'}^\tau d\tau'' E(\tau'')\right]. \tag{4.9}$$

Clearly, $f^{1bc} A^1 Q^b \frac{\partial}{\partial Q^c} f(x,p,Q) = 0$, as S, f_{eq} and ξ' only depend on Q_1

With this final simplification, we get a set of three equations, one each for quark, antiquark and gluon respectively. They are, explicitly,

$$
\left[\frac{\partial}{\partial \tau} - \left(\frac{\tanh \xi}{\tau} + \frac{g \cos \theta_1 E(\tau)}{p_t \cosh \xi} \right) \frac{\partial}{\partial \xi} \right] f_{q,g}(\tau, \xi, p_t, \theta_1)
$$
$$
+ \frac{f_{q,g}}{\tau_c} = \frac{f_{q,g}^{eq}}{\tau_c} + \frac{S_{q,g}(\tau, p_t, \xi, \theta_1)}{p_t \cosh \xi} \tag{4.10}
$$

for quarks and gluons, and

$$
\left[\frac{\partial}{\partial \tau} - \left(\frac{\tanh \xi}{\tau} - \frac{g \cos \theta_1 E(\tau)}{p_t \cosh \xi} \right) \frac{\partial}{\partial \xi} \right] \bar{f}_q(\tau, \xi, p_t, \theta_1)
$$
$$
+ \frac{\bar{f}_q}{\tau_c} = \frac{f_q^{eq}}{\tau_c} + \frac{S_q(\tau, p_t, \xi, \theta_1)}{p_t \cosh \xi} \tag{4.11}
$$

for antiquarks.

In the process where the field and the particles are present the conservation of energy-momentum is expressed in the form:

$$
\partial_\mu T_{mat}^{\mu\nu} + \partial_\mu T_f^{\mu\nu} = 0, \tag{4.12}
$$

where

$$
T_{mat}^{\mu\nu} = \int p^\mu p^\nu (2f_q + 2\bar{f}_q + f_g) d\Gamma d\Omega_7, \tag{4.13}
$$

and

$$
T_f^{\mu\nu} = \mathrm{diag}(E^2/2, E^2/2, E^2/2, -E^2/2). \tag{4.14}
$$

Here $d\Gamma = d^3p/(2\pi)^3 p_0 = p_t dp_t d\xi/(2\pi)^2$, and $d\Omega_7$ is the angular integral measure in the color space. The factor 2 in the equation (4.13) is for two flavors of quarks. Now since energy and

momentum are conserved in each collision, we have:

$$\int p^\nu C d\Gamma d\Omega_7 = 0. \qquad (4.15)$$

Taking the first moment of the Boltzmann equation, integrating over the color degrees of freedom for f_q, $\bar{f}_q$ and f_g and making use of equations (4.12) and (4 15), we obtain from equation (4.1)

$$\partial_\mu T_f^{\mu\nu} + gE(\tau) \int d\Gamma d\Omega_7 p^\nu \frac{\partial(2f_q - 2\bar{f}_q + f_g)}{\partial\xi} + 4 \int d\Gamma d\Omega_7 p^\nu S_q + 2 \int d\Gamma d\Omega_7 p^\nu S_g = 0 \quad (4\ 16)$$

In the above equation the factor 4 in third term arises because we have two separate transport equations for quark and antiquark, each coming with two flavors, and the factor 2 in fourth term is due to gg pair production, although there is only one transport equation for gluon. Putting ν = 0 and 3 in (4 16) we get two equations, which then yield the following equation for the decay of the electric field:

$$\frac{dE(\tau)}{d\tau} - \frac{2g\gamma}{2\pi} \int_0^\infty dp_t p_t^2 \int_0^\infty d\xi \sinh\xi \int_0^\pi d\theta_1 [2f_q - 2\bar{f}_q + f_g] + (\pi^3/6)\bar{a}|E(\tau)|^{3/2} = 0. \quad (4.17)$$

Here $\bar{a} = a\zeta(5/2)\exp(0.25/\alpha)$, $a = c(g/2)^{5/2}\frac{7}{2(2\pi)^3}$ and $c = \frac{2.876}{(4-3)}$. Finally, $\zeta(5/2) = 1.342$ is the Riemann zeta function.

To solve this equation we fix the form of $T(\tau)$, by demanding that the particle energy density differ negligibly from the equilibrium energy density, in each collision. We then relate the proper energy density, which is defined by

$$\epsilon(\tau) = \int d\Gamma d\Omega_7 (p^\mu u_\mu)^2 (2f_q + 2\bar{f}_q + f_g), \qquad (4.18)$$

to the temperature by its equilibrium value, whence,

$$T(\tau) = [\frac{10\epsilon(\tau)}{\pi^6}]^{1/4}. \qquad (4.19)$$

We solve the equation (4 17) numerically to study the evolution of quark-gluon plasma.

4.2 Numerical procedure

The numerical procedure is already discussed in the earlier chapter. We use a double self-consistent method. The procedure follows the scheme $\{T(\tau)_{trial}, E(\tau)_{trial}\} \rightarrow \{f, \bar{f}, E(\tau)\} \rightarrow \{f, \bar{f}\} \rightarrow T(\tau) \rightarrow ..$ by repeated use of equations (4.8), (4.17), (4.8), (4.19), which is iterated until there is a convergence to the required degree of accuracy. We have in mind the LHC energies, and we have taken the initial energy density as $\epsilon_0 = 300 GeV/fm^3$. Compared to PCM[38] where the initial particle energy density is taken to be around 1300 Gev/fm^3 at RHIC, our choice of initial field energy density might appear some what low However, our choice is guided by the estimate that the formation time for a qgp is a fraction of a fermi, as we explained in the previous chapter. In any case it would not be very appropriate to compare the two initial conditions since the "initiality" is only in a limited sense. Indeed. it is the energy density at the location of the receding color plates, and being well in the fragmentation region at all later times after the collision, what matters is the energy in the central region, corresponding to larger and larger values of τ as the system evolves. It will be seen that in this region the results that our study yields are not unreasonable, if we make a judicious choice for the value of τ_c. We have studied, in this paper, the results for three different values of τ_c. For hydrodynamic and collisionless limits we have choosen $\tau_c = 0.001 \ fm$ and 5.0 fm. We have compared the results of these limitng value of τ_c to a realistic intermediate value $\tau_c = 0.2 fm$.

4.3   RESULTS AND DISCUSSIONS

The solution of the transport equations following the procedure outlined in the previous section allows us to determine directly the temporal evolution of the particle and energy densities, temperature and also the rate at which the field energy flows into the particle sector. These quantities are of intrinsic interest and are, in principle, amenable to experimental study via dilepton production. We present the results below. Also of interest are the broader questions: when the equilibration sets in, at what time the flow becomes hydrodynamic - with or without viscous flow[2, 41], etc.

Then there are features peculiar to our model. Since the color plates are receding away from each other, energy is continuously pumped into the field, which subsequently decays to produce particles. We study the relative rates at which these two dynamical processes proceed in URHIC. This process cannot of course proceed indefinitely. This has already been observed by Gyulassy and Csernai in their study of the dynamics of fragmentation region[48]. As the plates give up their energy, they decelerate. The deceleration sets limits on the times up to which the model is valid. Indeed, the assumption of boost invariance breaks down as it is strictly exact only if $v_{plate} = c$. It is safe to assume boost invariance so long as $v_{plate} \geq 0.9c$[49] A simple estimate shows that this condition, for our choice of initial energy density, holds up to $\sim 5 - 10 fm$ for LHC energies. There would be other competing processes in the fragmentation region, and the Bjorken scenario is probably valid upto $3 - 4 fm$. Keeping this in mind, we have restricted ourselves to (proper) times $\leq 1.5 fm$. Note that the results presented below will be applicable for RHIC energies only if $\tau < 1 fm$.

Finally, the formulation allows us to study an inherently non-abelian quantity, viz,

$< cos^2\theta >$, where θ is the angle between the charge and the field in the group space. Note that its abelian counterpart $\equiv 1$. Wherever possible, we have compared our results with the earlier $SU(2)$ study and PCM. We also display the distribution function(s) in the color space, which none of the other models can yield, be they flux tube based or pQCD based. All the results will be shown for the quarks and the gluons separately. We mention here that it is the color Flux-tube model within which one obtains the evolution of the mean background chromoelectric field, which is absent, either in HIJING or PCM. The evolution of such a background field has a greater impact on the acceleration of the partons present in the system, and hence on the observed signatures. For example the $c\bar{c}$ pair, which is produced in early collisions is acted by this back ground field along with $c\bar{c}$ potential, to evolve into a physical J/ψ

4.3.1   Comparison with SU(2) results
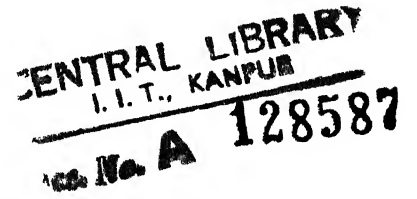
In the earlier chapter we had argued that the assumption of the so called abelian dominance which was made in a large number of transport studies[18, 19, 25] does not receive any justification from a proper study of a non-abelian transport equation. The present study reinforces the same idea, as it is only to be expected. In particular, note that a determination of quantities such as the vacuum current or the polarization current[41] will be particularly suspect in view of the fact that the effective charge will only be a fraction of the true charge (see below). There now arises the question of the dependence of the results on N if one employs the gauge group SU(N) in solving equation (4.1). Although we are not in a position to make a strict comparison between SU(2) and SU(3) in this chapter because the SU(2) study had ignored the gluonic terms altogether, it is still useful to see what a limited comparison can yield. We shall restrict ourselves to the value $\tau_c = 0.2 fm$ to contrast very briefly the results of SU(2) and SU(3).
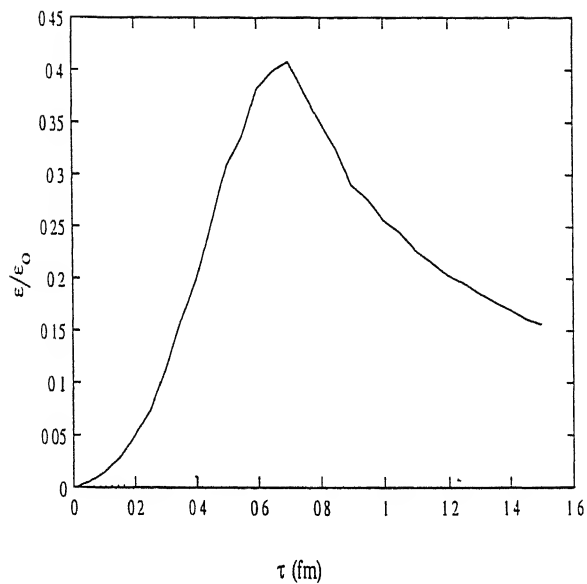
Figure 4.2. The particle energy density scaled w.r.t the initial field energy density as a function of proper time (in units of fermi), for $\tau_c = .2fm$. The solid line refers to SU(3) case, and the dashed line to SU(2) case.
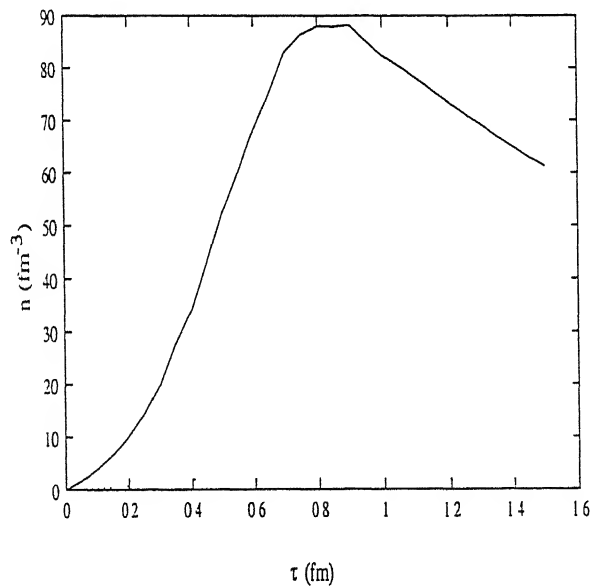
Figure 4.3: The particle number density as a function of proper time (in units of fermi), for $\tau_c = 2fm$. The solid line refers to SU(3) case, and the dashed line to SU(2) case.

flow in more detail in the next section. On the whole, the plasma is denser for SU(3) due to increased volume in phase space.

4.3.2   Discussion of the results

We now discuss the results for SU(3) in some detail, for three values of τ_c - 0.001, 0.2 and 5 fm. The first (last) choice corresponds to the instantaneous hydrodynamic (collisionless) case, in the time scale set by the initial energy density. The quark and the gluonic contributions will be shown separately. It is clear from Figs. 4.4 and 4.5 that the quarks and the gluons show
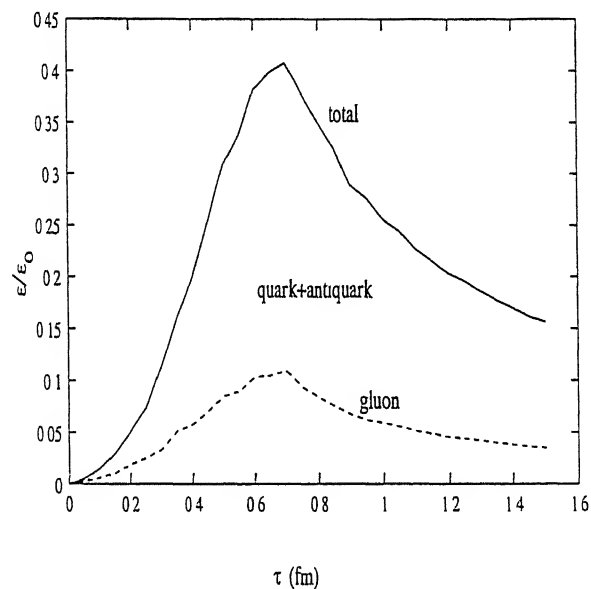
Figure 4.4   The particle energy density scaled w.r.t the initial field energy density as a function of proper time (in units of fermi), for $\tau_c = .2fm$. The solid line refers to total energy density, upper dashed line to quark plus antiquark energy density, and lower dashed line to the gluon energy density.

the same behaviour regarding the energy density and the number density as functions of proper time. The quark contribution is larger, partly because we have considered two flavors, although the source term[47] favors a larger rate for gluons in the color space. The situation will probably get reversed if we include the more correct perturbative source term for quark[39] and gluon
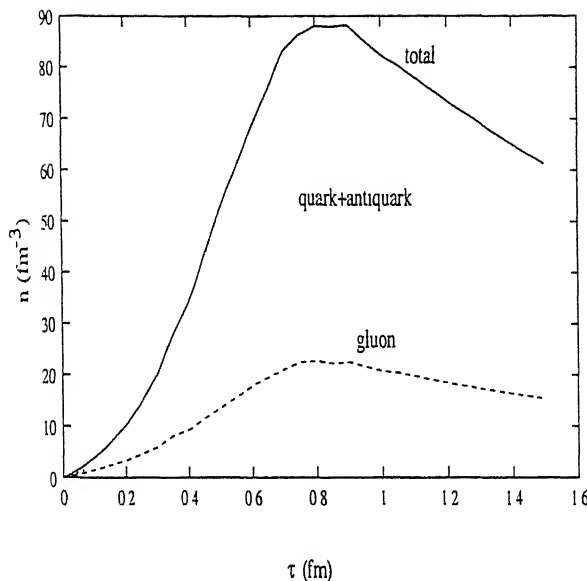
Figure 4.5. The particle number density as a function of proper time (in units of fermi), for $\tau_c = 2fm$. The solid line refers to total number density, upper dashed line to quark plus antiquark number density, and lower dashed line to the gluon number density.

production[50]. In that case, the single and three gluon production rates are of the same order as that of two gluons. That the two sectors will continue to show the same trend may be reliably assumed.

The important common feature that Figs. 4.1, 4.4 and 4.5 show is the nature of the evolution at times later than 1 fm. The curves suggest an approach to the hydrodynamic flow. Note that a hydrodynamic flow would imply that $n(\tau), \epsilon(\tau)$ and $T(\tau)$ behave like $\tau^{-1}, \tau^{-4/3}$ and $\tau^{-1/3}$ respectively. We find that the corresponding exponents are $-0.7, -1.23$ and -0.31 respectively. While the temperature scaling suggests a close approach to the free flow regime, the other two exponents show the presence of drag[51], implying that collisions have not completely ceased. It may be expected that full hydrodynamic flow will take over around $2fm$.

First of all let us compare the results for quarks and gluons separately, for $\tau_c = 0.2fm$ before presenting the results for different values of τ_c. In Fig-4.4 we have presented the scaled particle

energy densites. In contrast to HIJING and PCM, we obtain lower values for energy and number densities for gluons than that of quarks and antiquarks together (Fig-4 5). For a complete study, a source term for hard parton production is also required and this term can be obtained from minijet production at these collider energies, following say reference[41]. The importance of the non-perturbative contribution may be gauged qualitatively by noting that the peak number density for quark-antiquark together(for two flavors) in this model is $\simeq 60 \ /fm^3$ in contrast to the PCM value of $\simeq 120 \ /fm^3$ (for three massless flavors). The energy density for quark sectors in PCM is also larger by the same factor, implying that the average energy per particle is of the same order in both the cases.

Let us now consider $< cos^2\theta >$ (where θ is the angle between color charge and the chromoelectric field in color space). This quantity is a good bench mark to characterise the 'non-abelan'ness of the system, and we present our results in Fig-4 6. This quantity is gauge invariant and physical.
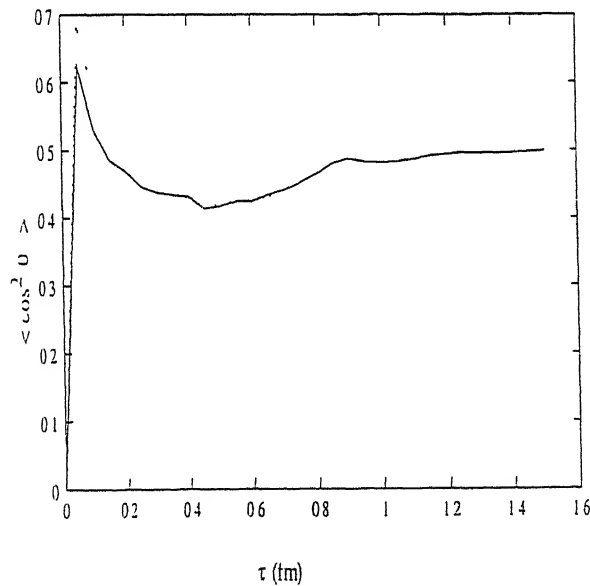
Figure 4 6: $< cos^2\theta >$ as a function of proper time (in fermi) at $\tau_c = .2fm$ for quark (solid line) and gluon (dashed line)

It may be seen that this value saturates at $\theta \simeq \pi/4$, for both quarks and gluons. This value was

always unity in an abelian plasma, as $\theta \equiv 0$ in that case.

This has a direct impact on the equilibration of the plasma. The equilibration is faster around $\theta \simeq \pi/2$ where the background field effect is zero, and is slower at $\theta \simeq 0$ This is understood as follows. At larger value of θ, say around $\pi/2$, there is no acceleration of partons by the background electric field. Only collisions are present at this angle, and hence the rate of equilibration is faster. On the otherhand when the angle $\theta = 0$, the acceleration of partons by background field retards the equilibration of the partons. At any intermediate values of θ, the rate of equilibration lies in between these two extreme values. So this average value, which is purely due to the non-abelian nature of the theory, has a major role in the equilibration of the plasma. This is more clearly shown in the distribution functions which carry the color degrees of freedom explicitly(Fig-4.7 and Fig-4.8).
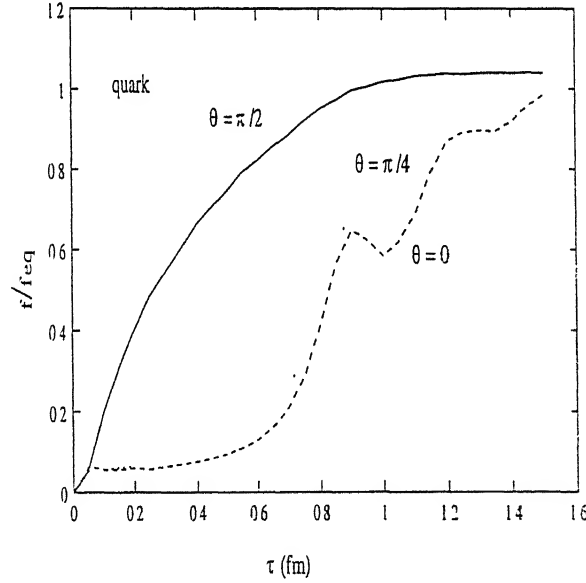
Figure 4 7: f_a/f_q^{eq} as a function of proper time at $p_t = 300 MeV$, $\xi = 0$ and $\tau_c = 0.2fm$, for different values of θ. Solid line corresponds to $\theta = \pi/2$.

We conclude the discussion at $\tau_c = 0.2fm$ by making an interesting observation. As can be seen in Fig-4.6, the value of $< cos^2\theta >$ fluctutates around its mean value for both quarks and gluons,
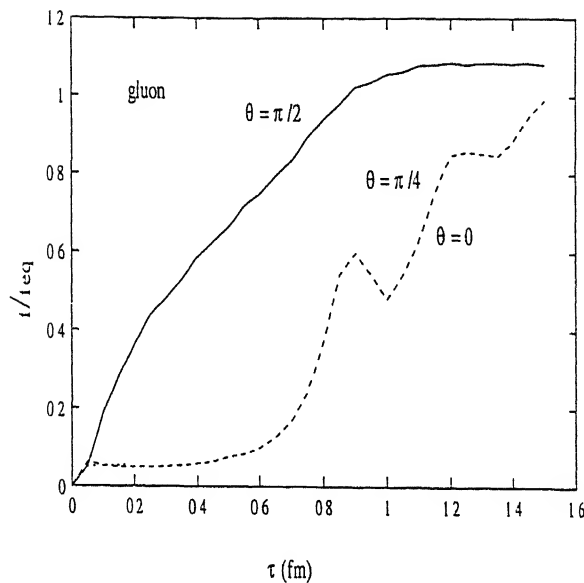
Figure 4.8: f_g/f_g^{eq} as a function of proper time at $p_t = 300 MeV$, $\xi = 0$ and $\tau_c = 0.2 fm$. for different values of θ Solid line corresponds to $\theta = \pi/2$.

with similar fluctuations in other quantities as well - although it is not that pronounced in them. While it certainly indicates that the distribution is approaching its equilibrium value asymptotically, the question is whether the fluctuations would persist even as the system hadronises. Unfortunately, it is difficult to make any definite assertion at this stage. Indeed, as pointed earlier, evolution of the system beyond $3 - 4fm$ requires a full treatment that goes beyond the assumption of the Bjorken scenario in the central region. It is also not known when the hadronization exactly sets in. However, if one assumes that the fluctuations do indeed persist. it may quite well happen that it will manifest as an anisotropy in the parton momentum distribution. This has been pointed out in a study of the related 'color filamentation' by Mrowczynski[52] It is also possible[53], although we do not know in what manner, that these fluctuations in the hadronic phase show up as disoriented chiral condensates. It is only a more complete and rigorous study that can settle the status of these speculations.

Now we present the data for the other two values of τ_c, namely $\tau_c = 0.001 fm$ and $\tau_c = 5fm$,

corresponding to hydrodynamic and collisionless limits respectively. These results are then compared with $\tau_c = 0.2fm$. Consider first the number density $n(\tau)$. This quantity is seen to be sensitive to the values of τ_c. As can be seen from Fig-4 9, $n(\tau)$ is larger in the hydrodynamic
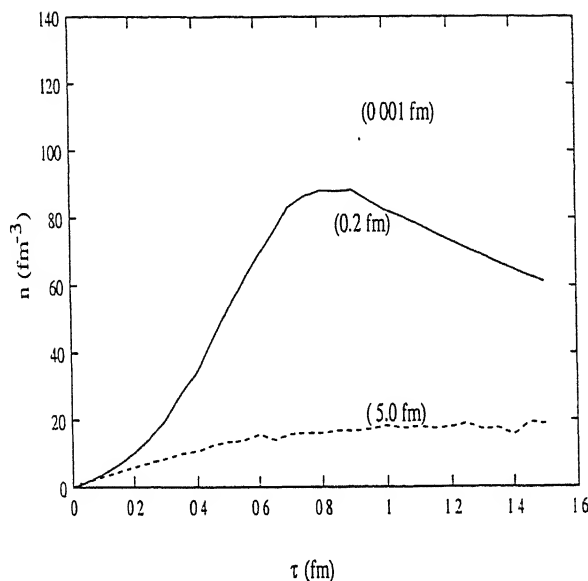
Figure 4.9: The particle number density as a function of proper time (in units of fermi), for $\tau_c = 2fm$ (solid line), for $\tau_c = 0\,001fm$ (upper dashed line) and for $\tau_c = 5fm$ (lower dashed line).

limit, where the maximum value is around 120 per fm^3, at $\tau \simeq 1.0fm$. As τ_c is increased to 0.2 fm we find a lesser value, the maximum value being around $80/fm^3$. This trend continues for collosionless limit where particle density is still less. The increase in number density as τ_c is decreased is expected in the context of classical theory. This is because, the collision time in any classical non-equilibrium theory depends roughly on the inverse of the number density, apart from the other factors. The behaviour of number densities in Fig-4.9 for different values of τ_c in our calculation also reflects the above fact.

In Fig-4.10 we present the scaled energy densities for different values of τ_c. Unlike the number density, there is no strong dependence on τ_c. This means that the average energy per particle is different for different values of τ_c. We find that for $\tau_c = 0.001fm$, the maximum average energy
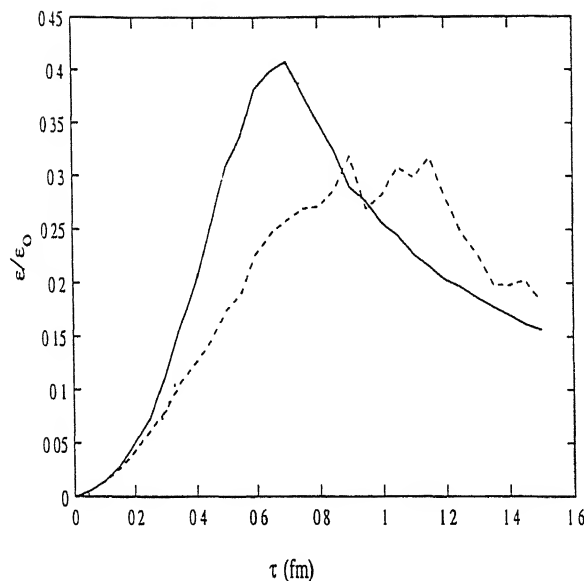
Figure 4.10: The particle energy density scaled w.r.t the initial field energy density as a function of proper time (in units of fermi), for $\tau_c = .2fm$ (solid line), for $\tau_c = 0\,001fm$ (upper dashed line) and for $\tau_c = 5fm$ (lower dashed line).

per particle is around 1.0 GeV, whereas it is around 2.0 GeV for $\tau_c = 0.2fm$ and 4.0 GeV for $\tau_c = 5.0fm$. Note that these high energy deconfined partons can produce secondary partons, such as strange quarks and also can break a fully formed J/ψ as analysed by short-distance QCD in reference[54].

Let us consider the electric field. It may be seen from Fig-4.11 that the decay of the field is very slow at $\tau_c = 0.001fm$, compared to $\tau_c = 0.2$ and 5 fm. Only 30 percent of the field has decayed in the hydrodynamic limit in comparison to collisionless and intermediate limits, where the decay is very large. At the other end in the collisionless limit, the decay is at a slightly slower rate in comparison to $\tau_c = 0.2$ fm, implying that the maximal conversion rate is for τ_c around 0.2 fm. As mentioned earlier, one peculiarity of the model is that the field energy is continuously created due to the recession of the plates even as the field itself decays to produce particles. To study this, in Fig-4.12 we present field energy per unit transverse area as a function of *ordinary* time. For $\tau_c = 0.2$ fm this energy is much less than that at $\tau_c = 5$
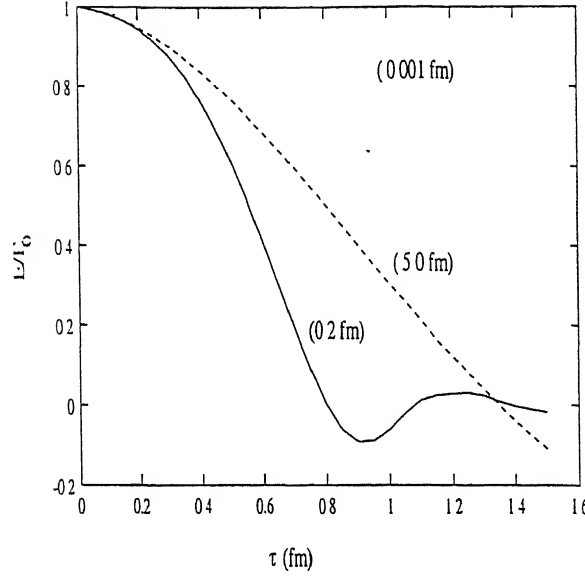
Figure 4.11: Decay of the chromoelectric field as a function of proper time (in units of fermi), for $\tau_c = .2fm$ (solid line), for $\tau_c = .001fm$ (upper dashed line) and for $\tau_c = 5fm$ (lower dashed line).

fm and $0.001\ fm$. This demonstrates that the conversion is indeed dominant at $\tau_c = 0.2\ fm$.

This is more clearly displayed in Fig-4 13, where we have plotted the ratio of particle energy

per unit transverse area to field energy per unit transverse area.

In Fig-4.14 we present the evolution of temperature at $\tau_c = 0.2\ fm$. The maximum temperature

we obtain in the color flux-tube model is around 300 MeV. Finally, a brief comment on the
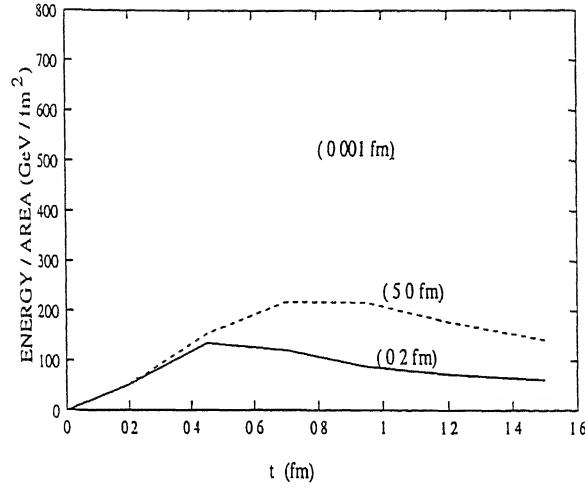
Figure 4.12: The field energy/unit transverse area(in units of GeV/fm^2) for $\tau_c = 0.2$ fm (solid line), for $\tau_c = 0.001$ fm (upper dashed line) and for $\tau_c = 5$ fm (lower dashed line), as a function of ordinary time (in fermi).
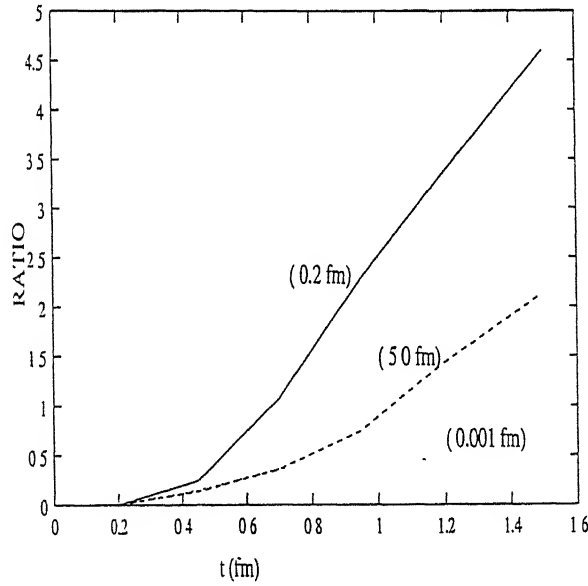
Figure 4.13: The ratio of particle energy per unit transverse area to field energy per unit transverse area for $\tau_c = 0.2$ fm (solid line), for $\tau_c = 5$ fm (upper dashed line) and for $\tau_c = .001$ fm (lower dashed line). as a function of ordinary time (in fermi).
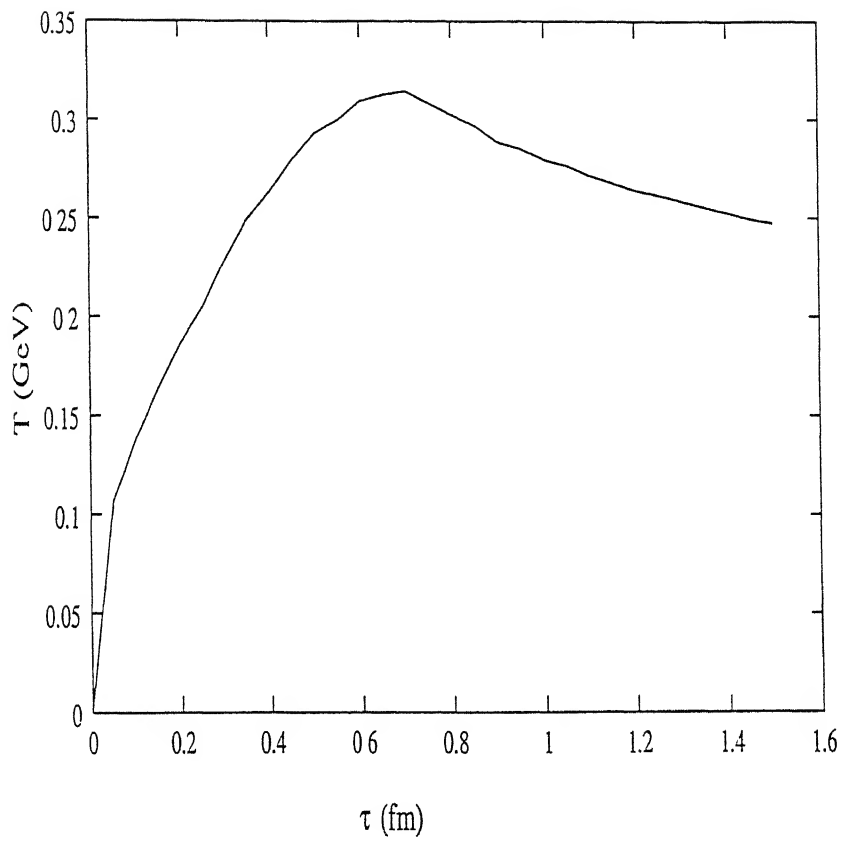
Figure 4 14: Evolution of temperature as a function of proper time (in fermi), for $\tau_c = 0.2$ fm.

distribution functions for quarks and gluons with explicit color dependence (Fig-4.7 and 4 8). As discussed earlier, it may be seen that the equilibration is fastest for $\theta = \pi/2$. where there is no background effect. At $\theta = \pi/2$ the thermal equilibration occurs at a common time $\tau \simeq 1\,0$ fm for both quarks and gluons.

4.4   Conclusion

We have studied the production and the equilibration of a genuinely non-Abelian plasma with the color degree of freedom incorporated in both the source term and the background term in the transport equation. With the realistic gauge group $SU(3)$ that we have considerd here, the distribution functions for quarks and gluons get defined in the extended phase space of dimension 14 We have added the gluonic component into the color flux-tube model, which was so far absent

The role of the color degree and that of gluons was found to be substantial, and non-trivial. The plasma is denser than the $SU(2)$ counter part but is comparable to the Abelian case. However, it is much cooler than the abelian plasma. where the corresponding temperature is $\sim 800 MeV$. The value of the effective charge is larger than that of its counterpart in $SU(2)$, contrary to naive expectations. The peak energy per particle is $\simeq 2$ GeV which indeed is the demarcating scale[37] between soft and hard processes. In short, the non-perturbative aspects of the evolution of QGP offer a rich variety of results which will have to be combined with the perturbative studies in order to abtain a complete description of the production and evolution of quark-gluon plasma.

Chapter 5

Dilepton production from a thermally equilibrating quark-gluon plasma

---

As mentioned earler, some of the major proposed signatures to detect quark-gluon plasma in URHIC are 1) J/ψ supression[5], 2) electromagnetic probes such as dilepton and direct photon production[6, 7]. and 3) strangeness enhancement[8]. It has been suggested that for an equilibrated quark-gluon plasma, J/ψ supression, due to screening, is a good probe[5]. However, due to the uncertainties in the study of production and evolution of QGP in these is experiments the results obtained by screening can not be taken too seriously. There are also calculations of J/ψ suppression in the equilibrating quark-gluon plasma[9, 10] using short-distance QCD which are different for different models (see chapter 7). The supression of J/ψ. infact, has been observed in reactions where there is no quark-gluon plasma phase, such as in p-A collisions and in collisions of light nucleus[55]. This suppression is well explained by the nuclear absorption

of J/ψ[56] Although, recently, NA50 collaboration[57] reports an excess in the supression of J/ψ, it is still not clear if a quark-gluon plasma phase has formed in this collisions. There are proposals that the data are explained by a deconfined partonic medium[58], or by a medium with high density[59]; but there are also other calculations which explain the data without assuming any quark-gluon plasma phase[60]. As far as the J/ψ supression in nucleus-nucleus collision is concerned, many aspects of it has to be studied in greater detail before unambigious conclusions can be drawn about the existence of quark-gluon plasma. It thus appears that there is a need to study more than one signature if one has to detect QGP. With that in mind we investigate another signature, $i.e.$ dilepton emission.

Dileptons and single photons have long been proposed as useful probes of the plasma[7]. Once produced, they hardly interact with the strongly interacting matter and thus carry the details of the circumstances of their production. There has been, however, uncertainties in the calculation in their spectra. This is due to lack of detailed knowledge about the space time evolution of quark-gluon plasma. Recall that the various stages by which the complete evolution of quark-gluon plasma is described in URHIC are, i) pre-equilibrium, ii) equilibrium, where one actually studies the equilibrated quark-gluon plasma, iii) cooling and iv) hadronisation. The pre-equilibrium stage of the collision which leads to thermal and then chemical equilibrium has a crucial role to play. From this point of view it is necessary to study what happens to the dilepton emissions from different stages of evolution of QGP, rather than estimating it in an equilibrated quark-gluon plasma.

We study the dilepton production in an equilibrating QGP employing the distribution functions determined in the previous chapter. The dominant process which produces a dilepton pair l^+l^-

is

$$q + \bar{q} \to \gamma^* \to l^+ + l^- \tag{5.1}$$

where γ^* is the intermediate virtual photon. The dilepton emission rate in a space time volume d^4x is written as

$$\frac{dN}{d^4x d^4P} = \frac{1}{(2\pi)^6} \int d^3p_1 d^3p_2 dQ\, f(x,p_1,Q)\bar{f}(x,p_2,Q)v_{rel}\sigma(M^2)\delta^4(P - p_1 - p_2). \tag{5.2}$$

Here P^μ is the four momentum of the lepton pair, with P_T its transverse momentum and $M_T(= \sqrt{M^2 + \mathbf{P_T}^2})$ its transverse mass. M is the invariant mass of the dilepton pair $(M^2 = P^\mu P_\mu)$ and $v_{rel} = M^2/2E_1E_2$ is the relative flux velocity of quark and antiquark pair in the above process. The distribution function of quark and antiquark is a function of the color charge Q. dQ is the integral of the the color part of the phase space. The dilepton production cross section for the above reaction is

$$\sigma(M^2) = \frac{4\pi\alpha^2}{3M^2}[1 + \frac{2m_l^2}{M^2}][1 - \frac{4m_l^2}{M^2}]F_q \tag{5.3}$$

where $F_q = N_s^2 \frac{1}{N}\sum_f e_f^2$ and m_l is the mass of the lepton. N is the color averaging factor (corresponds to the volume of the compact(color) space), N_s is the spin degeneracy $(N_s = 2s+1)$ and e_f is the fractional charge of the flavour. For a dilepton pair of large mass the emission rate in the midrapidity region (Y = 0) of lepton pair is given by[61]:

$$\frac{dN}{dM_T^2 dY dP_T^2} = \frac{5R^2\alpha^2}{72\pi^7} \int d\tau \tau W(f_1, f_2). \tag{5.4}$$

where

$$W(f_1, f_2) = \int_{-\infty}^{+\infty} d\eta \int_{-\infty}^{+\infty} d\xi_1 \int_{p_-}^{p_+} dp_{t1} \int dQ \frac{p_{t1} f(\tau, p_{t1}, \xi_1, Q)\bar{f}(\tau, p_{t2}, \xi_2, Q)}{[p_{t1}^2 P_T^2 - [p_{t1}M_t ch(\eta - \xi_1) - \frac{1}{2}M^2]^2]^{1/2}} \tag{5.5}$$

with $p_{t2} = \sqrt{M_T^2 - 2M_T p_{t1}ch(\eta - \xi_1) + p_{t1}^2}$, $sh\xi_2 = \frac{1}{p_{t2}}(M_T sh\eta - p_{t1}sh\xi_1)$ and $p_{\pm} = \frac{1}{2}M^2[M_T ch(\eta - \xi_1) \mp P_T]^{-1}$. In equation (5.4) we have used $d^4x = \pi R^2 d\tau\tau d\eta$ (where R is the radius of the radiating region). $\alpha(= 1/137)$ is the coupling constant of the electromagnetic interaction.

It has been shown[62] that the thermal dilepton rate does not depend on M and P_T separately, but only on M_T. This is known as M_T scaling in QGP. However this M_T scaling is violated in an equilibrating plasma, as can be seen from equation (5.4). In this case the dilepton rate depends on both M_T and P_T This would also be the case if one takes the transverse expansion of the plasma into account[63].

In our calculation we have taken $R = 7fm$ corresponding to Au-Au collisions. We have considered two different cases corresponding to two different relaxation times, $\tau_c = 5fm$ and $\tau_c = 0\,2fm$. The relaxation time $\tau_c = 5fm$ corresponds to collisionless limit and $\tau_c = 0.2fm$ corresponds to a more realistic limit of equilibration[38]. We have calculated the dilepton rate as a function of M_T for $P_T = 0$ and 1 GeV respectively. In Fig-5.1 we have presented the dilepton rate at $\tau_c = 0.2fm$. As can be seen from Fig. 5.1, the dilepton yield becomes smaller
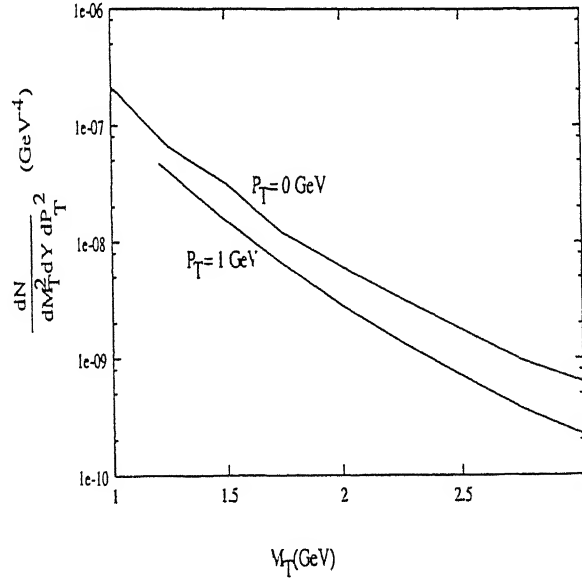
Figure 5.1: Dilepton rate from pre-equilibrium stage, as a function of M_T for $\tau_c = 0.2$ fm.

for higher values of transverse momenta. In Fig-5.2 we have shown our results for $\tau_c = 5fm$ which corresponds to the collisionless limit. The rate at higher M_T is found to be larger than that at $\tau_c = 0.2fm$. This is because the average energy per parton is higher at $\tau_c = 5fm$ than at

$\tau_c = 0.2 fm$ as observed in the last chapter. This is because in the collisionless limit the energy

per parton is larger (~ 4 GeV) than that at $\tau_c = 0.2$ fm (~ 2 GeV).

In Fig-5 3 and Fig-5.4 we have compared our results with the corresponding Drell-Yan predictions. The Drell-Yan results are taken from the reference[28]. It can be seen from Fig. 5.3 that
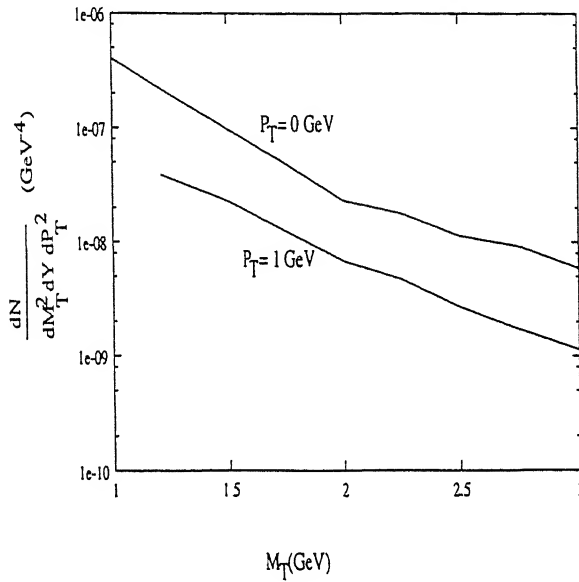
Figure 5.2: Dilepton rate from pre-equilibrium stage, as a function of M_T for $\tau_c = 5.0$ fm (collisionless limit).

the dilepton rate from pre-equilibrium stage is larger than the Drell-Yan production for very

small transverse momentum ($P_T \simeq 0 GeV$). This is true when $M_T \leq 2 GeV$. For $M_T \geq 2 GeV$,

the Drell-Yan production dominates over the pre-equilibrium dilepton production. For a large

transverse momentum ($P_T = 1 GeV$) of dilepton pair, the production from the pre-equilibrium

phase is lower than the Drell-Yan production in the whole range of dilepton transverse mass.

This can be seen from Fig-5.4. This is contrary to the earlier findings[64–66] where it is shown

that dilepton production from the pre-equilibrium stage dominates over the Drell-Yan produc-

tion. However the production of partons are not too hard in this model, and one expects to

have such a low rate in the dilepton spectra than the Drell-Yan emission.
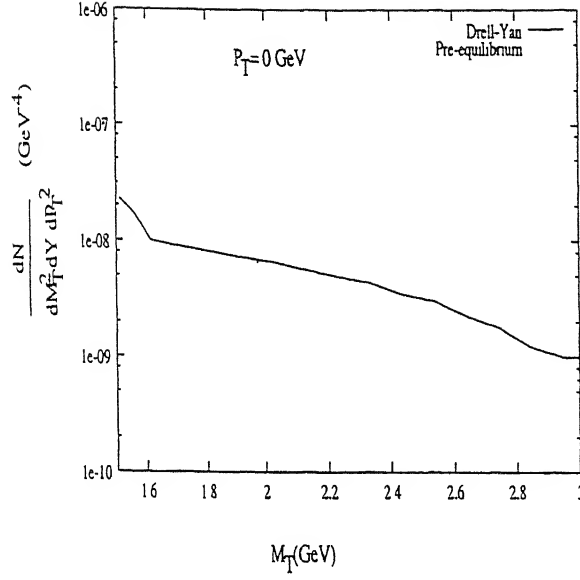
Figure 5.3. Drell-Yan and pre-equilibrium dilepton rate as a function of M_T for $\tau_c=0\,2$ fm ($P_T = 0$ GeV).

Summarizing the chapter, we have calculated the dilepton spectra in ultra relativistic heavy-ion collisions within color flux-tube model, with non-abelian features explicitly incorporated. In contrast to the earlier studies, we have found a smaller rate in dilepton production in the pre-equilibrium stage at high M_T and P_T than the Drell-Yan production. The production is larger in the collisionless limit of the plasma. An experimental measurement of the dilepton spectra in URHIC can shed light on the collision time (τ_c) and possibly on the initial field energy density that we have assumed in our model.
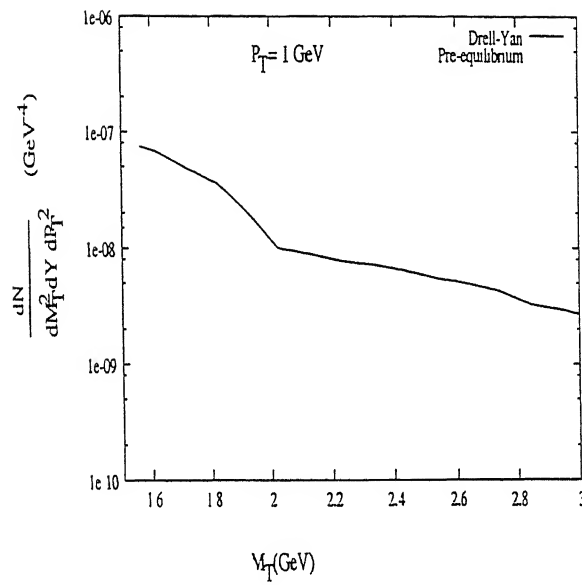
Figure 5 4   Drell-Yan and pre-equilibrium dilepton rate as a function of M_T for τ_c=0.2 fm ($P_T = 1$ GeV).

Chapter 6

A new source term for quark production from a space-time dependent chromoelectric field

6.1   Introduction

Over years there has been several devlopement on the production of charged particles from electric field, a phenomenon which was discovered nearly forty years ago by Schwinger[23]. By now the production of particles from a constant background electric field is extensively studied both theoretically and experimentally[67]. However, the subject matter of particle creation

from a time dependent field, and the dynamics of the 'field-particle' system is relatively new and is not fully solved. This aspect has been a subject of renewed and central interest in the context of heavy-ion collisions and QCD due to the suggestion that the receding nuceli might produce a strong chromoelectric field which creates quark/anti-quark pairs and gluons[19]. As the particles (quark/anti-quarks and gluons) are continously produced from the background field, the field becomes time dependent during the evolution of the system after the two nuclei collide with each other. Hence the source term for the production of particles which is taken in chapter 3 and 4 incorporating a constant field in its calculation is not strictly applicable and a determination of the particle production from a time dependent electric field becomes necessary. Indeed a complete quantum mechanical treatment of the problem is rather too involved. For our purpose, it should be sufficient to derive how a space-time dependent field produce particles as a function of time. The dynamics of the field is of course is coupled to that of the particles, and may be determined in a consistent (although not complete) manner by solving the transport equations as we have done in the previous chapters.

In this chapter we derive a source term for quark/anti-quark and gluon production from a time dependent electric field which is needed in the non-abelian transport equation[45], with the purpose of eventually studying the production and equilibration of quark-gluon plasma in ultra relativistic heavy-ion collisions. As described in the preceeding chapters the source term one needs is, $\frac{dN}{dt d^3 x d^2 p_t}$, which is the probability for particle production per unit time per unit volume per unit transverse momentum in the phase space.

Before deriving a source term for a time dependent electric field there are several physical features that needs to be clarified. First of all Schwingers's mechanism[23] incorporating a constant field in its calculation is an exact one loop non-paeturbative result, which can be

understood in terms of a semiclassical tunneling process[68]. However, for a time dependent electric field such a calculation is not necessary and particle production can directly take place by the perturbative mechanism. It can be further noted that a constant field can not produce pairs by this perturbative mechanism. Secondly, it is not possible to obtain a source term ($\frac{dN}{dtd^3xd^2p_t}$) in the usual phase space from a quantum processes This is because any attempt to obtain such a source term within zero uncertainty will violate quantum mechanics. Although a source term in the usual phase space has been proposed[68] by rewriting the Schwinger's source term as an integral over p_t^2, such proposals are ad hoc and are inconsistent with the minimum uncertainty requirement. In this chapter we overcome this problem by working in the coherent basis of coordinate, momenutm and color.

A coherent state ($|\alpha>$) is the eigen state of anihilation operator $\hat{a}(x,p)$ defined by[69]

$$\hat{a}|\alpha> = \alpha|\alpha> \qquad (6.1)$$

with α being its eigen value the real part of which is proportional to the expectation value of cordinate operator and the imaginary part is proportional to the expectation value of the momentum operator. W.r.t this coherent state the expectation value of coordinate operator $\hat{x}$ and momentum operator $\hat{p}$ can be written as

$$X = <\alpha|\hat{x}|\alpha> \qquad (6.2)$$

$$P = <\alpha|\hat{p}|\alpha> \qquad (6.3)$$

with $\Delta X \Delta P = h/4\pi$, which satishfy the minimum uncertainity. Here $(\Delta X)^2 = <\alpha|\hat{x}|\alpha>^2 - <\alpha|\hat{x}^2|\alpha>$ and $(\Delta P)^2 = <\alpha|\hat{p}|\alpha>^2 - <\alpha|\hat{p}^2|\alpha>$. We have used this coherent basis $|\alpha> (\equiv |X,P>)$ to derive a new source term which does not violate principles of quantum mechanics. To derive a source term for parton production from a time dependent electric field and to further

study its dynamics we have restricted our calculation to a finite time interval in the S matrix expansion (see below).

In the next section we derive the source term for the case of a purely time dependent electric field. Pending the determination of $E(t)$ from a self consistent study, we have employed a specific form for the electric field to get an understanding of the dynamics of the particle production. We have compared the results of this source term with that of Schwinger's source term (obtained for a constant field) by puting the same time dependence in the field (the time dependence in the electric field in Schwinger's source term was put by hand in chapter 3 and 4). In section 3 of this chapter we have derived a source term for quark production from a $\tau(= \sqrt{t^2 - z^2})$ dependent electric field. These source terms will be used in the transport equation to study production and equilibration of quark-gluon plasma in ultrarelativistic heavy-ion collisions.

6.2   Source term for a purely time dependent electric field

We start our derivation with a determination of the Feynmann amplitude for the production of quark from a time dependent electric chromoelectric field. The Feynmann amplitude is written either in momentum space or coordinate space. However, we need a source term ($\frac{dN}{dtd^3xd^p}$) in the usual phase space of coordinate and momentum from this amplitude. For this purpose, we have projected the Feynmann amplitude (in momentum space) to a coherent basis of coordinate and momentum. As described earlier this coherent state is the eigen state of anihilation operator and the expectation value of the coordinate and momentum with this coherent states satishfy the minimum uncertainty.

For a particle at mean position X, having mean momentum P, and color charge Q the amplitude in the coherent basis can be written as

$$< Q, X, P|S|0 > = \int d^3\vec{k} < Q, X, P|k > < k|S|0 >, \qquad (6.4)$$

where $|X, P, Q >$ is the coherent state of cordinate, momentum and color. Here the coherent state $|Q >$ for the color is defined as $|Q > = exp(\imath Q^a T^a)|0 >$ (see Eqn 6.14). To the leading order in perturbation series we have

$$S = \int_0^t dt' d^3x \mathcal{L}_\mathcal{I}(t', x). \qquad (6.5)$$

with $\mathcal{L}_\mathcal{I}(t', x)$ being the interaction lagrangian density. The time $(t = 0)$ refers to the initial state where there is no production (this replaces $t = -\infty$ in the usual scattering processes). For our dynamics here we have limitted the time integral to a finite limit t and not to ∞. For quark/anti-quark pair production the interaction lagrangian density is

$$\mathcal{L}_\mathcal{I} = -g\bar{\psi}_j T^a_{\imath j} \gamma_\mu A^{\mu a} \psi_\imath, \qquad (6\ 6)$$

with $\psi_\imath$ being the Dirac field for quark and A^a being the external color field. In the above equation $T^a_{\imath j}$ are the generators with $a = 1..,.,8$ and $\imath, \jmath = 1, 2, 3$. For quark/anti-quark pair production the corresponding amplitude is

$$< Q_1, Q_2, X_1, X_2, P_1, P_2|S|0 > = \Sigma_{\imath, \jmath} \int d^3\vec{k_1} d^3\vec{k_2} < Q_1, Q_2, X_1, X_2, P_1, P_2|k_1, k_2, \imath, \jmath >$$
$$< \imath, \jmath, s_1, s_2, k_1, k_2|S|0 >, \quad (6.7)$$

where X_1, X_2 are coordinates P_1, P_2 momenta and s_1 and s_2 are the spin indices of the quark and anti-quark respectively. Here $< i, \jmath, s_1, s_2, k_1, k_2|S|0 >$ is the usual Feynmann amplitude for quark/anti-quark pair production with i and j being the color index of quark and anti-quark.

After summing over spin and color the absolute square of this amplitude is written as:

$$|< Q_1, Q_2, X_1, X_2, P_1, P_2|S|0 >|^2 = \Sigma_{i,j,l,m} \Sigma_{s_1,s_2} \int d^3\vec{k_1} d^3\vec{k_1'} d^3\vec{k_2} d^3\vec{k_2'} < Q_1, Q_2, X_1, X_2, P_1, P_2|k_1, k_2, i, j;$$

$$< l, m, k_1', k_2'|Q_1, Q_2, X_1, X_2, P_1, P_2 >^* < 0|S|k_1', k_2', s_1, s_2, l, m >^* < i, j, s_1, s_2, k_1, k_2|S|0 >$$

In our calculation, we have made a suitable gauge choice such that $A^{(\mu=0)} = 0$. With this choice the potential $A^{\mu a}$ in the the above equation is related to the electric field by the simple expression.

$$E^a(t) = -\frac{dA^a(t)}{dt}. \tag{6.9}$$

Substituting

$$A(t, x) = \int d^3 K A(t, \vec{K}) \exp(-iK \cdot x) \tag{6.10}$$

we obtain (for massless quark)

$$\Sigma_{s_1,s_2} < 0|S|k_1', k_2' >^* < k_1, k_2|S|0 >= f(t_1, t_2, k_1, k_2, k_1', k_2'), \tag{6.11}$$

where $f(t_1, t_2, k_1, k_2, k_1', k_2')$ is given in the appendix for a fixed value of a in $A^{\mu a}$. The expression for color sum $(C(Q))$ is not included in $f(t_1, t_2, k_1, k_2, k_1', k_2')$ and is presented separately (see Eqn (6.14)). With the above fourier transformation (Eqn (6.10)) the time dependence in A appears finally in the source term. In most of the earlier studies[71] the source term is derived with some special form of the electric field. Such source terms are not necessarily applicable in the transport equations to study the production and equilibtation of quark-gluon plasma. In our study, here no specific form for electric field is assumed.

For the case of a single quark we project Feynmann amplitude to a coherent basis $|X, P, Q >$ rather than projecting it to $|X_1, X_2, P_1, P_2, Q_1, Q_2 >$. The later is needed if we are interested in pair (quark/anti-quark) production and corelations. For quark production at mean position X

having mean momentum P and color charge Q we have

$$|< Q, X, P|S|0 >|^2 = \Sigma_{i,j,l} \int d^3\vec{k_1} d^3\vec{k_1'} d^3\vec{k} < Q, X, P, |k_1, \; i > < j, \; k_1'|Q, X, P >^*$$

$$< 0|S|k_1', k, j, l >^* < l, i, k_1, k|S|0 > . \quad (6.12)$$

The above equation can be written as

$$|< Q, X, P|S|0 >|^2 = \Sigma_{i,j,l} \int d^3\vec{k_1} d^3\vec{k_1'} d^3\vec{k} < Q|i > < j|Q >^* T_{il}^a T_{lj}^{*b} < X, P, |k_1 > < k_1'|X, P >^*$$

$$< k_1, k|S^a|0 > < 0|S^b|k_1', k > \quad (6.13)$$

As was done in the previous chapters we fix the direction of the electric field and we take it to be along 8 direction in the color space (a=8 and b=8). The color factor C(Q) becomes,

$$C(Q) = \Sigma_{i,j,l} < Q|i > < j|Q >^* T_{il}^8 T_{lj}^{*8} = \frac{1}{4}[1 + 3| < Q|3 > |^2], \quad (6.14)$$

with $|Q > = exp(iQ^aT^a)|0 >$

Following the reference[70] we arrive at the expression $< Q|3 > = cos\theta \exp(i\gamma)$; so that $C(Q) = \frac{1}{4}[1 + 3cos^2\theta]$. *This is the univerasl form of the color dependence independent of the nature of the electric field.* Here $0 < \theta < \pi/2$ and $0 < \gamma \leq \pi$.

For a purely time dependent potential $A(t.\vec{k_1} + \vec{k_2} = 0)$ we obtain

$$|< Q, X, P|S|0 >|^2 = C(Q) \int d^3\vec{k_1} d^3\vec{k_1'} 2d^3\vec{k} < X, P, |k_1 > < k_1'|X, P >^*$$

$$\int_0^t dt_1 \int_0^t dt_2 f(t_1, t_2, k_1, k, k_1', k) \exp(i(k_1^0 + k^0)t_1) \exp(-i(k_1'^0 + k^0)t_2)\delta^3(\vec{k_1} + \vec{k})\delta^3(\vec{k_1'} + \vec{k}) \quad (6.15)$$

The coherent state wave function $< X, P|k >$ which satisfies minimum uncertainty is

$$< X, P|k > = N \exp(-(\vec{P} - \vec{k})^2/2Q^2) \exp(i\vec{k} \cdot \vec{X}), \quad (6.16)$$

with N being the normalisation constant. Putting the the above form for the coherent state in equation (6.15) we get

$$|< Q, X, P|S|0 >|^2 = N^2 C(Q) \int d^3\vec{k} \exp(-(\vec{k}-\vec{P})^2/Q^2) \int_0^t dt_1 \int_0^t dt_2$$
$$\exp(2\imath k^0(t_1-t_2)) \frac{1}{4k^{02}} [\vec{k}^2(\vec{A}(t_1) \cdot \vec{A}(t_2)) - (\vec{k} \ \vec{A}(t_2))(\vec{k} \cdot \vec{A}(t_2))], \qquad (6\ 17)$$

with $k^0 = |\vec{k}|$ (for massless quark) Without any loss of generality one can assume z-axis to be along the direction of A and obtains

$$|< Q, X, P|S|0 >|^2 = C(Q)N^2 \int d^3\vec{k} \exp(-(\vec{k}-\vec{P})^2/Q^2) \int_0^t dt_1 \int_0^t dt_2 (A(t_1)A(t_2)) \exp(2\imath|\vec{k}|(t_1-t_2))$$
$$\frac{1}{4}[(1-\cos^2\theta_k)]$$
$$-(6\ 18)$$

with θ_k being the angle between z-axis and $\vec{k}$. This is the probability of quark production per unit volume per unit momentum having a color charge Q from a time dependent electric field $E(t)$ related to $A(t)$ by Eqn (6.9). The required source term is then

$$\frac{dN}{dt d^3 X d^2 P_T} = \int dP_3 \frac{d|< Q, X, P|S|0 >|^2}{dt}. \qquad (6.19)$$

To make sure that a constant potential and a constant field (which is obtained from a linear time dependent potential (Eqn. (6.9)) do not contribute to the above time dependent source term we project out only the time dependent part by the replacement $A(t) \rightarrow A(t) - A(0) - tA'(0)$ in the Eqn. (6.19). After singling out the contributions from this constant potential and the constant field we obtain a genuinely time dependent source term from Eqn. (6.19).

Now by putting some specific form of the electric field we compare the results obtained by this source term with that of Schwinger's source term. For the choice $A(t) = \exp(-t/t_0)$ we present the results of both the cases below. We have choosen Q_T and Q_3 in the coherent state wave function (Eqn. 6.16) corresponding to a 1+1 dimensional expanding plasma. For Q_T the scale

is the transverse diameter of the nucleus ($\simeq$ 14 fm for Au nucleus) and for Q_3 it is determined from the total length traveled by the two nuclei (2z or 2t, as nuclei travel almost at a speed of light.) In Fig-6.1 we have plotted the production rate ($\frac{dN}{dt d^3 X d^2 P_T}$) for P_T 0.5 GeV as a function of t. The production rate increases as time increases in contrast to the Schwinger's results

Figure 6.1: The rate of quark production ($\frac{dN}{dt d^3 X d^2 P_T}(GeV^2)$) obtained by the new source term from a time dependent electric field for $P_T = 0.5$ GeV, $t_0 = 0.5$ fm and $\theta = 0$

which is shown in Fig-6.2 for the same input parameters. This is because, in the newsource term we have taken a finite limit in the time integration in the feynmann amplitude. As time increases, the absolute value of this amplitude increases and hence a large production rate is obtained. However, the schwinger formula is valid for a constant field. But for a comparison with our new source term we have taken the same time dependence in the electric field in both the cases. In Fig-6.3 we present the results for $P_T = 1.0$ GeV. The production rate decreases as P_T increases, which is in accordance with the Schwinger's result (presented in Fig-6.4). This is more clearly seen in Fig-6.5 where where we have plotted the production rate of the new source term for $P_T = 5.0$ GeV. To get a feeling on the total production of particles rather
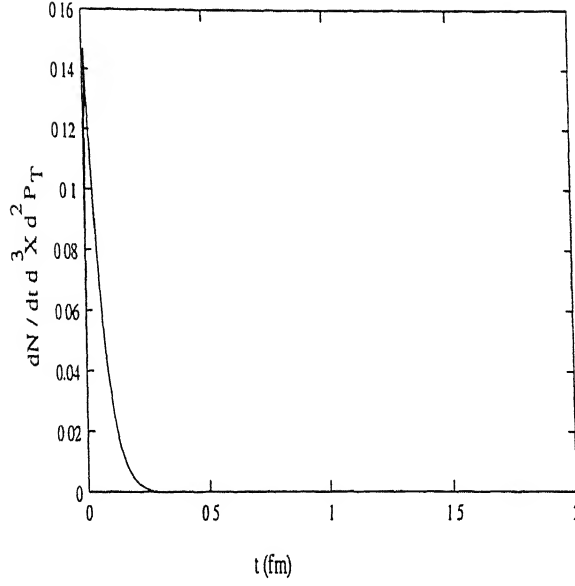
Figure 6 2: The rate of quark production ($\frac{dN}{dt d^3 X d^2 P_T}(GeV^2)$) obtained from Schwinger's source term with the same time dependent electric field (as described in the text) for $P_T = 0.5$ GeV, $t_0 = 0.5$ fm and $\theta = 0$

than its production rate we have plotted the total production ($\frac{dN}{d^3 X d^2 P_T}$) in Fig-6.6 and 6.7 for $P_T = 0.5$ and 5.0 GeV up to $t = 2.5$ fm. It is seen that total number of particle production per unit volume per unit transverse momentum is an increasing function of time. This has a strong impact on the particle production in relativistic heavy-ion collisions where the plasma would be very dense even at a later time (up to 2.0 fm). Such a calculation of the quark-gluon plasma production and its evolution within the frame work of non-Abelian transport equation will be performed and reported elsewhere.

Figure 6.3: The rate of quark production ($\frac{dN}{dtd^3Xd^2P_T}(GeV^2)$) obtained by the new source term from a time dependent electric field for $P_T = 1.0$ GeV, $t_0 = 0.5$ fm and $\theta = 0$
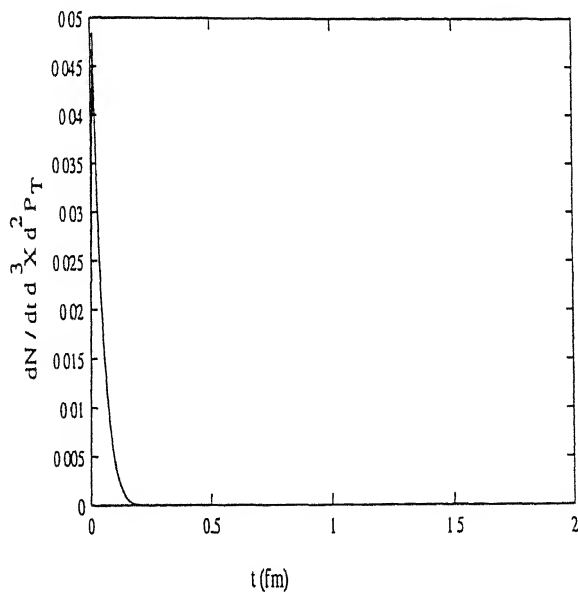
Figure 6.4: The rate of quark production ($\frac{dN}{dtd^3Xd^2P_T}(GeV^2)$) obtained from Schwinger's source term with the same time dependent electric field (as described in the text) for $P_T = 1.0$ GeV, $t_0 = 0.5$ fm and $\theta = 0$
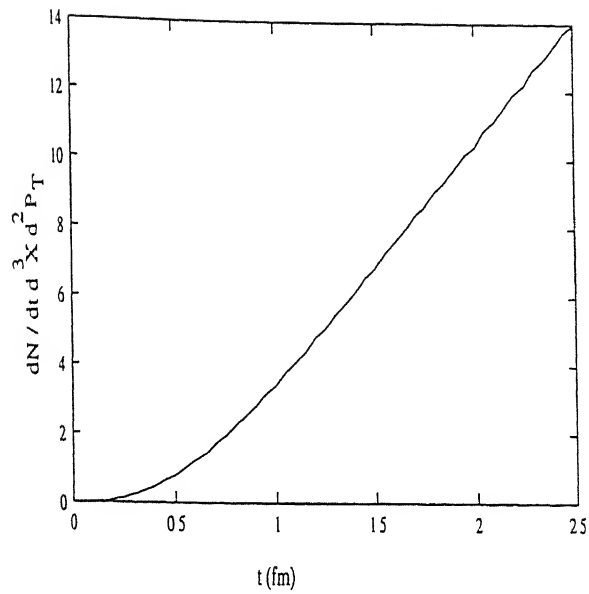
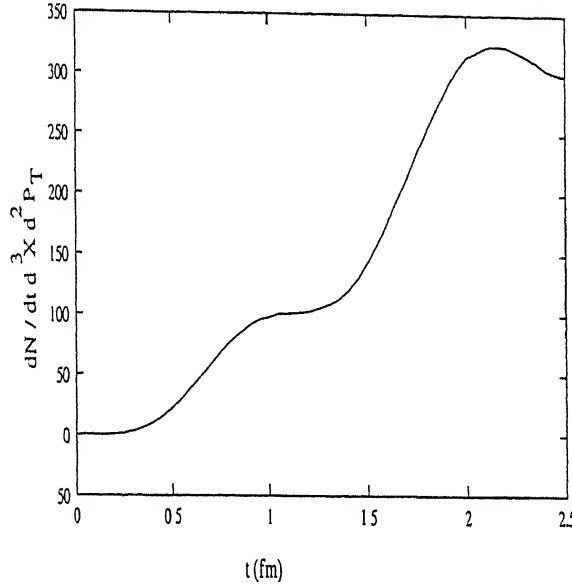Figure 6.5 The rate of quark production ($\frac{dN}{dt d^3 X d^2 P_T}(GeV^2)$) obtained by the new source term from a time dependent electric field for $P_T = 5\,0$ GeV, $t_0 = 0.5$ fm and $\theta = 0$
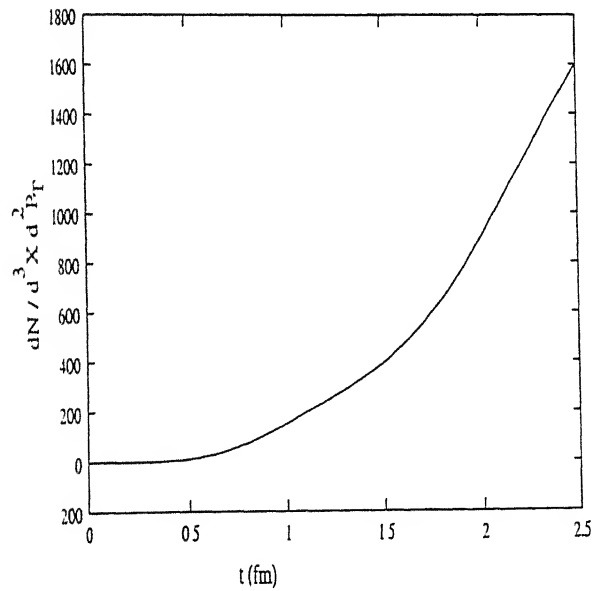
Figure 6.6: The quark production ($\frac{dN}{d^3 X d^2 P_T}(GeV\ )$) obtained by the new source term from a time dependent electric field for $P_T = 0.5$ GeV, $t_0 = 0.5$ fm and $\theta = 0$
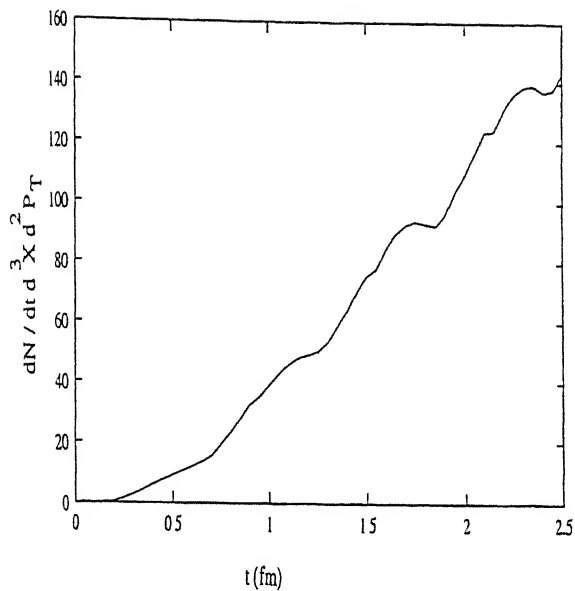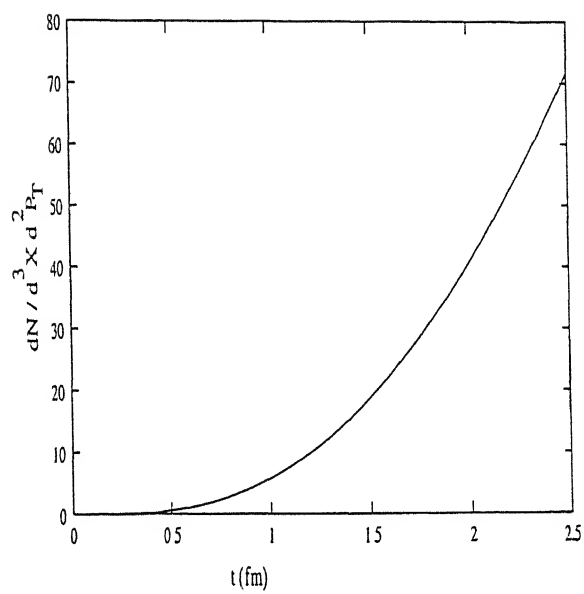
Figure 6.7: The quark production ($\frac{dN}{d^3 X d^2 P_T}(GeV\ )$) obtained by the new source term from a time dependent electric field for $P_T = 5.0$ GeV, $t_0 = 0.5$ fm and $\theta = 0$

6.3 Source term for a τ dependent electric field

As seen in the previous chapters, for a 1+1 dimensional expanding quark-gluon plasma we have employed Bjorken's boost invariance formalism according to which the longitudinal boost are the symmetry operations on the particle production. The boost invariant parameters are $\tau = \sqrt{(t^2 - z^2)}$, P_T and $\xi = \eta - y$ with $\eta = tanh^{-1}(z/t)$ and $y = tanh^{-1}(P_3/P_0)$. The source term for particle production ($\frac{dN}{dtd^X d^2 P_T}(\tau, \xi, P_T)$), needed in the transport equation depends only on these boost invariant parameters. In this section we derive such a source term which is needed in the transport equation to study production and equilibration of quark-gluon plasma in ultrarelativistic heavy-ion collisions.

In terms of these variables we get $dtdz = \tau d\tau d\eta$ and

$$S = \int_0^\tau \tau' d\tau' d\eta dx dy \mathcal{L}_I(\tau', \eta, x, y). \tag{6 20}$$

(this equation is analogous to Eqn. (7) for a purely time dependent electric field). To be consistent with the previous chapters we work in the Lorentz gauge $\partial^\mu A^\mu = 0$ with $A^\mu = \epsilon^{\mu\nu}\partial_\nu G(\tau)$ where $\mu, \nu = 0, 3$. Due to this choice the chromo-electric field depends only on the boost invariant quantity τ which is given by

$$E(\tau) = [\frac{d^2}{d\tau^2} + \frac{2}{\tau}\frac{d}{d\tau}]G(\tau) = [\frac{d}{d\tau} + \frac{2}{\tau}]G'(\tau). \tag{6.21}$$

Following the same procedure as was done for the time dependent case above, we get

$$|< Q, X, P|S|0 >|^2 = \Sigma_{i,j,l} \int d^3\vec{k_1} d^3\vec{k_1'} d^3\vec{k} < Q|i > < j|Q >^* T_{il}^a T^{*b} l_j < X, P, |k_1 > < k_1'|X, P >^*$$

$$\int_0^\tau d\tau_1 \tau_1 \int_0^\tau d\tau_2 \tau_2 d\eta_1 d\eta_2 g(k_1, k, k_1', k, \tau_1, \tau_2, \eta_1, \eta_2) \exp(i(k_1^0 + k^0)\tau_1 cosh\eta_1)$$

$$\exp(-i(k_1'^0 + k^0)\tau_2 cosh\eta_2)\exp(-i(k_{1z} + k_z)\tau_1 sinh\eta_1)\exp(i(k_{1z}' + k_z)\tau_2 sinh\eta_2)$$

$$\delta^2(\vec{k_{1T}} + \vec{k_T})\delta^2(\vec{k_{1T}'} + \vec{k_T}) \tag{6.22}$$

where the expression for $g(k_1, k, k_1', k, \tau_1, \tau_2, \eta_1, \eta_2)$ is given in the appendix for massless quark. In the above equation we have used the fourier transformation $A(t, z, X_t) = \int d^2 K_t A(t, z, \vec{K}_t) \exp(-\imath K_t \cdot X_t)$, with $A(t, z, K_t = 0)$ for the vector potential which depends only on t and z. Eqn (6.22) can be further simplified and is written as

$$|< Q, X, P|S|0 >|^2 = N^2 C(Q) \int dk_{1z} dk_{1z}' d^2 \vec{k}_T dk_z \exp(-(k_T - P_T)^2/Q_T^2)$$

$$\exp(-((k_{1z} - P_3)^2 + (k_{1z} - P_3)^2)/2Q_3^2) \int_0^\tau d\tau_1 \tau_1 \int_0^\tau d\tau_2 \tau_2 d\eta_1 d\eta_2$$

$$g(k_1, k, k_1', k, \tau_1, \tau_2, \eta_1, \eta_2) \exp(\imath(k_1^0 + k^0)\tau_1 \cosh\eta_1) \exp(-\imath(k_1'^0 + k^0)\tau_2 \cosh\eta_2)$$

$$\exp(-\imath(k_{1z} + k_z)\tau_1 \sinh\eta_1)\exp(\imath(k_{1z}' + k_z)\tau_2 \sinh\eta_2) \exp(-\imath(k_{1z} - k_{1z}')X_3), \qquad (6.23)$$

with $k^0 = \sqrt{(k_T^2 + k_z^2)}$, $k_1^0 = \sqrt{(k_T^2 + k_{1z}^2)}$ and $k_1'^0 = \sqrt{(k_T^2 + k_{1z}'^2)}$. Substituting $X_3 = \tau \sinh\eta$ and $P_3 = P_T \sinh y$ with $\xi = \eta - y$ we get

$$|< Q, X, P|S|0 >|^2 = N^2 C(Q) \int dk_{1z} dk_{1z}' d^2 \vec{k}_T dk_z \exp(-(k_T - P_T)^2/Q_T^2)$$

$$\exp(-((k_{1z} - P_T \sinh y)^2 + (k_{1z} - P_T \sinh y)^2)/2Q_3^2) \int_0^\tau d\tau_1 \tau_1 \int_0^\tau d\tau_2 \tau_2 d\eta_1 d\eta_2$$

$$S(k_1, k, k_1', k, \eta_1, \eta_2) G'(\tau_1) G'(\tau_2) \exp(\imath(k_1^0 + k^0)\tau_1 \cosh\eta_1)\exp(-\imath(k_1'^0 + k^0)\tau_2 \cosh\eta_2)$$

$$\exp(-\imath(k_{1z} + k_z)\tau_1 \sinh\eta_1)\exp(\imath(k_{1z}' + k_z)\tau_2 \sinh\eta_2)\exp(-\imath(k_{1z} - k_{1z}')\tau \sinh(\xi + y)) \qquad (6.24)$$

where

$$S(k_1, k, k_1', k, \eta_1, \eta_2) G'(\tau_1) G'(\tau_2) = g(k_1, k, k_1', k, \tau_1, \tau_2, \eta_1, \eta_2). \qquad (6.25)$$

Integrating this expression over P_3 and taking derivative w.r.t. τ we arrive at the new source trem,

$$\frac{dN}{dt d^3 x d^2 P_T} = P_T \frac{d}{d\tau} \int dy \cosh y |< Q, X, P|S|0 >|^2. \qquad (6.26)$$

which depends only on the boost invariant quantities τ, ξ and P_T. This source term will be used in the transport equation to study the production and equilibration of quark-gluon plasma in ultrarelativistic heavy-ion collisions. This work will be taken up separately.

6.4 APPENDIX

For $m = 0$ one obtains

$$f(t_1, t_2, k_1, k_2, k_1', k_2') = \frac{1}{B}(I_1 + I_2) \tag{6 27}$$

where

$$B = \sqrt{k_1^0 k_1'^0 k_2^0 k_2'^0} \tag{6.28}$$

and

$$I_1 = [(k_1 \cdot A)(k_2 \cdot A^*)(4k_1'^0 k_2'^0 - (k_1' \quad k_2)) + (k_1' \cdot A)(k_2 \cdot A^*)(k_1 \cdot k_2') + (k_1 \quad A)(k_1' \cdot A^*)(k_1' \cdot k_2)$$

$$- (k_1' \cdot A)(k_2' \quad A^*)(k_1 \cdot k_2)] + [(k_1 \cdot A^*)(k_2 \quad A)(4k_1'^0 k_2'^0 - (k_1' \cdot k_2)) + (k_1' \cdot A^*)(k_2 \cdot A)(k_1 \quad k_2') +$$

$$(k_1 \cdot A^*)(k_1' \cdot A)(k_1' \cdot k_2) - (k_1' \cdot A^*)(k_2' \cdot A)(k_1 \cdot k_2)] + (\vec{A} \cdot \vec{A^*})[4k_1'^0 k_2'^0 (k_1 \cdot k_2) + (k_1 \cdot k_1')(k_2 \cdot k_2')$$

$$+ (k_1 \cdot k_2)(k_1' \cdot k_2') - (k_1 \cdot k_2')(k_1' \cdot k_2)] + [((k_1 \cdot A)(k_1' \cdot A^*) - (k_1 \cdot A^*)(k_1' \cdot A))(k_1 \cdot k_2') + ((k_2 \cdot A^*)$$

$$(k_2' \cdot A) - (k_2 \cdot A)(k_2' \cdot A^*))(k_1 \quad k_1'] \tag{6.29}$$

and

$$I_2 = (k_1 \cdot A)(k_2 \cdot A^*)[2k_1'^0 k_2'^0 - (k_1' \cdot k_2')] + (k_1 \quad A)(k_2' \cdot A^*)[(k_2 \cdot k_1') - 2k_1'^0 k_2^0] + (k_1 \cdot A^*)(k_2 \cdot A)$$

$$[2k_1'^0 k_2'^0 - (k_1' \cdot k_2')] + (k_1 \cdot A^*)(k_2' \cdot A)[(k_2 \cdot k_1') - 2k_1'^0 k_2^0] + (k_1' \cdot A)(k_1 \cdot A^*)(k_2 \cdot k_2') -$$

$$(k_1' \cdot A^*)(k_1 \cdot A)(k_2 \cdot k_2') + (k_1' \cdot A^*)(k_2 \cdot A)[(k_1 \cdot k_2') - 2k_1^0 k_2'^0] + (k_1' \cdot A^*)(k_2' \cdot A)[-(k_1 \cdot k_2)$$

$$+2k_1{}^0k_2{}^0] + (k_1' \cdot A)(k_2 \cdot A^*)[(k_1 \cdot k_2') - 2k_1{}^0k_2'{}^0] + (k_1' \cdot A)(k_2' \cdot A^*)[-(k_1 \cdot k_2) + 2k_1{}^0k_2{}^0]$$

$$+(k_2 \cdot A)(k_2' \cdot A^*)[(k_1 \cdot k_1') - 2k_1{}^0k_1'{}^0] + (k_2' \cdot A)(k_2 \cdot A^*)[-(k_1 \cdot k_1') + 2k_1{}^0k_1'{}^0] - \vec{A} \cdot \vec{A}^*$$

$$[2k_1{}^0k_2'{}^0(k_2 \cdot k_1') - 2k_1{}^0k_2{}^0(k_1' \cdot k_2') + k_1'{}^0k_2{}^0(k_1 \cdot k_2') - k_1'{}^0k_2'{}^0(k_1 \cdot k_2)] \quad (6.30)$$

More generally $f(t_1, t_2, k_1, k_2, k_1', k_2') = f^{a,b}(k_1, k_2, k_1', k_2')$ where $A = A^a \, and \, A^* = A^b$.

and

$$g(k_1, k_1', k_2, \tau_1, \tau_2, \eta_1, \eta_2) = \frac{I}{C} \quad (6.31)$$

with

$$C = k_2^0 \sqrt{k_1^0 k_1'^0} \quad (6.32)$$

and

$$I = A \cdot A^*[2k_2^{0^2}(k_1 \cdot k_1') + 2k_1{}^0k_2{}^0(k_2 \cdot k_1') - 6k_1'{}^0k_2{}^0(k_1 \cdot k_2)] + (k_1 \cdot A)(k_2 \cdot A^*)(6k_1'{}^0k_2{}^0)$$

$$+(k_2 \cdot A)(k_1 \cdot A^*)(6k_1'{}^0k_2{}^0) - (k_1' \cdot A)(k_1 \cdot A^*)(2k_2{}^0k_2{}^0) + (k_1' \cdot A^*)(k_1 \cdot A)(2k_2{}^0k_2{}^0)$$

$$-(k_1' \cdot A)(k_2 \cdot A^*)(2k_1{}^0k_2{}^0) - (k_1' \cdot A^*)(k_2 \cdot A)(2k_1{}^0k_2{}^0) + A^0[(k_1 \cdot A^*)2k_2^0(k_2 \cdot k_1')$$

$$+(k_2 \cdot A^*)2k_2^0(k_1 \cdot k_1') - (k_1' \cdot A^*)2k_2^0(k_1 \cdot k_2)] + A^{0*}[(k_1' \cdot A)2k_2^0(k_2 \cdot k_1)$$

$$-(k_1 \cdot A)2k_2^0(k_2 \cdot k_1') - (k_2 \cdot A)2k_2^0(k_1 \cdot k_1')] \quad (6.33)$$

$(in \; Eqn. \; 6.31)$

Here $A_0 = -sinh\eta_1 G'(\tau_1)$, $A_3 = cosh\eta_1 G'(\tau_1)$, $A_0^* = -sinh\eta_2 G'(\tau_2)$, $A_3^* = cosh\eta_2 G'(\tau_2)$ and

other A's are zero.

Chapter 7

J/Ψ suppressions in a thermally equilibrating quark-gluon plasma at RHIC

7.1 INTRODUCTION

As mentioned earlier, dileptons and single photons have long been proposed as useful probes of the plasma[7], as once produced, they hardly interact with the strongly interacting matter and thus carry the details of the circumstances of their production. However, as they are also produced via hadronic decays in the later stages of evolution, where plasma expands and cools,

ıt becomes difficult to distinguish between them. In that sense the production of $c\bar{c}$ is a clean process, as it is not produced ın the later stages due to its heavy mass. The production of $c\bar{c}$ takes place mainly at the hard vertex. Once produced, $c\bar{c}$ will evolve in to open D mesons and charmonium states, such as J/ψ, χ, etc., while travellıng through this dense phase of matter. Unlike hadronic collisions, where an enhancement of J/ψ is found at tevatron energy[72], both $c\bar{c}$ and J/ψ get suppressed while travelıng through different stages of quark-gluon plasma. There might be thermal charm productions in the very early stage of the plasma, where the temperature is very hıgh, but no production of $c\bar{c}$ can occur in the later stages due to decrease ın the temperature.

We agaın mention that. the various stages by which the complete evolutıon of quark-gluon plasma is descrıbed in URHIC are, i) pre-equilibrium, ii) equilibrium, where one actually studies the thermalised quark-gluon plasma, iii) cooling and iv) hadronisatıon. The production of an equilibrated quark-gluon plasma in stage (ii) crucially depends on the pre-equilibrium evolutıon, ı.e. on stage (i). Matsui and Satz[5] have suggested the suppressıon of J/ψ in the equilibrıum phase. In their study, the debye screening length whıch ıs calculated from lattice QCD, is found to be less than the J/ψ radius. This forbids the binding of $c\bar{c}$ to J/ψ in the equilibrated quark-gluon plasma. However. such a study ıs not available for an equilibrating quark-gluon plasma. There could be many interesting effects in the pre-equilibrium stage, when $c\bar{c}$ or J/ψ travel before reaching the equilibrium stage. As high energy deconfined partons are also present in the pre-equilibrium stage, J/ψ is suppressed due to its interaction with these deconfined partons. Since the J/ψ dissocıation cross section inside a deconfined partons is very different from that inside a hadronic gas (see section II), the study of J/ψ suppression can then provide us information on color deconfinement in the quark-gluon plasma.

Another outcome of the pre-equilibrium study is the prediction of the equilibration time, the time at which quark-gluon plasma equilibrates. A detailed knowledge of equilibration time and J/ψ formation time is very crucial in determining the J/ψ suppressions in URHIC. This is because, a large equilibration time may permit a J/ψ formation from $c\bar{c}$ pairs before plasma equilibrates. Then the interaction of a fully formed J/ψ with deconfined partons is prefered than screening. If the J/ψ formation time is greater than the equilibration time or comparable to it, then $c\bar{c}$ interacts with the deconfined partons before screening starts operating in the equilibrium stage. The interaction of a $c\bar{c}$ with the partons before plasma equilibriates is not studied yet, and such a calculation is beyond the scope of this thesis.

As mentioned earlier, a careful study of pre-equilibrium evolution of quark-gluon plasma is the consistent way to study production and equilibration of quark-gluon plasma in URHIC. From this point of view it is necessary to study what happens actually to the J/ψ suppressions at different stages of evolution of QGP, rather than estimating it in an equilibrated quark-gluon plasma. We study here the suppression of a fully formed J/ψ in equilibrating quark-gluon plasma using short distance QCD. The J/ψ may also be suppressed in later stages due to inelastic collisions with hadrons, but we do not consider it here. This suppressions will be less due to lesser value of the hadron-J/ψ inelastic cross section (described in section II).

However, J/ψ suppression is also measured in p-A collisions where there is no existence of quark-gluon plasma[73, 55]. At these experiments the suppression of J/ψ is due to the presence of a nuclear medium. The prominent mechanism by which these datas are explained at SPS is via nuclear absorption, the suppression of a nascent J/ψ before it forms a physical resonance[56, 74]. Within this mechanism, one does not assume the existence of a quark-gluon plasma phase or a highly densed deconfined partonic medium. This is the case with some light nuclei collisions

at SPS[73, 55]. However the recent measurements of J/ψ suppression by NA50 collaboration[57] (Pb-Pb collisions at $\sqrt{s} = 17 GeV$) yeild an excess suppression of J/ψ, which is not explained by the above conventional approach. Presence of a nuclear medium may not be enough to explain this data. There are speculations that this suppression is due to the existence of a deconfined partonic medium[58] or a high energy density matter[59].

Whether an equlibrated plasma has formed in Pb-Pb collisons at SPS($\sqrt{s} = 17 GeV$) or not, is debatable, but at RHIC(Au-Au collisions at $\sqrt{s} = 200 GeV$) we may go closer to the equilibrated quark-gluon plasma. In this chapter we estimate the J/ψ suppressions at RHIC for a thermally equilibrating quark-gluon plasma.

However before studying charmonium suppressions in quark-gluon plasma it is essential to study the corresponding situations in hadronic collisions. The experimental analysis of quarkonia production in high energy hadronic collisions at tevatron energy[72] revealed a drastic disagreement with the predictions from color singlet model[75]. A substantial fraction of quarkonium production at very high energy arises from intermediate color octet fluctuation during the evolution into final state color singlet $Q\bar{Q}$ pair. Now a rigorous theoretical foundation has been achived by Bodwin, Braaten, and Leepage[76], who devloped a QCD formalism by marrying pQCD and an effective field theory within non-relativistic QCD(NRQCD). This formalism accounts for the production of both color singlet and color octet $c\bar{c}$ states, that evolve in to final color singlet quarkonium. Within NRQCD, the production amplitude is expanded in powers of both the strong coupling α_s and the velocity of heavy quark($v^2 = .23$ for $c\bar{c}$ system), which includes higher fock-state components. The long distance non-pertubative matrix element is either fitted from experiments or taken, in principle, from lattice QCD[77]. This technique has been used to study many heavy quarkonium production processes in hadronic collisons. However a space

time evolution of quarkonium using this technique has not been achived. This is crucial for studying the evolution of J/ψ in nuclear collisions. The existence of background chromoelectric field[45] and high dense partonic medium complicates the study of the evolution of $c\bar{c}$ to J/ψ, both at RHIC and LHC. As $c\bar{c}$ takes $\simeq 1.0$ fm (time in $c\bar{c}$ rest frame) to form a J/ψ bound state, it interacts with the nearby light partons and with the background chromoelectric field during this period. No attempts is made on this line to study J/ψ production and its subsequent evolution in nucleus-nucleus collisions. This might be the consistent way to study J/ψ suppression in URHIC.

Since we study the suppression of J/ψ in equilibrating quark-gluon plasma, it is relevant to discuss the process of equilibration of QGP in URHIC, which is not completely studied yet. The rate of equilibration is different for diiferent models (see chapter 8). Some relevant models that describe the equilibration of QGP are parton cascade model(PCM)[17], heavy-ion jet interaction generator(HIJING)[78] and color flux-tube model. PCM and HIJING are both perturbative QCD based models, and color flux-tube model is a field theoritical model. The former models describe the evolution of hard and semihard partons and the later describes the production of soft partons via non-perturbative Schwinger mechanism. For a complete study of production and equilibration of quark-gluon plasma, color flux-tube model may be combined with the pQCD based models. We use here the distribution of partons from parton cascade model to study J/ψ suppressions in a thermally equilibrating quark-gluon plasma at RHIC. A study of J/ψ suppressions in a chemically equilibrating quark-gluon plasma within HIJING model can be found in the ref.[10]. As mentioned in chapter 4 the J/ψ suppressions in a thermally equilibrating quark-gluon plasma within color flux-tube model will be calculated once hard partons are added to it via a minijet source term. Within parton cascade model, a relativistic transport equation is solved to study the distribution of partons by considering the direct collision processes $2 \rightarrow 2$,

the inelastic collision processes $2 \to 1$, and the decay processes $1 \to 2$[17]. More explicitely, this is written as

$$p^\mu \partial_\mu f_i(x,p) = C_i(x,p) \qquad (7.1)$$

where $f_i(x,p)$ is the distribution of a particular type of parton i in the usual phase space. The collisions term $C_i(x,p)$ is derived from pQCD taking all the processes mentioned above. The initial condition on $f_i(x,p)$ is the distribution of partons inside the nucleus before the two nuclei collide with each other[38]. However for a complete study, the addition of soft partons and the effect of background field has to be taken into account. These backgruond electric field may not exit in the very early stage where pQCD is applicable[41], but in later times this will have an important role in the equilibration of the plasma[41, 40]. Such calculations may be available once the color flux-tube model is combined to the pQCD based models.

In section **II** we describe the short-distance QCD and the dissociation of J/ψ. Results and discussions are presented in section **III**, for RHIC energy. We summarise and conclude the main results in section **IV**

7.2 J/ψ dissociation by deconfined gluons

In the framework developed by Bhanot and Peskin[79, 80], interactions between light hadrons and deeply bound, heavy quarkonium states, such as the J/ψ, are mediated by short-range color dipole interactions. For sufficiently heavy quarks, the dissociation of quarkonium states by interaction with light hadrons is fully accounted for by short-distance QCD[79, 80]. Because of its small size, a heavy quarkonium can probe the short distance properties of light hadron. A parton based calculation of the J/ψ-hadron cross section is thus possible via an operator product

expansion method, similar to that used in deeply inelastic lepton-hadron scatterings[79–82]. These pertubative calculations become valid when the space and time scale associated with the quarkonium state, r_Q and t_Q, are small in comparison to the nonperturbative scale λ_{QCD}^{-1}, which is the characteristic size of the light hadrons, i.e. $r_Q <<< \lambda_{QCD}^{-1}$, and $t_Q <<< \lambda_{QCD}^{-1}$. For J/ψ ground state $r_{J/\psi} \simeq 0.2 fm = (1 GeV)^{-1}$ and $E_{J/\psi}(2M_D - M_{\psi'}) \simeq 0.64$ GeV. With $\lambda_{QCD} = 0.2 GeV$, the above inequalities seem to be well satisfied[54] and one expect that the dissociation of J/ψ by hadron will be governed by the J/ψ-hadron break-up cross section as calculated in short distance QCD. The operator product expansion allows one to express the hadron-J/ψ inelastic cross section in terms of the convolution of the gluon-J/ψ dissociation cross section with the gluon distribution inside the hadron. The gluon-J/ψ dissociation cross section is given by[79, 80, 82]:

$$\sigma(q^0) = \frac{2\pi}{3}(32/3)^2(\frac{16\pi}{3g_s^2})(1/m_Q^2)\frac{(q^0/\epsilon_0 - 1)^{3/2}}{(q^0/\epsilon_0)^5}. \qquad (7.2)$$

Here g_s is the coupling between gluon and charm quark, m_Q the charm quark mass, and q^0 the gluon energy in the J/ψ rest frame. The heavy quarkonium is coulomb like, and one writes, $\epsilon_0 = (\frac{3g_s^2}{16\pi})^2 m_Q$[79, 82].

The gluons which are soft inside a pion are not capable of dissociating a charmonium. Hence they give a low π-J/ψ cross-section. However, deconfined gluons, which carry enough energies, are sufficient to break a charmonium[54]. These high energy partons are present in URHIC, as observed in several calculations, such as[45, 17]. These deconfined gluons can break a fully formed J/ψ that exit inside QGP. This conclusion does not seem to be affected substantially by nonperturbative effects[83].

We use the above g-J/ψ dissociation cross section to study the J/ψ suppressions in a thermally equilibrating quark-gluon plasma at RHIC. For the central collisions, the J/ψ survival probab-

ility is:

$$S_{g-J/\psi}(P_T) = \exp[-\int d\tau n_g(\tau) < v_{rel}\sigma(k\cdot v) >_k]. \tag{7.3}$$

Here $n_g(\tau)$ is the gluon number density which evolves as system expands longitudinally. According to Bjorken scenerio[2], this number density is a function of the boost invariant parameter τ ($\tau = \sqrt{(t^2 - z^2)}$) The thermal average g-$J/\psi$ cross section, $< v_{rel}\sigma(k\cdot v) >_k$, is

$$< v_{rel}\sigma(k\cdot v) >_k = \frac{\int d^3k v_{rel}\sigma(k\cdot v)f(k^0, T(\tau))}{\int d^3k f(k^0, T(\tau))}. \tag{7.4}$$

Here $v(\equiv (M_T, \vec{P_T}, 0)/M_{J/\psi})$ is the four-velocity of J/ψ in central rapidity region and k is the four-momentum of gluon in the parton gas. In the thermal average cross-section we use the distribution function, $f(k^0, T(\tau)) = \frac{a(\tau)}{\exp(k^0/T(\tau))-1}$ for gluon. Here $a(\tau)$ captures the deviation from equilibrium, which in principle, is determined from the relation, $n_g(\tau) = \int d\Gamma(p^\mu u_\mu)f(p, T(\tau))$, by knowing the evolution of temperature and n_g, for an equilibrating quark-gluon plasma. Here $d\Gamma = \frac{\gamma d^3 p}{(2\pi)^3 p_0}$ with $\gamma = 2 \times 8$(the product of spin and color degeneracy), and u(= (t/τ, 0, 0, z/τ)) is the flow velocity. However, as $a(\tau)$ cancels both from numerator and denominator of equation(7.4), we need not know its form. What matters is $n_g(\tau)$ and T(τ) whose evolutions are taken from PCM[17]. Within PCM, $n_g(\tau) \simeq 0.72 n(\tau)$, with $n(\tau) = 565 fm^{-3}(\frac{\tau}{\tau_0})^{-0.90}$ and $T(\tau) = 950 MeV(\frac{\tau}{\tau_0})^{-0.30}$, for a thermally equilibrating quark-gluon plasma at RHIC. Here $\tau_0 = .05 fm$. Using this distributions the integration in equation (7.3) is performed numerically to study the J/ψ survival probability.

7.3 Results and discussions

In Fig-7.1 we present the thermal averaged gluon-J/ψ cross section as a function of J/ψ transverse momentum P_T, for different values of temperature. It can be seen that this value is de-

creased as the temperature of the plasma is increased. Also for J/ψ with high P_T this thermal
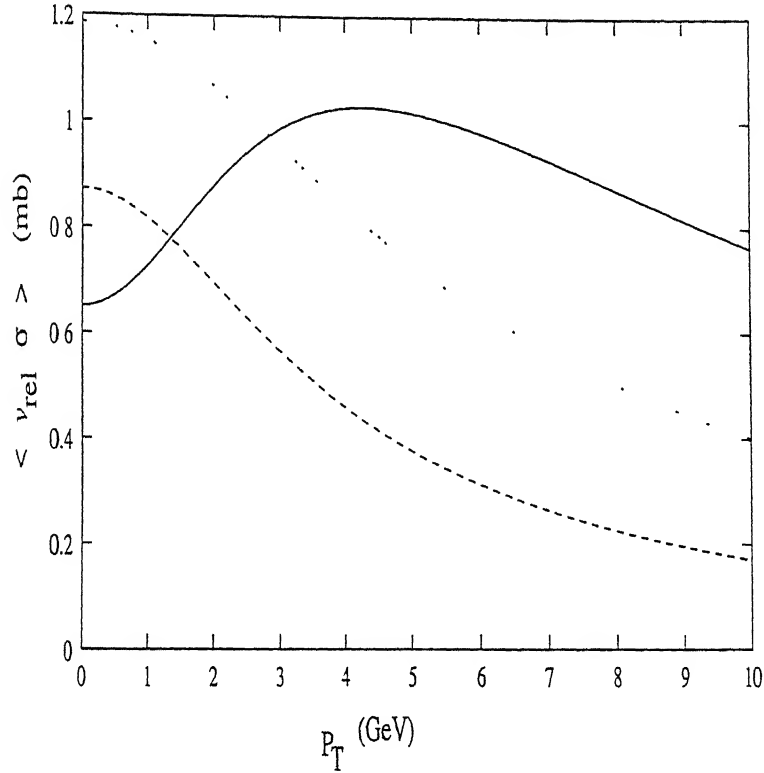
Figure 7.1: The thermal averaged gluon-J/ψ cross section $< v_{rel}\sigma >$ (mb) as a function of transverse momentum P_T at different temperatures. Solid line refers to T= 0.2 GeV, upper broken line corresponds to T= 0.4 GeV and lower broken line refers to T=0.8 GeV.

cross section becomes less. This has a direct impact on J/ψ suppression. As P_T becomes large

the survival probability must increase. However, due to large initial parton density formed in

the initial stage of the plasma, these smaller thermal cross sections do not have a large effects

on the total survival probability. This is shown in Fig-7.2 where we have plotted the survival

probability $S_{g-J/\psi}$ as a function of P_T for a thermally equilibrating QGP at RHIC within PCM.

As can be seen, the suppression is almost 100 percent for J/ψ with low transverse momentum.

Even for J/ψ with high $P_T(\simeq 10 GeV)$ the suppression is about 95 percent. This huge suppres-

sion is due to the presence of a highly densed deconfined partonic medium at RHIC. As can

be seen from equation(7.3) and Fig-7.1 this suppression will be more for a plasma with larger
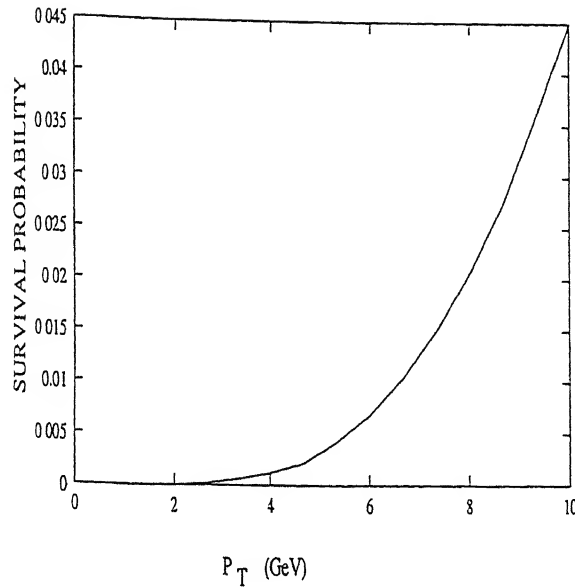
Figure 7.2: The survival probability of J/ψ in a thermally equilibrating plasma at RHIC.

number density and lower temperature. A denser and cooler plasma is obtained once the soft partons studied within the color flux-tube model in earlier chapters are added to pQCD based models such as PCM. The measurement of such huge suppression will reveal the existence of such a deconfined partonic medium, possibly a thermalised quark-gluon plasma, at RHIC.

However, what one actually measures experimentally is the total survival probability. This implies that other sources of J/ψ suppression, without the existence of a QGP phase, have to be singled out from the total survival probability in order to see the suppressions only from this deconfined partonic medium. If the estimated suppression due to all sources without QGP phase is much less than the experimental findings, one may then hope that the rest of the suppressions is due to the existence of a highly densed deconfined partons. The experimental measurement of J/ψ at RHIC will be able to reveal all the possibilities and may explain the existence of such a deconfined partonic medium, possibly a thermalised quark-gluon plasma.

On the other hand J/ψ enhancement can occur due to an increase in the (thermal)charms

produced at a very high temperature, especially in the initial stage of the evolution of the system[85, 86] We recall that screening of J/ψ was originally[5] proposed without taking production of thermal charms into account, which was argued to be negligible at $T \simeq 200$ - 300 MeV However, the system may approach a temperature which is as large as 900 MeV initially, and can therefore produce a large number of thermal charms at RHIC So to make resonable estimates at RHIC and LHC, one has to take into account both thermal and hard J/ψ. For simplicity, we have not considered here those J/ψ which are created from thermal charms.

7.4 Conclusion

Applying short distance QCD mechanism and taking parton cascade model for the evolution of quark-gluon plasma at RHIC we have found a huge suppression (almost 100 percent) of J/ψ which are produced from primary charm quarks. In principle, the total survival probability is written as

$$S_T = S_{g-J/\psi} S_{other} \tag{7.5}$$

where first one ($S_{g-J/\psi}$) is due to g-J/ψ dissociation, and the last one(S_{other}) is due to any other possible sources of suppression[11–14] such as nuclear absorption, final state comover scatterings etc. As the hadron-J/ψ cross section is smaller than g-J/ψ cross section[54], we expect a lesser suppression of J/ψ in the hadronisation stage. The prominent suppression seems to be due to the nuclear absorption (60 percent at RHIC[9]) and J/ψ dissociation in the deconfined partonic system. Hence the measurement of a huge J/ψ suppression at RHIC may suggest the existence of a partonic plasma. However, many refinements, such as space time evolution of quarkonium production in nucleus-nucleus collision using NRQCD has to be worked out, before unambigous

conclusions can be drawn for the pre-resonance suppression of J/ψ. Also, the contribution from thermal J/ψ, which may not be neglible at RHIC and LHC, has to be taken into account. It is only after incorporating the above features the certainty of screening can be justified.

In any case, we have shown here the importance of the thermally equilibrating quark-gluon plasma on J/ψ suppression. This suppression depends on variuos models which describes the thermal evolution. From the measurement of this suppression, the validity of these models for thermal evolution of quark-gluon plasma at RHIC can be checked.

Chapter 8

A brief description of other Models and approaches

8.1 Dynamical Models in heavy-ion collisions

8.1.1 Hevy-ion jet interaction generator (HIJING)

Heavy-ion jet interaction generator model[37] is a pQCD inspired model where the non-perturbative part is modeled phenomenologically The evolution of hard and semihard partons are described by pQCD. The intitial condition is estimated by HIJING monte carlo code in which initial direct parton scatterings are taken into account. The produced parton gas in the central rapidity region approaches thermal and chemical equilibrium through elastic scatterings and induced ra-

diations. In an overlap region of 1fm thickness (of the two nuclei) a local isotropy in momentum distributions assumed and is estimated to be achieved in a time period of 0.5-0.7 fm through free-streaming evolution. It is further assumed that this is the actual kinetic equilibration (or thermalisation) time for the partonic system. Though this assumption is not well founded, this is the best that the model incorporates in the absence of a complete calculation of the relaxation time. Within this model the scattering processes which maintain thermal equilibrium are $gg \leftrightarrow gg, gq \leftrightarrow gq$ etc.. Further chemical equilibration of partons is studied by by solving master rate equations, where $gg \leftrightarrow ggg$ and $gg \leftrightarrow q\bar{q}$ processes are taken into account. Asssuming that the parton scatterings are sufficiently rapid so as to mainatin thermal equilibrium, and therefore neglecting the effects of viscosity due to elastic and inelastic scatterings, one determines the evolution of the energy density from the hydrodynamic equation. The master equations are solved self consistently[37] to obtain the time evolution of the temperature and fugacities. It is found that the parton gas cools considerably faster than the Bjorkens scaling law ($T^3\tau = cons.$), because the production of additional partons during the approach to chemical equilibrium consumes an appreciable amount of energy. It is shown within this model that the equilibration can hardly reach before the temperature drops below $200 MeV$ in the short period time of 1-2 fm at RHIC energy. However, at LHC energy the parton gas, especially the gluon component, becomes very close to equilibrium and the plasma may exist in a deconfined phase for as long as 4-5 fm. One observation of this model is that the quarks never reach chemical equilibrium at both energies.

8.1.2   Parton Cascade Model (PCM)

The parton cascade model[17] is a relativistic kitetic model for high energy nuclear collisions which is inspired by the parton picture of hadronic collisions. The dynamics of the space time evolution of quarks and gluons is studied by the interaction of partons in the framework of perturbative QCD. The time devlopment of parton cascades is taken in six-dimensional phase space of coordinate and momenta according to a semiclassical, relativistic transport equation with a collision kernel that contains the asymptotically dominant perturbative QCD interaction processes among the partons. The time devlopement of the parton distributions, the number and type of interactions is determined by the dynamics itself. The transport equation which is solved is

$$p^\mu \partial_\mu F_a(r,p) = \Sigma_k I_a^(k)(r,p) \qquad (8.1)$$

where $F_a(r,p)$ is the phase-space distribution of the parton of type a and $I_a^(k)$ is the collision kernel for the collision terms. The initial state for the parton phase space distribution is taken from the experimantally measured nucleon structure functions and elastic nucleon form-factors, as well as nuclear shadowing corrections. The general form of collision term, $\sigma_k I_a^(K)(r,p)$, in the above equation includes a subset of all possible $n \rightarrow n'$ interaction proceses. These processes consists of $2 \rightarrow 2$ colisions, $2 \rightarrow 1$ fusions and $1 \rightarrow 2$ decays of partons in the lowest order perturbative QCD, plus higher order corrections which are associated with multiple emissions and absorptions of partons.

Within this study it observed that isotropy in the momentum distribution is reached very quickly, leading to very rapid thermalisation, almost after $0.2fm$ of maximum overlap of two nuclei at RHIC. The system is very dense ($n(\tau) = 565 fm^{-3}(\frac{\tau}{0.5})^{-0.90}$) and very hot ($T(\tau) = 950 MeV(\frac{\tau}{0.5})^{-0.90}$) within this study.

8.2   Lattice QCD studies

In the high temperature limit of QCD, the short range interactions among the partons become weak and the long range interactions become dynamically screened. As a consequence, hadronic matter at very high temperature do not exhibit confinement and chiral symmetry breaking. Lattice gauge theory which allows nonperturbative numerical calculation of observables in QCD predicts that the transition between low-temperature and high-temperature phases of QCD is not smooth but discontinuous. The order of chiral phase transition is sensitive to the number of light, dynamical quark flavors. This phase transition is of second-order for two massless flavors and is of first-order for three massless flavors. The numerical simulations of lattice gauge theory have predicted that the transition temperature lies in the range 150±10 MeV at vanishing net quark density. The simulations without dynamical quarks clearly exhibit a first-order phase transition at a temperature $T_c \simeq 260 MeV$. The quarks are not confined in the high temperature phase. The quark condensate $< \psi\bar{\psi} >$ shows a strong drop over the same temperature range, indicating that deconfinement and restoration of chiral symmetry go hand-in-hand. However, the simulations of lattice QCD with dynamical quarks have not yet overcome the limitations due to finite lattice size. More works in this area are now in progress regarding the order of phase transition.

Bibliography

[1] J. W. Harris and B. Muller, in Annual Review of nuclear and particle sciences, Vol. **46** 71 (1996) edited by Chris Quigg *al.* .

[2] J. D. Bjorken, Phys. Rev D27 (1983)140

[3] S. E. Eiseman *et al.*, Phys. Lett. **B297**, 44 (1992).

J. Barrette *et al.*, Z. Phys. **C59**, 211 (1993).

T. Abbott *et al.*, Phys. Rev. **C50**, 1024 (1994).

S. E. Eiseman *et al.*, Phys. Lett **B325**, 322 (1994).

J. Barrette *et al.*, Phys. Lett. **B351**, 93 (1995).

[4] E. Andersen *et al.*, Phys. Lett. **B327**, 433 (1994).

M. Gadzicki *et al.*, Nucl. Phys. Lett. **A590**, 197c (1995).

D. D. Bari *et al.*, Nucl. Phys. Lett. **A590**, 307c (1995) and refernces therein.

[5] T. Matsui and H. Satz, Phys. Lett . B178 416 (1986)

[6] M. T Strickland, Phys. Lett. B331 245 (1994).

[7] Jan-e Alam, Sibaji Raha and Bikash Sinha, Phys. Rep. **273** 243 (1996).

[8] J. Rafelski and B. Muller, Phys . Rev. Lett. 48 1066 (1982), C. P. Singh. phys. Rev. Lett. 56 870 (1990).

[9] Gouranga C Nayak, Journal of High Energy Physics 02 (1998) 005.

[10] Xiao-Ming Xu *et al.*, Phys. Rev. C 53, 3051 (1996).

[11] S. Gavin and R. Vogt, Phys. Rev. Lett. 78, 1006 (1997).

[12] C. Y. Wong, Phys. Rev. C 55, 2621 (1997).

[13] R C Hwa, T. Pisut and N. Pisutova, OITS 628 (1997).

[14] Rajiv V Gavai and Sourendu Gupta, TIFR/TH/97-07, Report No:- hep-ph/9703300, To appear in Phys. Lett. B.

[15] J. Rafelski and R. Hagedorn, in statistical Mechanics of Quarks and Hadrons, Ed. H. Satz, (North Holland, Amsterdam, 1981).

[16] S. Nagamiya, Nucl. Phys. A544 5c (1992).

[17] K. Geiger and J. Kapusta, Phys Rev D47 4905 (1993), and references therein.

[18] G. Baym, Phys. Lett. B138 18 (1984).

[19] K. Kajantie and T. Matsui, Phys. Lett B164 373 (1985).

[20] B. Andersson *et al.* Phys. Rep. 97, 31 (1983), Nucl. Phys B 281, 289 (1987).

[21] F E. Low, Phys. Rev. D12 163 (1975).

[22] S. Nussinov, Phys. Rev. Lett. 34 1286 (1975).

[23] J. Schwinger, Phys. Rev. 82 664 (1951).

[24] A Bialas et el. Nucl. Phys. B296 611 (1988).

[25] B. Banerjee, R. S. Bhalerao and V Ravishankar, Phys. Lett. B224 16 (1989).

[26] T T. Wu and C. N. Yang, Phys. Rev. D12 3843 (1975).

[27] R V Gavai, private communication.

[28] M. Asakawa and T. Matsui, Phys. Rev. D43 2871 (1991).

[29] U. Heinz. Phys. Rev. Lett. 51 351 (1983).

[30] S. K. Wong, Nuovo Cemento A65 689 (1970).

[31] H-T Elze and U. Heinz, Phys. Rep. **183** 81 (1989)

[32] U. Heinz. Ann. of Phys. (NY) **161** 48 (1985).

[33] R. Pisarski, Phys Rev. Lett. 63 1129 (1989).

[34] P. F. Kelly, Q. Liu, C. Lucchesi and C. Manuel, Phys. Rev Lett. 72 3461 (1994)

[35] P. F. Kelly, Q. Liu, C. Lucchesi and C. Manuel, Phys. Rev. 50 4209 (1994)

[36] B. Svetitsky, Phys. Rev D37 2484 (1988).

[37] X. N. Wang, Phys. Rep. **280**, 287 (1997).

[38] K. Geiger, Phys. Rep. **258**, 237 (1995).

[39] R. S. Bhalerao and V. Ravishankar, Phys. Lett B **409**, 38 (1997).

[40] K. J Eskola, B. Muller and X. N. Wang, Phys. Lett. B **374**, 20 (1996).

[41] K. J. Eskola and M. Gyulassy, Phys. Rev. C **47**, 2329 (1993).

[42] L. S. Brown and W. I. Weisberger, Nucl. Phys B. **157**, 285 (1979).

[43] H. Heiselberg and X. N. Wang, Phys. Rev. C **53**, 1892 (1996).

[44] C M. Hung and E.V Shuryak, report no hep-ph/9709264

[45] Gouranga C. Nayak and V. Ravishankar, Phys. Rev. **D55**, 6877 (1997): and references therein.

[46] Gouranga C Nayak and V. Ravishankar, Phys. Rev **C58** 356 (1998).

[47] M. Gyulassy and A. Iwazaki, Phys. Lett. B **165B**, 157 (1985).

[48] M. Gyulassy and L. P. Csernai, Nucl. Phys. A **460** 723 (1986).

[49] Increasing the accuracy by another 5 percent does not substantially alter the estimate.

[50] G. C. Nayak and V. Ravishankar, in preparation.

[51] see ref[41]. The Ohmic heating in the reference is realised by the particle production in our model.

[52] Stanislaw Mrowczynski, Phys. Lett. B **393** 26 (1997).

[53] see, e.g., K. Rajagopal, CALT-68-2104, who has discussed the possible impact of non-equilibrium state on the formation of disoriented chiral condensates.

[54] D. Kharzeev and H. Satz, *in Quark-Gluon plasma II, edited by* R. C Hwa (World Scientific , Singapore, 1995), p. 395

[55] C. Baglin *et al.* Phys Lett. B **270**, 105 (1991);
C. Baglin *et al. ibid* **345**, 617 (1995).

[56] C. Gerschel and J. Hufner, Z. Phys. C **56**, 171 (1992).

[57] M. Gonin et al. Nucl Phys. A **610**, 404c (1996).

[58] D Kharzeev, C. Lourenco, M. Nardi and H. Satz, Z. Phys C **74**, 307 (1997)

[59] J. P. Blaziot and J. Y. Ollitrarault, Phys. Rev. Lett. **77**, 1703 (1996)

[60] R. C Hwa, T. Pisut and N. Pisutova, **OITS** 628 (1997)

[61] B. Kampfer and O. P. Pavlenko, Phys. Lett. **B289** 127 (1992).

[62] L. D. McLerran and T. Toimela, Phys. Rev D 23 545(1985)

[63] K. Kajantie, M. Kajata, L. McLerran and P. V. Ruuskanen, Phys Rev. D 34 811 (1986).

[64] A. Bialas and J. P. Blaizot, Phys. Rev. D 32 2954 (1985).

[65] K. Geiger and J. I. Kapusta, Phys. Rev. Lett 70 1920 (1993).

[66] J. Kapusta, L. McLerran and D. K. Srivastava, Phys. Lett. **B283** 145 (1992).

[67] A. Karman, T. Matsui and B. Svetitsky, Phys. Rev. Lett. **56** 219 (1986) and references therein.

[68] A. Casher, H. Neuberger and S. Nussinov, Phys. Rev. **D20** 179 (1979).

[69] Coherent states, Applications in Physics and Mathematical Physics, edited by J. R. Klauder and Bo-Sture Skagerstam (World scientific, 1985).

[70] Mark Byrd, DOE-ER-40757-104, UTEXAS-HEP-97-18 (1997), Report No:- physics/9708015.

[71] A. K. Ganguli, P. K. Kaw and J. C. Parikh, Phys. Rev. **D48** R2983 (1993) and references therein.

[72] M. Mangano, proceedings of the X'th Topical Workshop on $p\bar{p}$ physics, Fermilab publication 1995(hep-ph/9507353).

[73] J. Badier *et al.* Z Phys. **20**, 101 (1983); D. M. Alde *et al.* Phys. Rev. Lett. **66**, 133(1991).

[74] D. Kharezeev and H. Satz, Phys. Lett. B **366**, 316 (1996).

[75] R. Baier and R. Ruckl, Z. Phys. C **19**, 251 (1992).

[76] G. T. Bodwin, E. Braaten and G. P. Lepage, Phys. Rev. D. **51**, 1125 (1995).

[77] Peter. Cho, and Adam. K. leibovich, Phys. Rev. D **53**, 150 (1996).

[78] T. S. Biro, E. Van Doorn, B. Muller and X. N. Wang, Phys. Rev. C **48**, 1275 (1993).

[79] M. E. Peskin, Nucl. Phys. B **156**, 365 (1979).

[80] M. E. Peskin and G. Bhanot, Nucl. Phys. B **156**, 391 (1979).

[81] A. Kaidalov, in QCD and High Energy Hadronic interactions, edited by J.Tran thanh Van (Edition Frontier,Gif-sur-Yvette,1993)

[82] D. Kharezeev and H. Satz, Phys. Lett. B **334**, 155 (1994).

[83] D Kharezeev, L. McLerran, and H. Satz, Phys. Lett. B **356**, 349 (1995).

[84] C Y. Wong, Phys. Rev. Lett. **76**, 196 (1997); C. W Wong, Phys. Rev. D **54**, R4199 (1996).

[85] K. Geiger, Phys Rev. D **48**, 4129 (1993).

[86] A. Shor, Phys. Lett. B **246**, 207 (1990).